5-2016

Quantification and Characterization of Fracture Resistance in Asphalt Concrete Based on R-Curve Method

Shu Yang
University of Arkansas, Fayetteville

Quantification and Characterization of Fracture Resistance in Asphalt Concrete Based on R-Curve Method

A dissertation submitted in partial fulfillment
of the requirements for the degree of
Doctor of Philosophy in Engineering

by

Shu Yang
Southeast University
Bachelor of Science in Civil Engineering, 2006
Southeast University
Master of Science in Highway and Railway Engineering, 2011

May 2016
University of Arkansas

This dissertation is approved for recommendation to the Graduate Council.

_____
Dr. Andrew F. Braham
Dissertation Director

_____
Dr. Kevin D. Hall
Committee Member

_____
Dr. Zahid Hossain
Committee Member

_____
Dr. Gary S. Prinz
Committee Member

_____
Dr. Shengfan Zhang
Committee Member

Abstract

The application of fracture energy is widely applied in the evaluation of cracking in the laboratory for asphalt concrete. However, this single number does not provide information on the characterization of the initiation and propagation of cracks. The Resistance Curve method, or R-Curve, is widely applied in characterizing various materials including, but not limited to, metal, polymer, rock, and composite. This research R-Curve method introduces asphalt concrete through a stepwise approach. First, in chapter one, there is a literature review of the history of fracture mechanics, fracture research in asphalt concrete, and an examination of the role of R-Curve application in various materials. Second, the current widely applied fracture energy analysis techniques are studied comprehensively for three types of asphalt concrete, three levels of aging, and two levels of moisture condition. The main limitation of fracture energy found in this chapter is that fracture energy alone is not always able to differentiate the fracture resistance of the three different materials examined. Third, the R-Curve method is applied to analyze and evaluate the same materials examined in chapter two. It is found that R-Curve can characterize and quantify the crack initiation and propagation, and the effects of aging and moisture damage on crack propagation are captured. Finally, a further investigation of R-Curve is performed to establish the envelope R-Curve considering the internal factors of aggregate size and binder grade, and the external factors of testing temperature and loading rate. The effects of aggregate size, binder grade, temperature, and loading rate on crack initiation and propagation are found by the parameters of cohesive energy and energy rate that are extracted from R-Curve. In conclusion, it is found that the R-Curve method can characterize and quantify the crack initiation and propagation for asphalt concrete.

Acknowledgement

I want to say thank you to my parents, Yang Hualin and Yang Yulan for the support as always. I am heartily thankful to my advisor, Dr. Andrew Braham, for the encouragement, support and advice in the past five years. Besides my advisor, I also want to sincerely thank the rest of my committee: Dr. Kevin Hall, Dr. Zahid Hossain, Dr. Gary Prinz, and Dr. Shengfan Zhang.

I cannot have the great experience in the past five years without my coworkers: Cory Bramlett, Leslie Parker, Slater Smith; and my friends: Robert Hill and Amanda Garbacz, my first classmates in the UofA; Alex Jackson and John Ryan, my first research workmates in the UofA; Chase Henrichs and Sadie Smith, my second research workmates in the UofA; Elvis Castillo, Airam Morales, and Erica Yeung, my third research workmates in the UofA; Nazmul Chowdhury, my project colleague from Arkansas State University.

Table of Contents

List of Figures

List of Tables

List of Published Papers

Chapter 2: Shu Yang, Andrew Braham, Lianfang Wang, and Qingkai Wang. "Influence of Aging and Moisture on Laboratory Performance of Asphalt Concrete", Construction and Building Materials 115:527-535., 2016

Chapter 3: Shu Yang, and Andrew Braham. "R-Curves Characterisation Analysis for Asphalt Concrete", International Journal of Pavement Engineering:1-10., 2016

Chapter 1 Introduction of Fracture in Asphalt Concrete

1.1 General research history

Cracking is one of the common distresses and premature failures in asphalt concrete (Birgisson, *et al.* 2007). It is generally defined and separated into mechanisms: thermal cracking, reflective cracking, and fatigue cracking. In cold climate regions, thermal cracking in asphalt pavement is one of the prominent distresses (Dave *et al.,* 2011). Like many other materials, asphalt concrete has a thermal response to the environmental temperature change. When the environmental temperature is low and decreasing, asphalt concrete shrinks and stress grows in the material to deteriorate the material to form a crack at the weakest defect point. Reflective cracking of asphalt overlay is an extensive pavement distress and damage in composite pavement structures. (Dave and Buttlar, 2010). If asphalt course layer paved on the Portland Cement Concrete (PCC), as the wheel moves from the existing PCC slab joint or crack, shear stress could be generated to create a crack that initiates from the bottom of asphalt layer and finally reflects to the top. (Braham, 2008). Fatigue cracking occurs in the area of wheel path because of the repeated traffic load (Miller and Bellinger, 2003). Fatigue cracking is also a major distress in asphalt pavement, in which researcher put to study in the past twenty years (Luo, 2012).

From 1987 to 1993, Strategic Highway Research Program (SHRP) performed a significant amount of research to improve the performance of asphalt pavement. The SHRP introduced the Superior Performing Asphalt Pavement (Superpave) asphalt mixture design and analysis system in 1992 after five years' research to control the thermal cracking, fatigue cracking, and rutting (Kavanagh, 2004). The current mix design method – Superpave considered cracking as one of the major concerns.

Research on cracking in asphalt concrete developed from the empirical method to the target of mechanistic method. The earlier stage of the studies on cracking in asphalt concrete is empirical. For example, National Cooperative Highway Research Program (NCHRP) Report 747 is a guide of forensic analysis. It lists out the causes of cracking including: low strength in mix, low asphalt content, high air void content, low HMA thickness, poor subgrade or base compaction, high asphalt binder viscosity, rapid aging of binder, exposure to moisture, high traffic volume, inadequate structure, and poor drainage. Researchers collected and are collecting large amount of cracking data that could be used for forensic analysis or statistical analysis. It is important that the correlation between the cracking performance and these empirical parameters as it can be used to guide the design and construction of the pavement directly to prevent from cracking in asphalt concrete. However, empirical research is not adequate to understand the mechanism behind the correlation. It is even more important to understand the fundamental cause of the cracking because the environmental that the asphalt concrete work in and the material itself always vary in huge from one road to another.

In a more advanced stage to the research, studies have moved on to the perspective of fracture mechanics to discover the fundamental of cracking in asphalt concrete. Single Edge Notched Beam [SE(B)] test was applied to study the strain energy release rate, which marks the first application of fracture mechanics in asphalt concrete (Moavenzadeh, 1967). The concept of Paris' Law (Paris, 1963) from Linear Elastic Fracture Mechanics (LEFM) was applied in the studies of the fatigue cracking in asphalt concrete (Majidzadeh *et al.*, 1970), which is another significant milestone in the history of application of fracture mechanics in asphalt concrete.

Later, researchers start to apply more concepts in fracture mechanics that first developed for other materials, especially in metal, to the studies of the cracking resistance in asphalt concrete. For example, LEFM concepts include fracture toughness (Ramsamooj *et al.,* 1991), and stress intensity factor (Dongre *et al.,* 1989) was applied to asphalt concrete. Although these research were based on fracture mechanic, the asphalt concrete was over simplified as linear elastic material. More recently, researchers apply the non-liner theory concept, fracture energy to the investigation of cracking in asphalt concrete. The concept of fracture energy in asphalt concrete has been studied intensively and comprehensively by a vast amount of researchers. For example, Li and Marasteanu (2004) applied studied the fracture energy of asphalt concrete with Semi-Circular Bend [SC(B)] configuration.

1.2 Fracture mechanics history

The development of the fracture mechanics was first motivated and developed by the aircraft industry. Thus, the fracture mechanics was developed by studying the material of metal. The application of fracture mechanics in asphalt concrete can be benefit from the review of mechanic history. Asphalt concrete is a complex material with the following characterizations: Non-linear, heterogeneous, non-isotropic, viscoelastic. It is important to apply the appropriate theory in fracture mechanics to asphalt concrete due to its material characterization. Thus, it is important to review the development history of the fracture mechanics.

When looking at the development history of fracture mechanics, it experienced three decades from linear elastic theory to non-linear theory, and time-dependent theory. By mid 1950s, LEFM was developed by the driven of aircraft industry. (Saxena, 1998). Griffith (1921) first proposed

the energy release rate, however, Irwin and Kies (1954) defined energy release rate (G) as a rate of change in potential energy with the crack area. G is also called a crack driving force because it is the derivative of a potential as seen in Equation 1.1, and it has the same unit as force.

$$\boldsymbol{G = -\frac{d\Pi}{dA}} \qquad \textbf{Equation 1.1}$$

Where;

G = energy release rate,

ΠΙ= potential energy, and

a = crack area.

Irwin (1957) derived the stress near the crack tip for mode I cracking as seen in Equation 1.2-1.4:

$$\boldsymbol{\sigma_x = \sqrt{\frac{EG}{\pi}}\frac{1}{\sqrt{2r}}cos\frac{\theta}{2}(1 - sin\frac{\theta}{2}sin\frac{3\theta}{2})} \qquad \textbf{Equation 1.2}$$

$$\boldsymbol{\sigma_y = \sqrt{\frac{EG}{\pi}}\frac{1}{\sqrt{2r}}cos\frac{\theta}{2}(1 + sin\frac{\theta}{2}sin\frac{3\theta}{2})} \qquad \textbf{Equation 1.3}$$

$$\boldsymbol{\tau_{xy} = \sqrt{\frac{EG}{\pi}}\frac{1}{\sqrt{2r}}cos\frac{\theta}{2}sin\frac{\theta}{2}cos\frac{3\theta}{2}} \qquad \textbf{Equation 1.4}$$

Where;

σ= normal stress near the crack tip,

τ = shear stress near the crack tip,

E = young's modulus,

G = energy release rate, and

r, θ, x, y =coordinate parameter.

$K_I = \sqrt{EG}$ is now known as the single parameter concept of stress intensity factor by which the stress field at the crack tip could be calculated.

Paris law (Paris, 1963) stablished the relation between crack growth and cyclic stress intensity factor under the LEFM. However, it is realized that LEFM is only limited to the material of cracked body are dominated with linear elastic behavior, and asphalt concrete is viscoelastic material at all but lowest service temperatures. In 1960s, nuclear power industry development leads to develop Elastic-Plastic Fracture Mechanics (EPFM) as the industry uses the ductile steels in which fracture was associated with plastic deformation. There are two concepts that are critical to EPFM, Crack Tip Opening Displacement (CTOD) and J-Integral. As defined in equation 1.5, J-Integral has a similar definition as energy release rate, but for nonlinear material. J-integral is a more general concept than energy release rate and when the material is linear elastic, J-integral equals to energy release rate. (Anderson, 2005)

$$\mathbf{J} = -\frac{\boldsymbol{d}\Pi}{\boldsymbol{dA}} \qquad \textbf{Equation 1.5}$$

Where;

J = J integral,

Π= potential energy, and

A= crack area.

In early to mid-1970s, crack growth under creep condition was complimented to the fracture mechanics by Siverns and Price (1973). And Time-Dependent Fracture Mechanics (TDFM) was established.

1.3 Application of fracture mechanics in asphalt concrete

The development of fracture mechanics in asphalt concrete is not as advanced as in metal material. Asphalt concrete is complex in mechanics. In lieu of pure linear elastic, it is a heterogeneous, non-liner, viscoelastic material. It is reasonably found that the application history of fracture mechanics in asphalt concrete moved on from linear theory to non-linear, from elastic to non-elastic, similar to the history of fracture mechanics in metals.

Initially it started with the application of LEFM concepts, Kim *et al.* (1997) studied the stress intensity of asphalt concrete at low testing temperature, Majidzadeh *et al*. (1970) and Ramsamooj *et al.* (1991) used stress intensity factor to predict the fatigue life of asphalt concrete. Tsai *et al.* (2010) applied Paris Law to predict reflection cracking of HMA overlays.

The research then moved on to non-liner theory by using the concept of Crack Tip Opening Displacement (CTOD). Wagoner *et al.* (2005), Braham (2008) investigated the CTOD because asphalt concrete is not a linear elastic material, and the research on CTOD contributes to understanding of the "plastic zone" ahead the crack tip. Kuai *et al.* (2009) applied J-Integral to crack propagation modeling of asphalt concrete, as J-integral does not require the crack body behave in linear manner.

In addition to the research discussed above, other research groups have investigated fracture energy as well. For example, At the University of Illinois, the effects of critical factors on fracture energy has been well established: binder type, aggregate, composition, (Braham *et al.*, 2007), aging (Braham *et al.*, 2009), gradation (Ahmed *et al., 2010*), temperature, air void level,

(Dave *et al.,* 2011). Different test configurations have been transmitted from other material to asphalt concrete to capture fracture energy: indirect tension (Kim *et al.,* 2012), single edge notched beam (Wagoner *et al.,* 2005), disk-shaped compact tension (Wagoner *et al.,* 2006), and semi-circular bending (Li and Marasteanu, 2005). In addition, the effects of the geometry on fracture energy have been investigated by Wagoner *et al.* (2007).

In the University of Florida, the fundamental study of fracture energy in asphalt concrete was performed considering the effects of the material components and the environment. For example, Ruth *et al.* (2002) studied the relationship between gradation and fracture energy. Birgisson *et al.* (2004) measured the fracture energy before and after moisture condition to evaluate the moisture susceptibility in HMA. More recently, some more in depth research has been performed on fracture energy in asphalt concrete, the fracture energy analysis was evaluated by microstructure level analysis (Birgisson *et al.,*2006). Koh and Roque (2010) used no uniform stress-state tests to determine fracture energy and claimed that these tests can accurately determine fracture energy over a range of testing temperature and aging conditions. Birgisson *et al.* (2008) applied digital image correlation on IDT and SC(B) test to accurately capture the fracture energy density for polermer modified asphalt concrete. Kim *et al.* (2008) developed a rigorous analytical model to consider the effect of dissipated creep strain energy in cracking.

At Texas A&M University, Texas overly test protocol is a commonly used fracture test. The concept of fracture energy index was applied in the overlay tester to characterize the cracking resistance potential of asphalt concrete (Walubita, *et al.,* 2012). A lot more advanced research

was focused on the components of energy in fracture of asphalt concrete. Howson *et al.* (2012) separate the total work in a fracture into bond energy, surface free energy, dissipated plastic energy, and dissipated viscoelastic energy. By review the research from Texas A&M, it was fatigue cracking was investigated comprehensively by using the energy theory. Although the fatigue cracking and thermal cracking are considered fundamentally different, the point of view in fracture of asphalt concrete can be valuable in understanding both fatigue and thermal cracking. In the research of fatigue cracking in asphalt concrete at Texas A&M, the concept of surface energy was promoted. It was claimed that the crack in pavement mainly occurs between the interface of aggregate and asphalt bind or within the asphalt mastic. And the energy used to separate aggregate and asphalt binder was defined as adhesive energy, while the energy used to create crack within mastic was defined as cohesion energy. Cheng *et al.* (2002) applied the "Principle of Wilhelmy Plate Method" to test and analyzed the surface energy. The fracture energy was separated into surface free energy, dissipated plastic energy, and dissipated viscoelastic energy. In addition, Walubita *et al.* (2012) promoted the concept of pseudo-strain energy and surface energy to analyze the fracture and fatigue cracking resistance. Luo *et al.* (2015) identified the energy in the local nonlinear zone, the energy in the local energy release zone, and the surface energy in the material to define the energy-based crack initiation criterion.

At the University of Taxes, Bhasin *et al.* (2009) used the energy methods to characterize fatigue cracking in asphalt concrete. Bhasin and Little (2009) used the microcalorimeter to directly measure the surface free energy components: the total energy of adhesion from asphalt binder and aggregate. It should be noticed that the new created surface area is always rough surface, the

measurement of this area can introduce the inaccuracy of the measurement of fracture energy as it eliminates surface irregularities.

Fracture energy in literatures is normally defined in the Equation 1.6:

$$G_f = \frac{W_f}{A_{lig}} \qquad \textbf{Equation 1.6}$$

Where;

W_f = work has been done to create a new crack surface, J/m^2, and

A_{lig} = new created surface area, m^2.

At Louisiana State University, the parameter "critical strain energy release rate" was applied to characterize the fracture resistance of asphalt concrete. This parameter was defined as the area under the load-displacement curve in the pre-peak area divided by the new created surface area. (Kim *et al.* 2012). A tremendous amount of typical mixes in Louisiana were tested by using semi-circular bending test at 25ºC. The critical strain energy release rate, also known as critical value of J-integral was utilized to evaluate the fracture resistance (Wu *et al.*, 2005). The finite element method with the cohesive model was performed, and the simulation results agreed with the semi-circular bending test (Elseifi, *et al.*, 2012)

Fracture energy is currently a most widely used concept to quantify the crack resistance in asphalt concrete. Based on large amount for research, Marasteanu *et al.* (2012) claimed that 400J/m^2 is sufficient for the asphalt concrete to resist to thermal cracking. It is an easy single number for the agency to control the quality of asphalt concrete in crack resistance.

1.4 Problem statement

In general, there are two approaches for fracture analysis (Anderson, 2005). First approach is stress intensity analysis: Failure occurs when $K_I = K_{Ic}$, and K_I is stress intensity factor while K_{Ic} is the critical stress intensity factor of mode I, it is a measure of material resistance to fracture. Stress intensity analysis will not include the crack propagation; it is a failure analysis. And also it is not appropriate to be applied in asphalt concrete as stress intensity factor cannot address the viscous behavior of asphalt concrete. The second approach is Energy criterion: "Crack extension occurs when energy available for crack growth is sufficient to overcome the resistance of the material." One of the benefits of this approach is that: instead of a single static number, this approach views the cracking process in a dynamic way because it defines the necessary condition of a crack growth. Thus, it can be used to characterize the whole procedure of a cracking. The other benefit of this approach is that it quantifies the resistance in measurement of energy. Thus, the material in fracture analysis does not need to be linear in mechanic property.

As asphalt concrete is a viscoelastic material, due to the nonlinear behavior of the material and the benefits of the energy criterion, the second approach is appropriate to be applied to quantify and characterize the resistance to cracking in asphalt concrete. However, as seen in the history of the fracture mechanics application, no research actually performed this energy criterion to investigate the reason of crack growth.

1.5 What is R-Curve?

Irwin and Kies (1954) developed the concept to quantify the crack growth resistance: Resistance-Curve or R-Curve. The R-Curve method considers fracture resistance as a function of crack

extension, and crack extension occurs when energy release rate equals to the material resistance. A plot of resistance vs. crack extension is the defined as the resistance curve, or R-Curve.

The application of R-Curve is the case of fracture analysis using the energy criterion (Anderson, 2005). Crack occurs when the energy release rate equals to the resistance of the material. Crack could be stable or unstable. The stable crack growth condition is expressed in Equation 1.7, and unstable condition is shown in equation 1.8:

$$\frac{dG}{da} < \frac{dR}{da} \qquad \textbf{Equation 1.7}$$

$$\frac{dG}{da} > \frac{dR}{da} \qquad \textbf{Equation 1.8}$$

Where;

G = crack driving force,

R = fracture resistance, and

a = crack length.

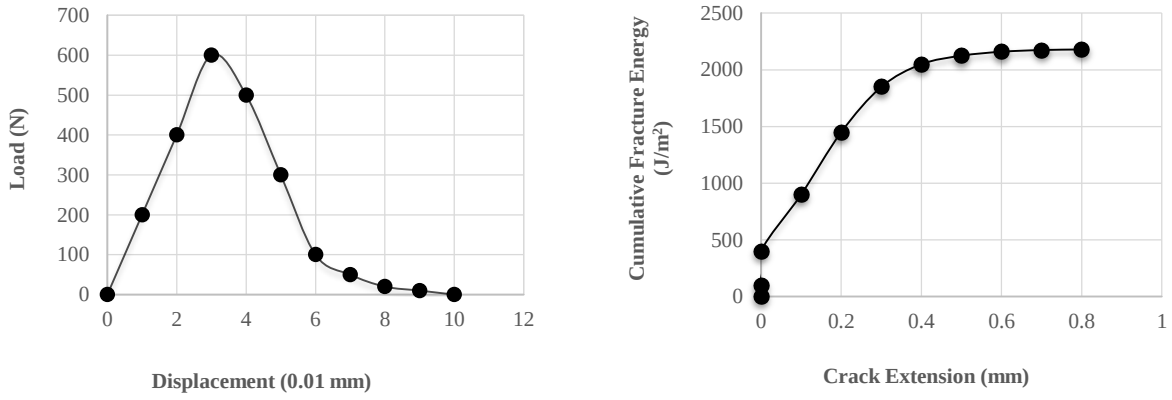

Figure 1.1 Load Displacement Curve and R-Curve

R-Curve is constructed by plotting crack resistance versus crack extension. If the stress at the low level, the crack cannot grow, the crack will begin to grow a little bit when the stress reaches to higher level when the crack driving force equals fracture resistance, but cannot grow any

further unless the stress increases. If the stress is at the level when the driving force increases at a slower rate than R, the cracking is stable when the stress is at the level that Equation 1.7 expressed. When stress reaches the level that expressed in Equation 1.8, the driving force increases at a rate quicker than R, the crack growth is unstable. Figure 1.1 illustrates the method to construct of R-Curve in this research by following the following steps:

1. Run fracture test;
2. Record load and load-line-displacement data;
3. Record images of surface to capture crack extension;
4. Sum up fracture energy at increment of crack length to plot R-Curve.

There are occasional deviations in the R-Curve construction due to the formation of cohesive zone and complexity of crack patterns, this method referred the construction of R-Curve by Braham and Mudford (2013).

Many studies use the concept of fracture energy was applied in asphalt concrete. But as a single number insufficient fracture energy cannot be the fundamental reason of crack initiation and propagation. Little research in asphalt area was found to characterize the fracture in a dynamic way. If compare energy release rate and fracture energy: they both share the same unit, because they both represent the energy to create a unit new surface. The different is that fracture energy is an overall average energy over the new surface area, so it is a single number of the cracking result. While energy release rate is the derivative of energy to crack extension increment, it is not a single number but a dynamic parameter to characterize the cracking process.

If fracture test performed at low temperature, chances are the material is very brittle, and the crack initiates and propagates in a very short time (less than one second). In this case, the R-Curve is a flat curve and energy release rate is a constant that has no difference with fracture energy. Thus, fracture energy is a special case of the energy release rate at a special condition when the cracking is brittle. However, asphalt concrete behaves more ductile when the temperature is high or the loading rate is low. Only asphalt concrete at brittle condition (proper temperature and loading rate combination) could be quantified properly with fracture energy. If the cracking is ductile rather than brittle, the criteria of fracture energy could be misleading, because it is just an empirical number at a certain condition. The application of R-Curve has the potential to solve this problem because energy release rate is a dynamic parameter. In addition, the way R-Curve method defines the crack growth is exactly the same as the second fracture analysis approach. Thus, R-Curve application to quantify the resistance of fracture has the support of fracture mechanics rather than empirical numbers. Although energy release rate is still under LEFM, however, if apply J-integral in R-Curve instead of energy release rate, non-linear property can be captured. This research will start the investigation of R-Curve from energy release rate.

In all, in area of asphalt concrete, fracture energy is now widely used to evaluate the material resistance to thermal cracking. However, cracking occurs because the energy release rate exceeds the material resistance, no matter it is thermal, load related, or other causes. Fracture energy is only a specific case of energy release rate when the cracking is a low temperature thermal cracking. There is a gap between the energy criterion in fracture mechanics and the practice of evaluation for asphalt concrete's cracking resistance. The application of R-Curve is expected to

fill this gap to evaluate the cracking resistance of asphalt concrete from the perspective of fracture mechanics.

1.6 Application of R-Curve in other area

R-Curve has been successfully applied in a vast range of material, especially, R-Curve has been widely applied in the areas such as metal (de Castro, 1984), composite (Fleck *et al.*, 1996), Ceramic (Yang, 1994), human tooth enamel (Bajaj *et al.*, 2009), human bone (Chan *et al.*, 2012), epoxy adhesives (Ameli *et al.*, 2009), alloy (Reynolds, 1996), dental porcelain (Cesar *et al.*, 2011), polymer (Schmit *et al.*, 1990), rock (Ouchterlony, 1982), and Concrete (Xi and Bazant, 1996). It is noticed that there is R-curve application in polymer, which has similar chemical structural as asphalt cement, and rock, the other important component in asphalt concrete. If R-Curve could be successfully applied in this large range of materials, there is a potential that this technique can be successfully applied in asphalt concrete. However, only a few literature of the application of R-Curve on asphalt concrete was found. Braham and Mudford (2013) applied the R-Curve for asphalt concrete. Multiple R-Curves at different testing temperatures for the same mixture were built. By shifting the curves at different temperature, a master R- Curve was constructed. This study used the master R-Curve to quantify and characterize the cracking resistance of asphalt concrete. It is noticed that this research used CMOD as the crack extension.

The further literature focusses on answering the following three questions: first, why the R-Curve was applied for other materials? Second, how R-Curve can be applied in other materials? Third, what can be found by using R-Curve?

Conventionally, it is widely believed that a singular constant fracture toughness (K_c) can be used to demonstrate the instability conditions in all test geometry size. However, this contradicts to the concept of R-Curve, which consider the fracture toughness as the resistance is a function of crack extension. The ASTM committee E-24 on fracture testing metals found that in order to capture the constant Kc, the specimen need to be as wide as 48 in. R-Curve method can be applied with a much thinner specimen in a sheet specimen testing, or plain stress problem testing, which significantly reduces the cost of testing. (ASTM, 1973). Based on literature review, Heyer (1973) concluded that R-Curve method had been found to be useful to capture fracture toughness over a large range of material properties and specimen thickness. It is known that brittle material has a flat R-Curve while ductile material has rising R-Curve. Judy and Goode (1973) applied R-Curve on three high-strength steels and found that the slope of R-Curve was dependent on the specimen thickness.

As R-Curve consider the resistance as the function of crack extension, it can be used to demonstrate the extensive crack tolerance by the minimum fracture toughness. For example, R-Curve was applied on ASTM A572 grade 50 steel, to investigate the plane-stress fracture toughness from temperature range -40°F to +72°F, and this fracture toughness can be translated into critical flaw length. (Novak 1976). In this research, the author used two methods of loading to capture the R-Curve: displacement control and load control. It was found that load control method captured a higher measure of the fracture toughness. One of the most interesting findings was that the critical flaw size was seven times larger than the specimen in all geometry and testing temperature combinations.

In lieu of directly capturing the crack extension and resistance in testing, there are alternative methods to construct R-Curve indirectly. Zhou, *et al.* (2015) and Lin, *et al.* (2015) applied indentation-strength method developed by Anderson and Braun (1990) to construct R-Curve of the ceramic material. In this method, the R-curve is determined as the common envelope o the tangency points of the family of stress intensity factor curves from the strength data sets. The reason that researchers in ceramic material use R-Curve was that it was found to be hard to identify the contribution of crack deflection, crack bridging, fiber pull out and transformation to the toughening of the ceramic composite material. By plotting R-Curve of three materials using indentation-strength method, analysis of the toughness increment at different crack length stage showed agreement with the quantitative toughening analysis. At the short crack region, the increment of the toughness was limited as the fiber behind the crack tip was not functional in initial indentation flaws. But at a larger crack region, the fresh material was transformed at advancing tip, caused a significant bridging effect to toughening. It was found that quantitative of toughening theory analysis agree with the R-Curve results.

R-Curve in its application has alternative of the crack resistance. Usually, accumulative fracture energy, crack driven force can be used as the measure of resistance. However, this can be replaced as other measure measurement to address specific material behavior. For example, J-integral is commonly used in elastic-plastic material to address plastic behavior. Sahu *et al.* (2012) applied J-R Curve on characterizing the elastic-plastic fracture behavior of ferritic and austenitic steel. J-R Curve is the R-Curve that constructed by plotting J-integral as crack resistance vs. crack extension. Sahu *et al.* (2012) studied the transferability of fracture toughness

properties from specimen to structure components, and it was found that J-R curve were geometry independent within the limited range of loading and geometric restrictions.

In addition, R-Curve can help to explain the mechanism of crack initiation and propagation, and the phenomenon that associated during a cracking process. For example, Jeon *et al.* (2015) applied R-Curve on Ti-based amorphous alloy containing ductile dendrites. It can explain the mechanism of blocking of the crack growth and crack blunting and deformation band formation at dendrites.

Another example is the cohesive energy that associated with cracking process. Gutkin *et al.* (2011) studied the R-Curve and its specimen dependence for IM7/8552 unidirectional carbon/epoxy using Double cantilever beam (DCB) and Compact Tension (CT) test. It was found that the analytical predicted R-Curve showed agreement with the Finite Element Method (FEM) R-Curve. It was found that cohesive law model can be used to predict accurate R-Curve. This research proved that R-Curve can characterize the cohesive zone and cohesive energy. In addition, the specimen dependent effect under large scale bridging condition was a concern when applying the R-Curve.

In summary, R-Curve method was comprehensively studied and established in a vast amount of materials. Due to three most important founds in literature: First, R-Curve can be applied in a large range of material. Second, R-Curve considers fracture resistance as function of crack extension instead of constant, which can be applied on thin specimen. Third, R-Curve give information of cracking initiation such as cohesive energy, and propagation such as the R-curve

slope. In conclusion of literature review, there is a research value to transit this R-Curve method to asphalt concrete.

1.7 Dissertation objectives

The first objective of this research is the review the application of R-Curve in other materials. This work is discussed as above in chapter one, the other three objectives will be covered from chapter two to chapter four and listed as below:

- Review of the current widely used quantification of fracture resistance in asphalt concrete, fracture energy, across various moisture and aging levels, while performing a viscoelastic analysis of the material by using dynamic modulus.
- Initial investigation of R-Curves by constructing R-Curves from the data in Chapter two
- A full investigation of R-Curves across multiple gradations and asphalt binder types to determine the potential extremes of R-Curve application.

1.8 Reference

Ahmed, Sarfraz, Eshan V. Dave, Behzad Behnia, William G. Buttlar, and Marvin Exline. "Fracture Characterization of Gap-Graded Asphalt Mixtures and Thin Bonded Wearing Courses." *International Journal of Pavement Research and Technology* 3, no. 3 (2010): 128-34.

Ameli, A., M. Papini, J. A. Schroeder, and J. K. Spelt. "Fracture R-Curve Characterization of Toughened Epoxy Adhesives." *Engineering Fracture Mechanics* 77, no. 3 (2010): 521-34.

Anderson, Richard M., and Linda M. Braun. "Technique for the R-Curve Determination of Y-Tzp Using Indentation-Produced Flaws." *Journal of the American Ceramic Society* 73, no. 10 (1990): 3059-62.

Anderson, Ted L., and T. L. Anderson. *Fracture Mechanics: Fundamentals and Applications*. CRC press, 2005.

Bajaj, Devendra, and Dwayne D. Arola. "On the R-Curve Behavior of Human Tooth Enamel." *Biomaterials* 30, no. 23-24 (2009): 4037-46.

Bhasin, Amit, and Dallas N. Little. "Application of Microcalorimeter to Characterize Adhesion between Asphalt Binders and Aggregates." *Journal of Materials in Civil Engineering* 21, no. 6 (2009): 235-43.

Birgisson, B., A. Montepara, E. Romeo, R. Roncella, G. Tebaldi, and R. Roque. "The Use of Digital Image Correlation for Accurate Determination of Fracture Energy Density in Hot Mix Asphalt (Hma)." Paper presented at the 6th RILEM International Conference on Cracking in Pavements, June 16, 2008 - June 18, 2008, Chicago, IL, United states, 2008.

Birgisson, Bjorn, Antonio Montepara, John Napier, Elena Romeo, Riccardo Roncella, and Gabriele Tebaldi. "Micromechanical Analyses for Measurement and Prediction of Hot-Mix Asphalt Fracture Energy." Paper presented at the Bituminous Paving Mixtures, 2006.

Birgisson, Bjorn, Antonio Montepara, Elena Romeo, Reynaldo Roque, Riccardo Roncella, and Gabriele Tebaldi. "Determination of Fundamental Tensile Failure Limits of Mixtures." Paper presented at the Asphalt Paving Technology 2007 AAPT, March 11, 2007 - March 14, 2007, San Antonio, TX, United states, 2007.

Birgisson, Bjorn, Reynaldo Roque, and Gale C. Page. "Performance-Based Fracture Criterion for Evaluation of Moisture Susceptibility in Hot-Mix Asphalt." 2004.

Braham, Andrew F., William G. Buttlar, Timothy R. Clyne, Mihai O. Marasteanu, and Mugurel I. Turos. "The Effect of Long-Term Laboratory Aging on Asphalt Concrete Fracture Energy." Paper presented at the Asphalt Paving Technology 2009, AAPT, March 15,

2009 - March 18, 2009, Minneapolis, MN, United states, 2009.

Braham, Andrew F., William G. Buttlar, and Mihai O. Marasteanu. "Effect of Binder Type, Aggregate, and Mixture Composition on Fracture Energy of Hot-Mix Asphalt in Cold Climates." *Transportation Research Record*, no. 2001 (2007): 102-09.

Braham, Andrew Franz. *Fracture Characteristics of Asphalt Concrete in Mode I, Mode Ii, and Mixed-Mode*. ProQuest, 2008.

Braham, Andrew, and Caleb Mudford. "Development of Fracture Resistance Curves for Asphalt Concrete." *Journal of Materials in Civil Engineering* 25, no. 11 (2013): 1631-37.

Cesar, Paulo Francisco, Vinicius Rosa, Marcelo Mendes Pinto, Humberto Naoyuki Yoshimura, and Luoyu Roy Xu. "Effect of Ion Exchange on R-Curve Behavior of a Dental Porcelain." *Journal of Materials Science* 46, no. 1 (2011): 117-22.

Chan, Kwai S., and Daniel P. Nicolella. "Micromechanical Modeling of R-Curve Behaviors in Human Cortical Bone." *Journal of the Mechanical Behavior of Biomedical Materials* 16, no. 1 (2012): 136-52.

Cheng, DingXin, Dallas N. Little, Robert L. Lytton, and James C. Holste. "Surface Energy Measurement of Asphalt and Its Application to Predicting Fatigue and Healing in Asphalt Mixtures." 2002.

Dave, Eshan V., Behzad Behnia, Sarfraz Ahmed, William G. Buttlar, and Henrique Reis. "Low Temperature Fracture Evaluation of Asphalt Mixtures Using Mechanical Testing and Acoustic Emissions Techniques." Paper presented at the Asphalt Paving Technology 2011, AAPT, March 27, 2011 - March 30, 2011, Tampa, FL, United states, 2011.

Dave, Eshan V., and William G. Buttlar. "Thermal Reflective Cracking of Asphalt Concrete Overlays." *International Journal of Pavement Engineering* 11, no. 6 (2010): 477-88.

de Castro, P. M. S. T. "R-Curve Behaviour of a Structural Steel." *Engineering Fracture Mechanics* 19, no. 2 (1984): 341-57.

Dongre, Rai, M. G. Sharma, and D. A. Anderson. "Development of Fracture Criterion for Asphalt Mixes at Low Temperatures." *Transportation Research Record*, no. 1228 (1989): 94-105.

Elseifi, Mostafa A., Louay N. Mohammad, Hao Ying, and Samuel Cooper Iii. "Modeling and Evaluation of the Cracking Resistance of Asphalt Mixtures Using the Semi-Circular Bending Test at Intermediate Temperatures." Paper presented at the Asphalt Paving Technology 2012, AAPT, April 1, 2012 - April 4, 2012, Austin, TX, United states, 2012.

Fleck, N. A., M. P. F. Sutcliffe, S. Sivashanker, and X. J. Xin. "Compressive R-Curve of a Carbon Fibre-Epoxy Matrix Composite." *Composites Part B: Engineering* 27, no. 6

(1996): 531-41.

Griffith, Alan A. "The Phenomena of Rupture and Flow in Solids." *Philosophical transactions of the royal society of london. Series A, containing papers of a mathematical or physical character* 221 (1921): 163-98.

Gutkin, R., M. L. Laffan, S. T. Pinho, P. Robinson, and P. T. Curtis. "Modelling the R-Curve Effect and Its Specimen-Dependence." *International Journal of Solids and Structures* 48, no. 11-12 (2011): 1767-77.

Howson, Jonathan, Eyad Masad, Dallas Little, and Emad Kassem. "Relationship between Bond Energy and Total Work of Fracture for Asphalt Binder-Aggregate Systems." Paper presented at the Asphalt Paving Technology 2012, AAPT, April 1, 2012 - April 4, 2012, Austin, TX, United states, 2012.

Irwin, G. R., and J. A. Kies. "Critical Energy Rate Analysis of Fracture Strength." *Welding Journal* 33, no. 4 (1954): 193-8.

Jeon, Changwoo, Choongnyun Paul Kim, Hyoung Seop Kim, and Sunghak Lee. "Interpretation of Fracture Toughness and R-Curve Behavior by Direct Observation of Microfracture Process in Ti-Based Dendrite-Containing Amorphous Alloys." *Metallurgical and Materials Transactions A: Physical Metallurgy and Materials Science* 46, no. 4 (2015): 1588-96.

Kavanagh, Leonnie N. "A 9-Year Evaluation of Field Cracking and Rutting Performance of Sps-9 Superpave Experiment." 2004.

Kim, Jaeseung, Reynaldo Roque, and Bjorn Birgisson. "Integration of Thermal Fracture in the Hma Fracture Model." Paper presented at the 2008 Annual Meeting of the Association of Asphalt Paving Technologists, AAPT, April 25, 2008 - April 30, 2008, Philadelphia, PA, United states, 2008.

Kim, Minkyum, Louay Mohammad, and Mostafa Elseifi. "Characterization of Fracture Properties of Asphalt Mixtures as Measured by Semicircular Bend Test and Indirect Tension Test." *Transportation Research Record*, no. 2296 (2012): 115-24.

Koh, Chulseung, and Reynaldo Roque. "Use of Nonuniform Stress-State Tests to Determine Fracture Energy of Asphalt Mixtures Accurately." *Transportation Research Record*, no. 2181 (2010): 55-66.

Kuai, Haidong, Hyun Jong Lee, Goangseup Zi, and Sungho Mun. "Application of Generalized J-Integral to Crack Propagation Modeling of Asphalt Concrete under Repeated Loading." *Transportation Research Record*, no. 2127 (2009): 72-81.

Li, Xue, and Mihai Marasteanu. "Evaluation of the Low Temperature Fracture Resistance of Asphalt Mixtures Using the Semi Circular Bend Test." Paper presented at the Asphalt

Paving Technology 2004, March 8, 2004 - March 10, 2004, Baton Rouge, LA, United states, 2004.

Li, Xue, and Mihai O. Marasteanu. "Cohesive Modeling of Fracture in Asphalt Mixtures at Low Temperatures." *International Journal of Fracture* 136, no. 1-4 (2005): 285-308.

Lin, Jia, Yu Huang, and Houan Zhang. "Damage Resistance, R-Curve Behavior and Toughening Mechanisms of Zrb2-Based Composites with Sic Whiskers and Zro2 Fibers." *Ceramics International* 41, no. 2 (2015): 2690-98.

Luo, Xue. "Characterization of Fatigue Cracking and Healing of Asphalt Mixtures." ProQuest LLC, 2012.

Luo, Xue, Rong Luo, and Robert L. Lytton. "Energy-Based Crack Initiation Criterion for Viscoelastoplastic Materials with Distributed Cracks." *Journal of Engineering Mechanics* 141, no. 2 (2015).

Majidzadeh, K., E. M. Kauffmann, and D. V. Ramsamooj. "Application of Fracture Mechanics in the Analysis of Pavement Fatigue." 1971 1970.

Marasteanu, Mihai, William Buttlar, Hussain Bahia, Christopher Williams, Ki Hoon Moon, Eyoab Zegey Teshale, Augusto Cannone Falchetto, *et al.* "Investigation of Low Temperature Cracking in Asphalt Pavements National Pooled Fund Study–Phase Ii." (2012).

Moavenzadeh, Fred. "Asphalt Fracture." 1967 1967.

Novak, Stephen R. "Resistance to Plane-Stress Fracture (R-Curve Behavior) of A572 Structural Steel." In *Mechanics of Crack Growth*: ASTM International, 1976.

Ouchterlony, Finn. "Simple R-Curve Approach to Fracture Toughness Testing of Rock Core Specimens." Paper presented at the Proceedings 23rd Symposium on Rock Mechanics, Berkeley, Calif, USA, 1982.

Paris, P., and F. Erdogan. "Critical Analysis of Crack Propagation Laws." *American Society of Mechanical Engineers -- Transactions -- Journal of Basic Engineering* 85, no. 4 (1963): 528-34.

Rada, Gonzalo R. *Guide for Conducting Forensic Investigations of Highway Pavements (with Supplemental Material on Cd-Rom)*. Vol. 747: Transportation Research Board, 2013.

Ramsamooj, D. V. "Prediction of Fatigue Life of Asphalt Concrete Beams from Fracture Tests." *Journal of Testing & Evaluation* 19, no. 3 (1991): 231-39.

Reynolds, Anthony P. "Comparison of R-Curve Methodologies for Ranking the Toughness of Aluminum Alloys." *Journal of Testing and Evaluation* 24, no. 6 (1996): 406-10.

Ruth, Byron E., Reynaldo Roque, Bensa Nukunya, Richard Davis, Mihai Marasteanu, William Vavrik, Frank Fee, *et al.* "Aggregate Gradation Characterization Factors and Their Relationships to Fracture Energy and Failure Strain of Asphalt Mixtures." Paper presented at the Asphalt Paving Technology 2002, March 18, 2002 - March 20, 2002, Colorado Springs, CO, United states, 2002.

Sahu, M. K., J. Chattopadhyay, and B. K. Dutta. "Transferability of Specimen J-R Curve to Straight Pipe with Circumferential Surface Flaw." *Fatigue and Fracture of Engineering Materials and Structures* 35, no. 5 (2012): 476-87.

Saxena, Ashok. *Nonlinear Fracture Mechanics for Engineers*. CRC press, 1998.

Schmit, F., D. Bouvart, and D. Francois. "Ductile Fracture Characterization of Polycarbonate by the R-Curve Method." *International Journal of Fracture* 43, no. 2 (1990): 83-96.

Siverns, M. J., and A. T. Price. "Crack Propagation under Creep Conditions in a Quenched 2 One Quarter Chromium 1 Molybdenum Steel." *International Journal of Fracture* 9, no. 2 (1973): 199-207.

Tsai, Fang-Ling, Robert L. Lytton, and Sangick Lee. "Prediction of Reflection Cracking in Hot-Mix Asphalt Overlays." *Transportation Research Record*, no. 2155 (2010): 43-54.

Wagoner, Michael P., and William G. Buttlar. "Influence of Specimen Size on Fracture Energy of Asphalt Concrete." Paper presented at the Asphalt Paving Technology 2007 AAPT, March 11, 2007 - March 14, 2007, San Antonio, TX, United states, 2007.

Wagoner, Michael P., William G. Buttlar, and Glaucio H. Paulino. "Development of a Single-Edge Notched Beam Test for Asphalt Concrete Mixtures." *Journal of Testing and Evaluation* 33, no. 6 (2005): 452-60.

Wagoner, Michael P., William G. Buttlar, Glaucio H. Paulino, and Philip Blankenship. "Investigation of the Fracture Resistance of Hot-Mix Asphalt Concrete Using a Disk-Shaped Compact Tension Test." 2005.

Wagoner, Michael P., William G. Buttlar, Glaucio H. Paulino, Philip Blankenship, Reynaldo Roque, Wu Rongzong, Adriaan De Bondt, *et al.* "Laboratory Testing Suite for Characterization of Asphalt Concrete Mixtures Obtained from Field Cores." Paper presented at the Association of Asphalt Paving Technologists -Proceedings of the Technical Sessions 2006 Annual Meeting, March 27, 2006 - March 29, 2006, Savannah, GA, United states, 2006.

Walubita, Lubinda F., Geoffrey S. Simate, Edward Ofori-Abebresse, Amy Epps Martin, Robert L. Lytton, and Luis E. Sanabria. "Mathematical Formulation of Hma Crack Initiation and Crack Propagation Models Based on Continuum Fracture-Mechanics and Work-Potential Theory." *International Journal of Fatigue* 40 (2012): 112-19.

Wu, Zhong, Louay N. Mohammad, L. B. Wang, and Mary Ann Mull. "Fracture Resistance Characterization of Superpave Mixtures Using the Semi-Circular Bending Test." *Journal of ASTM International* 2, no. 3 (2005): 135-49.

Xi, Yunping, and Zdenek P. Bazant. "Analysis of Crack Propagation in Concrete Structures by Markov Chain Model and R-Curve Method." Paper presented at the Proceedings of the 1996 7th Specialty Conference on Probabilistic Mechanics and Structural Reliability, August 7, 1996 - August 9, 1996, Worcester, MA, USA, 1996.

Yang, Kwanho, C. James Hwang, and John A. Rice. "New Testing Method for Ceramic R-Curve Determination at Elevated Temperatures." Paper presented at the Proceedings of the 1994 International Mechanical Engineering Congress and Exposition, November 6, 1994 - November 11, 1994, Chicago, IL, USA, 1994.

Zhou, Peng, Ping Hu, Xinghong Zhang, Wenbo Han, and Youhua Fan. "R-Curve Behavior of Laminated Zrbinf2/Inf-Sic Ceramic with Strong Interfaces." *International Journal of Refractory Metals and Hard Materials* 52 (2015): 12-16.

Chapter 2 Preliminary Fracture Energy Research*[1]

2.1 Background of preliminary fracture energy research

Based on the founding of the literature review in chapter one, it can be seen that fracture energy is an appropriate and widely applied quantification of crack resistance for asphalt concrete. As the preliminary research prior to the R-Curve study for asphalt concrete, a comprehensive study of asphalt concrete will be introduced in this chapter, including a standard analysis of cracking using only fracture energy, a study of the influence of moisture and aging, and a full viscoelastic quantification through dynamic modulus. It is known that asphalt concrete is a viscoelastic material, of whose performance is highly related to the environmental temperature. When the environmental temperature is relatively low, asphalt concrete tends to behave less viscous and more brittle, the material needs to be designed more flexible, or less tough to resist the crack; whereas when the environmental temperature is relatively high, asphalt concrete tends to behave more viscous and low in toughness, the material needs to be designed tougher, to resist permanent deformation or rutting. Obviously, the balance between flexibility and stiffness needs to be considered so that asphalt concrete has sufficient flexibility to resist cracking and sufficient toughness to resist rutting. Stiffness or toughness can be a vital role in this balance consideration. Thus, in addition to fracture energy, dynamic modulus as a toughness parameter is another study object in this preliminary fracture research.

1* The major work in this chapter was an article: Shu Yang, Andrew Braham, Lianfang Wang, and Qingkai Wang. "Influence of Aging and Moisture on Laboratory Performance of Asphalt Concrete", Construction and Building Materials 115:527-535., 2016

Besides the environmental temperature, moisture and aging are two other external factors which may significantly affect the performance of asphalt concrete. First, water in asphalt concrete may strip the asphalt binder from the aggregate, and result in less bonding at the interface. Also, the moisture in asphalt concrete can change the thermal dynamic of the material in a freeze-thaw cycle due to the environmental temperature change. Second, asphalt concrete is exposed to oxygen, sun radiation, and wind, which age it over time to build on toughness. In order to fully understand the crack resistance in asphalt concrete, these factors including temperature, moisture condition, and aging were added to the test matrix in this chapter.

Rather than external factors, asphalt concrete itself has a few variations due to the manufacture and new technique. Hot Mix Asphalt (HMA) is the most traditional one which needs to be mixed, transferred, placed, and compacted at high temperature range approximately from 150°C to 175°C depend on the viscosity of the asphalt cement. Except for the conventional HMA, warm mix technology and reclaimed material add new uncertainties to asphalt concrete. First, Warm Mix Asphalt (WMA) has been promoted in recent years to reduce the manufacturing (from mixing to compacting) temperature. By using lower temperature, warm mix technology should be able to reduce the aging of asphalt concrete during construction, and thus result in a better performance and longer service life. However, research need to be performed to verify this inference. Besides, warm mix has the advantage to reduce the emission of CO_2, improve the working condition at construction site, extend the construction season, extend the material transfer distance, etc. As a result, there is a huge driven to use this warm mix technology in industry, while there is concern about the long term performance because there is not much experience to apply this technology. Second, Reclaimed Asphalt Pavement (RAP) has been

utilized to add to HMA in many states. As RAP contains asphalt cement, the usage of RAP in HMA can reduce the new asphalt cement, which not only meets the demands of sustainability but also reduces the cost. However, as asphalt binder has the issue of aging as mentioned previously, RAP containing old binder attracts concerns in industry and academia on long term performance as well. In order to have a comprehensive understanding of the fracture resistance characterization of concrete, HMA, WMA, and WMA with usage of RAP (WR), as mixture type factor, was considered in the experimental matrix too.

In all, a comprehensive research of fracture energy coupled with consideration of toughness (dynamic modulus) for asphalt concrete is presented in this chapter to fully understand the current evaluation system of the fracture resistance in asphalt concrete.

2.2 Chapter objective

This chapter targeting using fracture energy and dynamic modulus to characterize the behavior of asphalt concrete considering aging and moisture condition.

2.3 Test materials

Three types of mixtures were used in this chapter: HMA without RAP (HMA), HMA with 25% RAP (HR), and WMA with 25% RAP (WR). In order to avoid another verbal of gradation by including 25% RAP in the HR and WR mixtures, the HMA mix design had to be slightly changed. The gradation was kept as close as possible to reduce conflicting variables when comparing the three mixtures. The gradation for the HR and WR mixtures was achieved by minimizing the sum of square errors (SSE, errors between HMA and HR/WR blend for each

size). In order to adjust the optimal asphalt cement content to accommodate the 25% RAP, the same air voids at N_{max} in the Superpave Gyratory Compactor were targeted to match the HMA, HR, and WR mixtures. While this is not as accurate as a complete mix design to determine the optimal asphalt cement content, due to limited materials available, this was deemed the best path forward.

The asphalt cement used in this study was SBS modified PG 76-22 binder. The RAP utilized in this study was unprocessed RAP shipped from Hebei Province. After solvent extraction, the PG grade of the binder in the RAP was determined to be a PG70-22, and the binder content in the RAP was determined to be 4.41% by taking the average of ignition oven and solvent extraction test. The total binder content for WR and HR incorporated this asphalt cement into the optimal asphalt cement content used in the samples fabricated in the lab. Since the RAP received was unprocessed, a lab processing procedure needed to be established.

The moisture conditioning procedure followed the AASHTO T 283 specification. Unconditioned samples were fabricated and tested with no temperature or moisture conditioning. The conditioning procedure can be described briefly in three steps: vacuum saturating, freezing, and thawing. This process may not be representative of the field situations, because the moisture damage may not be significant after one freeze-thaw cycle, and the conditioning was performed before the loading, which is not the field case. But this process is the current best way to simulate moisture damage. The samples were conditioned after they were cut. While this exposes cut aggregates directly to the moisture conditioning process, it can be very difficult to cut samples after the conditioning procedure, and many samples could be lost due to fabrication issues.

Along with moisture conditioning, aging was the second factor that was considered in the experimental matrix. AASHTO R 30 was followed to age the samples for testing. Three levels of this factor were considered: unaged, short term aged, and long term aged. These levels can be described as:

- Unaged: uncompacted samples were exposed to the "standard" aging time of two hours at compaction temperature before compaction as specified in the Superpave mix design procedure.
- Short term aged: uncompacted samples were aged for four hours at compaction temperature.
- Long term aged: samples were run through the short term aging protocol first and compacted. After compaction, the sample was placed at room temperature for sixteen hours, and then aged in an oven at a temperature of 85±3˚C for 120 hours (five days).

2.4 Test methods

2.4.1 Semi Circular Bend test

In this research, the fracture energy of asphalt mixtures is investigated by using the Semi-Circular Bend [SC(B)]. As mentioned before, in both the fracture test and dynamic modulus test, two factors were considered: moisture conditioning and laboratory aging. Two levels of moisture conditioning (conditioned and unconditioned) and three levels of aging (unaged, short term, and long term) were explored.

The fabrication of SC(B) sample, testing temperature and loading rate followed the specification of SC(B) test. Superpave Gyratory Compaction samples were compacted to N_{design}=100, targeting 4% air voids. Next, the samples were sliced into 3 disks, each with a thickness of 25mm. Finally, the sliced disks were cut in half into semi-circular shape and a 15mm in depth, 1mm in width notch was cut at the center bottom of each semi-circular sample.

Two testing temperatures in the specification were applied for each mix, -12°C and -24°C. The HMA, HR, and WR mixtures were placed in an MTS load frame with a clip gauge attached at the center bottom of sample. A load was applied to the sample, and the load line displacement (LLD) and Crack Mouth Opening Displacement (CMOD) were recorded by the MTS machine. All of the SC(B) tests were controlled with a constant COMD rate, set at 0.03mm/min. A preload of 0.3kN was applied before testing and the test stopped when the load drops below 0.5kN or when clip gauge range limit was reached.

2.4.2 Dynamic modulus test

As an important input of Mechanistic-Empirical Pavement Design Guide (MEPDG), dynamic modulus is very widely used to predict the rutting resistance for HMA. Pellinen and Witczak (2002) investigated the correlation between dynamic modulus and field performance including rutting, thermal and fatigue cracking, and dynamic modulus was suggested to be a parameter of the Simple Performance Test [SPT, known as asphalt mixture performance test (AMPT) later] for rutting.

The dynamic modulus test was performed by following AASHTO T 342. To fabricate the dynamic modulus samples, the Superpave gyratory compaction samples were compacted at N_{design}=100, targeting 4% air voids. Next, the samples were cored to a 100mm diameter and the ends were trimmed for a final height of 150mm. Three replicates were used for each test. The dynamic modulus testing was performed in the MTS loading frame with an environmental chamber at five temperatures (-10°C,+ 4°C, +21°C, +37°C, and +54°C) and 6 frequencies (25Hz, 10Hz, 5Hz, 1Hz, 0.5Hz, and 0.1Hz). AASHTO T 342 and AASHTO R 62 were followed to run the test and analyze the data.

2.5 Results and discussion

2.5.1 Discussion of SC(B) results

Figure 2.1 illustrated the results of the SC(B) tests with three types of mixture: HMA, HR, and WR at two conditions (unconditioned and moisture conditioned), three levels of age (two hours, four hours and five days), two testing temperatures (-24°C and -12°C). Fracture energy at each condition was captured to quantify the potential cracking characteristics of asphalt concrete mixtures.

As seen in Figure 2.1(a), the fracture energy of the SC(B) test at testing temperature -24°C with unconditioned samples. The average air voids of the sample tested are seen at the top of the bars in the figure. At testing temperature -24°C, and aging level two hours, WR indicates the highest fracture energy, HMA shows the lowest and HR is in between the other two. At aging level four hours, HMA indicates higher fracture energy than HR and WR. At aging level five days, HR and WR show higher fracture energy than HMA. However, the fracture energy trends are not

consistent between the three mixtures. It is disconcerting that the five days aging has such high variability between the replicates, especially with the HR and WR mixtures. This could indicate that the long term AAHSTO R 30 aging procedure does not consistently age samples, or creates significantly different crack patterns in the asphalt mixtures. It is also surprising that for the HR and WR mixtures, the five days aging has higher fracture energy. It was expected that as the samples were aged longer, they would become more quasi-brittle, and thus lose a significant amount of their fracture energy.

Figure 2.1(b) shows the fracture energy of the SC(B) test at testing temperature -24°C with moisture conditioned samples. At both aging levels two hours and four hours, HMA shows the highest fracture energy and WR shows the lowest. But at aging level five days, WR shows the highest fracture energy and HR shows the lowest; while WR does not show this fracture energy advantage in unconditioned samples, which may indicate that WR improves the moisture resistance in long term, but it does not improve the short-term cracking performance. It is encouraging that the variation between replicates on the moisture conditioned samples is lower than on the unconditioned samples. It is interesting to note that the fracture energy for the HMA mixtures is quite similar between conditioned and unconditioned samples, while the HR and WR mixtures show a larger decrease in fracture energy after moisture conditioning.

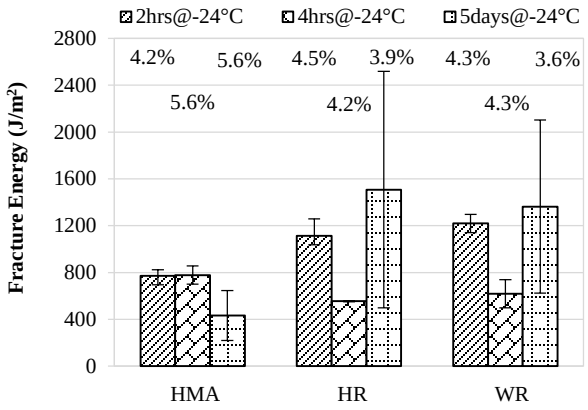

(a) Unconditioned

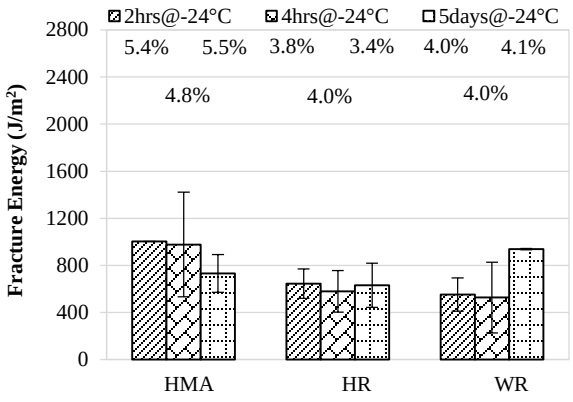

(b) Moisture Conditioned

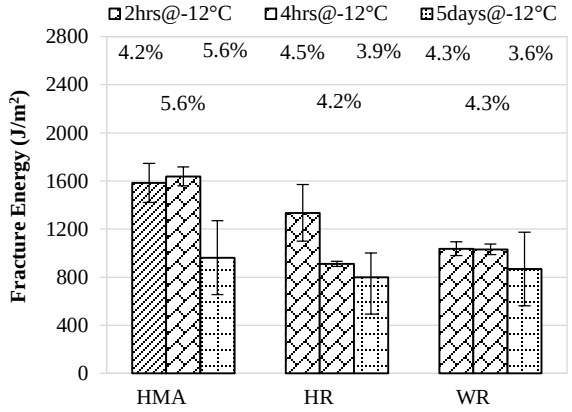

(c) Unconditioned

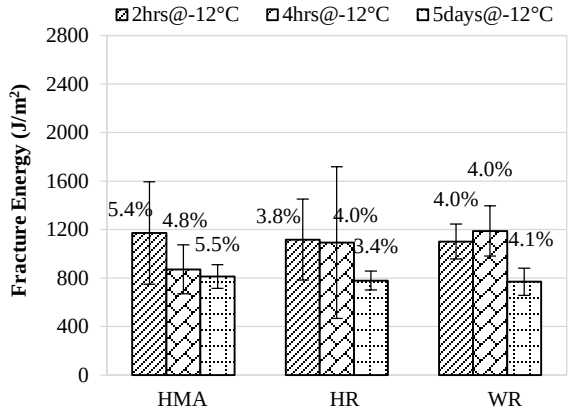

(d) Moisture Conditioned

*average air voids are shown above bars

Figure 2.1 SC(B) Fracture Test Results at -24°C and -12°C

Figure 2.1(c) and Figure 2.1(d) show the fracture data at -12°C. Specifically, Figure 2.1(c) shows the fracture energy of the SC(B) test at testing temperature -12°C with unconditioned samples. At both aging levels two hours and four hours, HMA shows the highest fracture energy and WR shows the lowest. At aging level five days, HMA still has the highest fracture energy but WR has slightly higher fracture energy than HR samples. A trend that is very apparent is that as the samples age, the fracture energy either remains essentially constant or decreases. This was the expected trend, as higher levels of aging in theory should make a mixture more brittle, thus, more susceptible to cracking. Another trend that was not observed at -24°C is that moisture

conditioning either does not affect the fracture energy or decreases it, as seen in Figure 2.1(d). It was expected that as a sample was moisture conditioned, the cracking resistance would decrease. These trends of aging and moisture conditioning indicate that in order to better capture the effects of aging and moisture conditioning, fracture testing at -12°C is preferred.

From Figure 2.1, there does not seem to be any detrimental effects on usage of RAP in mixtures. It also shows that the WMA technology is able to have equal performance to the HR technology, but at mixing and compacting temperatures that are 30°C lower. Therefore, by using the WMA technology, similar performance to standard RAP containing mixtures can be achieved in the lab, while reducing manufacturing temperatures. These effects are more beneficial to the environment through reduced energy use and emissions, and the WMA technology allows the opportunity to increase haul time.

As mentioned above, several of these sets of data have a high variability in fracture energy. The high COV shown by the bars in Figure 2.1 does not tend to appear for the unconditioned samples at two hours aging and four hours aging. It can be implied, therefore, that moisture conditioning and long term aging may be the reason for increased variability. In an attempt to more directly observe the effects of moisture conditioning at both -24°C and -12°C, equality line plots were made to compare the fracture energy of conditioned and unconditioned samples, as seen in Figure 2.2. It is apparent that the unconditioned fracture energy is higher than the moisture conditioned fracture energy in general. This is reasonable as one would expect moisture damage to occur during the conditioning process, and this would in turn decrease the fracture resistance of the mixtures.

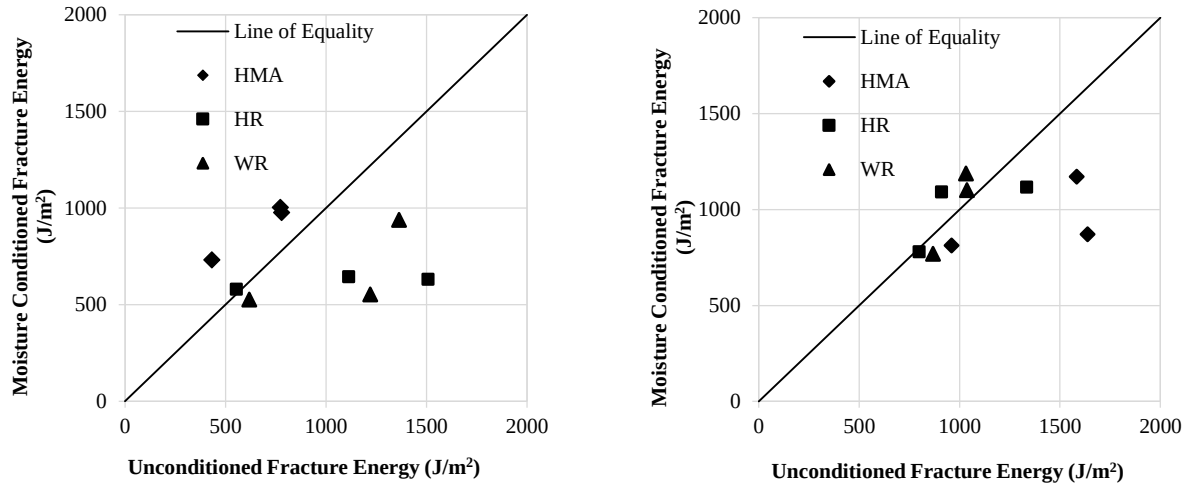

(a) -24 ˚C (b) -12 ˚C

Figure 2.2 Conditioned vs. Unconditioned SC(B) Test Results -24˚C and -12˚C

In order to find out the factor that impacts the fracture energy, Analysis of Variance (ANOVA) for SC(B) fracture energy is performed, and the result is shown in Table 2.1. Four factors including mixture type, moisture condition, testing temperature, and aging are considered. It is found that p-values (With a 95% confidence) of temperature is less than 0.05, which means that only testing temperature significantly affects fracture energy values, or the susceptibility of mixtures to cracking. In other words, RAP and warm mix do not statistically change the fracture energy significantly compare to traditional HMA. Considering WR has 0.46% lower binder content than HR, and is produced and placed at lower temperatures, WR and HR are statistically similar based on cracking performance.

Table 2.1 Analysis of Variance of Fracture Energy

Source	Sum Sq.	d.f.	Mean Sq.	F	p-value
Mix Type	20704.6	2	10352.3	0.13	0.8763
Aging	216469.1	2	108234.6	1.39	0.2658
Moisture	256171.0	1	256171	3.28	0.0803
Temperature	471923.2	1	471923.2	6.05	0.0201
Error	2262278.8	29	78009.6		
Total	3227546.7	35			

2.5.2 Discussion of dynamic modulus results

To visually simplify the dynamic modulus data, the master curve technique was applied in this study. Master curves were constructed by using the method from AASHTO PP 62-10. The effects of mixture type, aging duration, and moisture condition were analyzed in these master curves. The reference temperature is 21.1˚C.

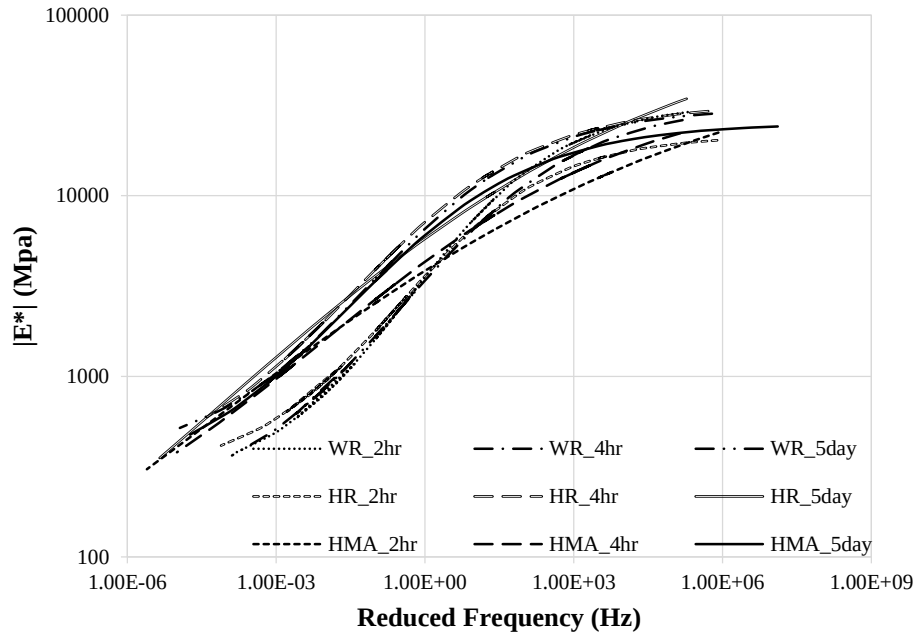

Figure 2.3 Master Curve for Unconditioned Sample (Reference Temperature: 21.1ºC)

As seen in Figure 2.3, the master curves for the three mixtures (unconditioned) at three aging level are plotted. In general, HR aged five days shows the highest |E*|, while HMA aged two hours shows the lowest |E*|at the high reduced frequencies area (low testing temperature area) and WR aged four hours shows the lowest |E*|at the low reduced frequencies area (high testing temperature area). The difference among the HR master curves is larger than WR curves, which indicates WR reduced the effect of aging on modulus. In addition, the curves of the three mixtures at five days aging level tend to be closer than at the other two aging levels. This result indicates all three mixtures show similar long term rutting resistance.

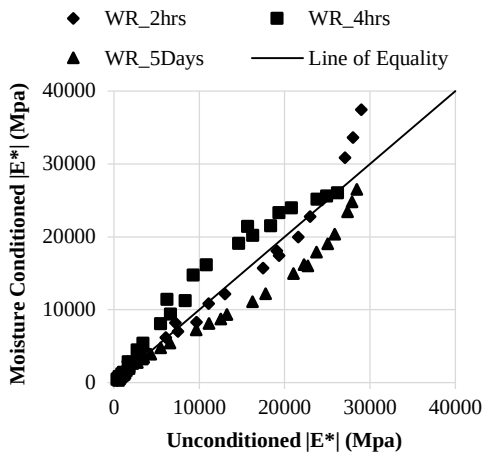

(a) WR

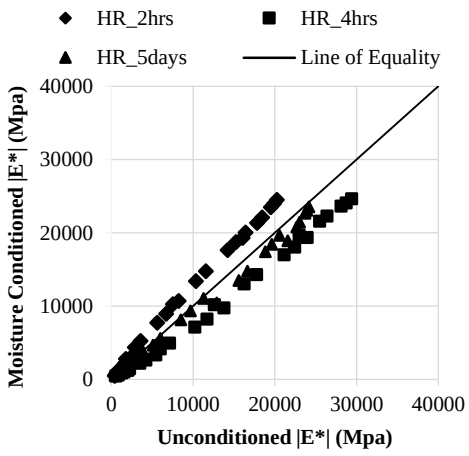

(b) HR

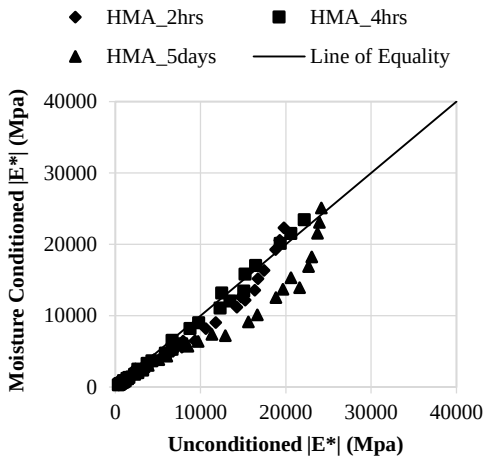

(c) HMA

Figure 2.4 |E*| Comparison for HMA (Moisture Condition vs. Unconditioned)

To look at the effect of moisture on |E*|, the entire |E*|values under moisture conditioned versus unconditioned are plotted as seen in Figure 2.4. If the points under the line of equality, it means that the modulus decreases after moisture condition. Otherwise, the modulus increases after the moisture condition. As seen in Figure 2.5 (a), the three levels of aging are considered for WR, the |E*| points of the sample under a normal two hours aging are closest to perfect line, which means the modulus does not change much because of the moisture condition. Four hours short term aging increases the modulus, while five days' long term aging decrease the modulus. HMA has the similar trend as WR does. HR shows different trends, moisture condition affect the |E*|

of HR at five days aging the least, |E*| increases after condition for two hours aging sample and reduces for four hours aging sample.

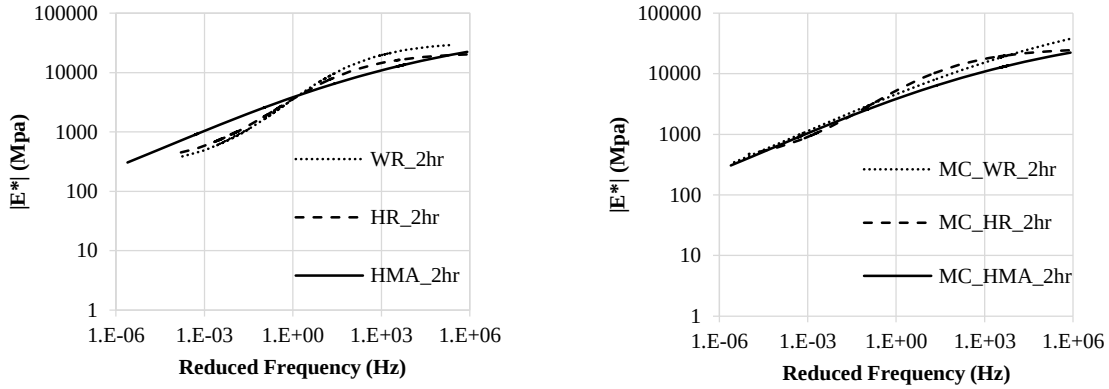

(a) Unconditioned (b) Moisture conditioned

Figure 2.5 Master Curve at Aging Level Two Hours (Reference Temperature: 21.1ºC)

Another difference between unconditioned and moisture conditioned samples is the shape of the master curve changed because of the moisture conditioning. In Figure 2.5 (a), the curves have well defined inflection points; the slope of the curves is lower as the distance increases from the inflection points. The curves for moisture conditioned samples don't contain these two inflection points, which indicate that the mixtures become stiffer more quickly faster as temperature decreases.

To investigate the significance of effects of mix type, aging, and moisture on dynamic modulus, ANOVA was performed. The p-value was calculated considering factor of mix type, aging, and moisture for the modulus at each temperature and frequency. As shown in Table 2.2, there are only 8 p-values out of 180(combination of five temperatures, six frequencies, three factors) are lower than 0.05. They are p-values of mixture type at -10ºC for all six frequencies, and moisture at -10 ºC for 25Hz and 0.5Hz. In other words, Warm mix and RAP make significant difference in

modulus at -10 ºC for all frequencies; moisture impacts the modulus at -10 ºC for 25Hz and 0.5Hz. The warm mix and RAP usage didn't impact the stiffness at higher temperatures, also, the effect of aging and moisture showed no significant different (95% confidence) at almost all temperatures and frequencies with two exceptions (moisture at -10 ºC, 25Hz and 5Hz) compare to HMA. The full ANOVA tables for all factors are attached in the appendix A.

Table 2.2 Analysis of Variance of |E*|

Temp (°C)	Frequency (Hz)	p-value		
		Mix type	Aging	Moisture
-10	25	0.020	0.567	0.044
	10	0.024	0.389	0.133
	5	0.022	0.368	0.097
	1	0.011	0.258	0.088
	0.5	0.006	0.339	0.034
	0.1	0.007	0.199	0.058
4	25	0.158	0.350	0.486
	10	0.190	0.408	0.702
	5	0.162	0.345	0.712
	1	0.153	0.346	0.870
	0.5	0.136	0.203	0.706
	0.1	0.124	0.139	0.712
21	25	0.066	0.754	0.118
	10	0.317	0.247	0.975
	5	0.372	0.232	0.939
	1	0.469	0.202	0.853
	0.5	0.455	0.176	0.902
	0.1	0.582	0.111	0.694
37	25	0.366	0.223	0.087
	10	0.663	0.295	0.106
	5	0.428	0.234	0.179
	1	0.392	0.199	0.251
	0.5	0.390	0.217	0.267
	0.1	0.362	0.181	0.365
54	25	0.109	0.174	0.366
	10	0.197	0.220	0.599
	5	0.221	0.251	0.705
	1	0.247	0.237	0.878
	0.5	0.225	0.263	0.561
	0.1	0.327	0.328	0.474

2.6 Summary and chapter conclusion

This preliminary research investigated the behavior of asphalt concrete materials in the perspective of fracture energy and dynamic modulus. Three different types of asphalt concrete mixtures were investigated: Hot Mix Asphalt without Recycled Asphalt Pavement (RAP), Hot Mix Asphalt with 25% RAP, and Warm Mix Asphalt with 25% RAP. After processing the RAP, mix designs were performed on the three mixtures. These mixtures, moisture conditioning, and aging procedures, were evaluated by fracture energy and dynamic modulus, the following conclusions were made:

- The Warm Mix Asphalt with RAP mixture performed very similar to the Hot Mix Asphalt with RAP mixture in terms of fracture according to the results of fracture energy from SC(B) test, but at mixing and compacting temperatures 30°C lower. It is expected that lower mixing and compacting temperature results in a lower aging and further higher fracture energy. But this didn't happen to fracture energy, which indicates that fracture energy didn't differentiate the cracking resistance performance of material of HMA, HR and WR.
- SC(B) fracture tests performed at -12°C (both conditioned and unconditioned) and the moisture conditioned samples at -12°C as expected, with decreasing fracture energy as more aging was applied. However, the -24°C unconditioned samples had large variability and did not follow logical trends. WR and HR performs similarly based on statistical analysis, even WR has 0.46% lower binder content than HR.
- Moisture conditioned samples tended to have flatter dynamic modulus master curves, indicating that they become stiffer more quickly as temperature decreases versus unconditioned samples.

- After long term aging, it appears that all three asphalt concrete mixtures perform in a similar manner in dynamic modulus.
- The statistical analysis shows that WMA and RAP application result in a significant different dynamic modulus at -10°C, but no significant difference at higher temperature. The effect of aging and moisture has no significant difference on WMA and WR compare to HMA.

After this fracture energy research, it is true that fracture energy does give an evaluation of the asphalt concrete as concluded above. Fracture energy in this study didn't differentiate the crack resistance capability of the three types of mixture. In addition, it didn't give information about the crack initiation and prorogation, and effects of the moisture and aging on them. In next chapter, a preliminary R-Curve method will be applied on the same raw data from the same test matrix to discover the information that fracture energy cannot provide. It is expected that R-Curve can provide more detailed crack resistance characterization and quantification of asphalt concrete.

2.7 Reference

American Association of State Highway and Transportation Officials."Mixture Conditioning of Hot Mix Asphalt (Hma)." Washington, D.C.: American Association of State Highway and Transportation Officials.

American Association of State Highway and Transportation Officials. "Standard Method of Test for Resistance of Compacted Asphalt Mixtures to Moisture-Induced Damage." Washington D.C.: American Association of State Highway and Transportation Officials.

Chapter 3 Preliminary R-Curve Research*[2]

3.1 Background of preliminary R-Curve research

Thermal and reflective cracking are two common types of cracking (Dave et al., 2011). Both of types of cracking need initiate from dislocation where stress concentrate on: defect for thermal cracking and joint for reflective cracking. Traditional cracking tests, for example, the Superpave Indirect Tension test (IDT) does not represent the crack propagation and post-peak behavior (Li and Marasteanu, 2010), as there is no stress intensity isolation in the bulk of the material. However, recent research has used the concept of fracture energy as an evaluation of the thermal and reflective cracking of asphalt pavement. The fracture energy is captured from the different fracture test configurations all have a notch in common. The most common fracture tests found in literature are: Semi-Circular Bend [SC(B)] (Li and Marasteanu, 2004), Disc-Shaped Compact Tension Test [DC(T)] (Wagoner *et al.*, 2005), and Single Edge notched Beam [SE(B)] (Mobasher, 1997). However, there is a disadvantage of these test configurations. The loading head pushing on the specimen can cause the localized deformation which may lead to the inaccuracy and inconsistency of the test results. University of Florida developed Dog-Bone Direct Tension (DBDR) test configuration, which can solve this problem. Also there is not a notch in DBDT configuration, the strain at the failure cross section are more determined by the actual failure plane and the measurement of fracture energy is less affect by the micro-damage. (Koh and Roque, 2010). Despite the disadvantage of notched-specimen, these tests configuration has one pre-cut notch on the specimen can lead to concentration of the stress at the notch tip and

2* The major work in this chapter was an article: Shu Yang, and Andrew Braham. "R-Curves Characterisation Analysis for Asphalt Concrete", International Journal of Pavement Engineering:1-10., 2016

initiate the crack start from the notch tip. In other words, the crack initiation and propagation can be expected in an under control range, and the crack initiation can be controlled from the notch rather than random defects. Fracture energy is at least a combination of two energies: the energy of both initiating a crack and propagating a crack. Therefore, when fracture energy is reported as a single number, there is no specific information on the behavior of the crack initiation and propagation. Reporting a single number may be too general and could mask important differences between asphalt concrete mixtures. A potential complementary alternative to fracture energy is the Resistance Curve, or R-Curves. R-Curves graphically show the cumulative fracture energy versus crack extension. Technically, if crack extension can be captured in a fracture test, the R-Curve method can be used to analyze the same fracture behavior.

As found in literature, R-Curve have been successfully used in a few fields that gain interests to application in asphalt concrete: steel (Tanaka and Harrison, 1978), polymer (Schmit et al., 1990), and composite (Fleck et al., 1996). Steel, polymer and composite are all different materials where fracture behavior is an important characteristic, but R-Curve can be successfully applied on all these different materials. In many industries, testing of material can be expensive due to the size of the specimen. However, if the testing is geometry dependent, the specimen needs to be thick to have plane strain status in testing to mimic the field condition. Haynes and Gangloff (1997) used R-Curve for small and thin aluminum alloy specimen, and compared with the R-Curve from large to middle specimen. It is found that the R-Curve results from thin specimen is still reasonable, which can improve the efficiency of the testing. Based on the investigation of aluminum alloy, Nesphor(1987) also claimed that R-Curve is dependent on the type and loading, the width of specimen, the ratio of the initial length of notch to specimen

width. This invariant characteristic benefited the testing of material with given test condition. Fett *et al.* (2000) also concluded that R-Curve can be the true material property for small crack extensions.

As R-Curve is a function of resistance to crack extension, it is often applied as the prediction of residual strength of metal. Wu and Wilson (1997) suggest that R-Curve is suitable approach for damage tolerance analysis in certain laminated materials. Cracking is usually a complicated process in many materials; R-Curve was reported to give information of the characterization of the cracking. For example, there are two stages in Portland Cement Concrete: deceleration stage and acceleration stage. Brake *et al.* (2012) captured the first stage that was neglected in normal Portland Cement Concrete testing. Lach *et al.* (2005) reported R-Curve can be used to describe the steady-state stable crack propagation in polymer as a three-phase kinetic phenomenon: crack tip blunting or crack initiation, non-stationary stable crack growth, and steady-state stable crack growth. In some cases, crack occurs in an instable manner. The initiation can be important in these cases. R-Curve has the capability to quantify the initiation of instability cracking. Sundaresan and Nageswara (2014) used R-Curve to evaluate the life expectancy of aerospace press vessels at the initiation of instability cracking. In addition, R-Curve can characterize both slow crack propagation (Suzuki, *et al*., 1995), and instantaneous crack propagation (Kim *et al*., 2005).

The application of R-Curve has been found to be powerful to solve mechanical and engineering problems for many other materials. Bertram and Kalthoff (2003) used R-Curve to study the crack propagation in rock, and it was found that the energy dissipated in crack propagation can be two

orders of magnitude larger than crack initiation. Fett *et al.* (2000) concluded that R-Curve for small crack extensions can be considered as a true material property. Wu and Wilson (1997) applied the concept of R-Curve to predict the residual strength of metal-matrix laminated panels, and it was found that R-curve was independent of the initial notch length and specimen thickness for aluminum alloy. Shah *et al.* (2009) evaluated fracture resistance of resin-based composite by using R-Curve, and use the R-Curve shape change explain the strength increment due to post-cure heat treatment of the dental composites. Du *et al.* (1999) used R-Curve to investigate the evolution of the process zone in rubber modified epoxy polymer. Therefore, this research looks to apply the of R-Curve method to quantify and characterize asphalt concrete cracking. Asphalt concrete is a composite (asphalt binder, rock, and air) and it has similar rheological characteristics as polymer, so R-Curve may have the potential to be able to provide similar benefits as the material discussed above to understand cracking behavior.

There is one research found using R-Curve on asphalt concrete to characterize the crack propagation, Ghafari and Nejad (2015) constructed R-Curve in asphalt concrete by using SE(B) test to characterize the crack propagation. Image analysis is used to capture the crack extension. It is claimed that crack extension form image analysis can be an alternative of compliance method. The critical crack length at crack propagation instability was found to be highly related to testing temperature. The critical crack length decreases as the testing temperature decreases.

In chapter two, fracture energy from SC(B) fracture test was investigated to quantify the crack resistance of three types of asphalt concrete at multiple aging levels and moisture conditions. Although there are advantages to use fracture energy, it did not give any information of crack

initiation and propagation. But stress intensity isolation (or notch) in fracture test supplies with the potential to evaluate crack initiation and propagation. The R-curve considers the crack resistance as a function of crack extension, which includes initiation and propagation. When performing the SC(B) fracture test discussed in chapter two, the crack growth of the fracture test was recorded by taking digital images of the specimen surface. Thus, R-Curve can be used to analyze the same fracture test matrix in chapter two: three asphalt concrete mixtures, including hot mix, hot mix with RAP, and warm mix with RAP were tested at two testing temperatures (-12°C and -24°C), three levels of aging (none aged, short term aged, and long term aged), and two levels of moisture condition (non-conditioned and moisture conditioned) by SC(B) fracture test. In this preliminary R-Curve study, it is found that the information of crack initiation and propagation can be captured.

3.2 Chapter objective

As a preliminary research, this chapter is introducing to extract crack initiation and crack propagation of asphalt concrete utilizing R-Curves method. This will be accomplished by applying the R-Curve method on the same experimental matrix in chapter two: asphalt concrete mixture types, two testing temperatures, moisture conditioning, and three levels of aging. The effects of mixture type, aging, and moisture condition on fracture resistance are expected to be seen by using R-Curve method.

3.3 Test materials

In order to discover the advantage of R-Curve method compare to fracture energy method, the test materials in this chapter is identical as the test material used in chapter two: Hot Mix Asphalt

without RAP (HMA), Hot Mix Asphalt with 25% RAP (HR), and WMA with 25% RAP (WR). The WMA utilized a chemical technology at 0.5% by weight of binder. The asphalt binder used in this study was a SBS modified PG 76-22 binder. The binder content in the RAP was determined to be 4.41% by taking the average of ignition oven and solvent extraction test. The total binder content for WR and HR incorporated this asphalt cement into the optimal asphalt cement content used in the specimens fabricated in the lab. The R-Curve analysis in this chapter is based on the same raw fracture test data in chapter two plus the image data. Thus, the factors of moisture condition and aging are the same in the experimental matrix.

3.4 Test methods

The SC(B) test configuration was introduced in chapter two. In order to have the crack extension to construct R-Curve, an industrial digital camera was used during testing to capture the crack growth on one side surface of the SC(B) specimen, the camera capture the image of the specimen surface at a rate of 0.2 frame per second, the images are 8-bit gray scale, and 18 megapixels in resolution.

3.5 Results and discussion

R-Curve tracks the energy dissipation history in the cracking process, so one potential application of R-Curve in asphalt concrete is the ability to characterize crack initiation and propagation. Two parameters were extracted from the R-Curves: cohesive energy and energy rate, which quantify crack initiation and propagation respectively. Figure 3.1 shows a typical R-Curve from asphalt concrete materials.

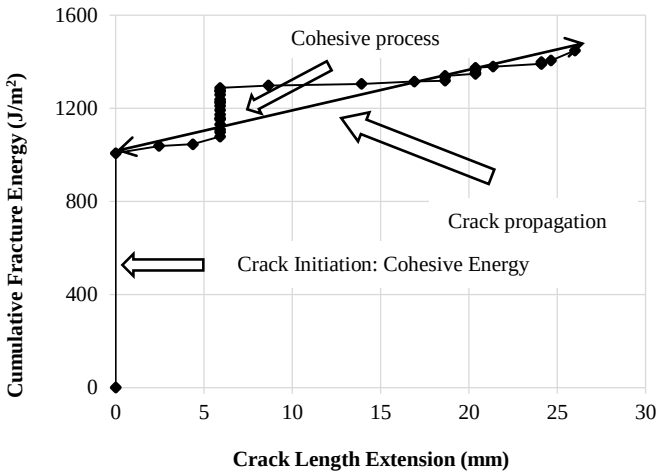

Figure 3.1 Typical R-Curve from Asphalt Concrete

As can be seen in the typical R-Curve of asphalt concrete in Figure 3.1, as the crack grew, more fracture energy was dissipated in the cracking process. There were a couple of common characterizations for all of the R-Curves constructed for asphalt concrete. First, there was always a vertical straight line at the beginning of the cracking procedure. This straight line indicated that there was no crack detected by image analysis the beginning of SC(B) test. During this stage of cracking, energy was dissipated throughout the specimen. In other words, the energy dissipated in the specimen didn't create a visible crack during this stage, which is termed the crack initiation stage. The energy consumed in this initiation stage processes can be defined as the cohesive energy, and is quantified by reading the maximum value of the vertical straight line of the R-Curve. Second, after the initiation stage, the crack grows as more energy consumed, which was defined as the propagation stage. Theoretically, the shape of R-Curve can be classified in two groups. The first group, when the R-Curve has a slope of zero, the material has brittle cracking behavior. However, the second group, when the R-Curve gradually increases, the material has ductile cracking behavior (Anderson, 2005). With asphalt concrete the propagation stage of the R-Curve for asphalt concrete was not consistently flat (brittle) or

gradually increasing (ductile). It was observed that there often was a localized vertical straight line in the propagation stage, which indicated that an additional area of the specimen experienced crack initiation without crack growth. Therefore, the traditional thought process of a single cohesive zone starting at crack initiation followed by pure crack growth may not be accurate, and cracks may experience more than one cohesive event with the crack growth. This phenomenon is also shown in Figure 3.1.

In order to characterize the general resistance of crack growth during the propagation stage, an energy rate was developed and is defined in Equation 3.1. Energy rates approaching zero indicate slopes approaching zero, or a brittle failure. However, as the energy rate increased, the cracking of the asphalt concrete is more ductile in nature.

$$\textbf{Energy Rate} = \frac{\textbf{Fracture Energy} - \textbf{Cohesive Energy}}{\textbf{Crarck Extention}} \qquad \textbf{Equation 3.1}$$

Where,

Energy rate – unit energy consumed in crack propagation stage, J/m^3,

Fracture energy - the energy consumed in both crack initiation stage and propagation stage, J/m^2,

Cohesive energy - the energy consumed in crack initiation stage, can be found in the R-Curve as the vertical axis reading of the top end of the vertical straight line, J/m^2, and

Crack extension - the crack length on one surface side of SC(B) specimen by image analysis, mm.

In order to characterize the initiation and propagation behavior in asphalt concrete, R-Curves were constructed for all of the mixtures shown in Table 3.1. The fracture energy was calculated traditionally (the area under the load/LLD curve divided by the area of the ligament), cohesive

energy, and energy rate were extracted from each R-Curve and are summarized in Table 3.2. The coefficient of the variance (COV) for fracture energy in the test results varied from 0.6% to 67.0%. An analysis of variance (ANOVA) was performed to determine that if the testing conditions (included mixture type, moisture condition, testing temperature, age) significantly affect the variance. The ANOVA results as shown indicated that none of the testing condition affected the COV significantly. In other words, the variance of the testing results tended to be from the heterogeneous of the material rather than the testing conditions.

Figure 3.2 shows two sets of example R-Curves. In Figure 3.2(a), three replicates are shown for Hot Mix Asphalt (HMA), tested at -12°C, with moisture conditioning, and two hours aging, while Figure 3.2(b) shows the influence of aging by examining three replicates of two hours aging (no aging), four hour aging (short), and 120 hour aging (long).

Table 3.1 Experimental Matrix for Chapter 3

Factors	**Number of levels**	**Level**
Mixture Type	3	• Hot Mix Asphalt (HMA) • Hot Mix Asphalt with 25% RAP (HR) • Warm Mix Asphalt with 25% RAP (WR)
Testing Temperature	2	• -12°C • -24°C
Moisture Conditioning	2	• Unconditioned • Conditioned
Aging	3	• Unaged • Short term • Long term

Table 3.2 Summary of Chapter 3's Test Results

Mix	Condition	Temp (°C)	Age	Fracture Energy	COV	Cohesive Energy	COV	Energy Rate
				(J/m^2)	(%)	(J/m^2)	(%)	(J/m^3)
HMA	Unconditioned	-12	2hours	1583.3	10.3	650.1	28.6	24.4
			4hours	1638.4	4.8	851.9	9.5	29.9
			5days	961.2	32.1	760.6	38.1	6.1
		-24	2hours	772.5	6.6	545.9	43.6	6.1
			4hours	778.4	10.1	636.3	14.2	6.3
			5days	432.8	49.3	383.7	48.5	1.6
	Conditioned	-12	2hours	1171.2	36.1	789.7	41.6	11.1
			4hours	871.4	23.1	555.5	36.9	8.6
			5days	813.3	12.0	625.7	7.3	5.5
		-24	2hours	1002.8	-	966.0	-	3.1
			4hours	977.6	45.3	794.1	45.6	5.1
			5days	731.2	21.9	652.7	26.1	2.1
HR	Unconditioned	-12	2hours	1334.6	17.7	655.6	33.7	29.3
			4hours	910.6	2.4	596.0	42.6	7.7
			5days	798.9	25.4	725.9	22.7	2.1
		-24	2hours	1113.2	12.9	845.4	71.5	7.1
			4hours	554.7	0.7	390.8	0.8	4.1
			5days	1507.6	67.0	537.9	23.7	18.5
	Conditioned	-12	2hours	1117.0	29.8	1031.8	35.7	2.0
			4hours	1092.2	57.2	867.2	86.2	6.3
			5days	779.5	10.1	690.1	22.5	2.4
		-24	2hours	644.4	19.5	452.7	48.1	5.2
			4hours	578.5	30.5	525.8	24.0	1.3
			5days	631.0	29.8	488.8	40.2	3.5
WR	Unconditioned	-12	2hours	1036.6	5.5	525.0	20.7	18.0
			4hours	1031.6	4.2	876.9	9.0	3.8
			5days	867.8	35.2	775.7	37.4	2.5
		-24	2hours	1219.6	6.4	1005.6	24.7	8.4
			4hours	618.5	19.4	460.5	15.5	4.7
			5days	1363.0	54.3	815.5	48.2	15.2
	Conditioned	-12	2hours	1101.4	13.0	832.8	19.1	7.3
			4hours	1187.6	17.4	915.3	5.0	7.3
			5days	769.2	14.5	596.0	35.4	4.9
		-24	2hours	552.2	25.7	479.9	50.6	1.9
			4hours	527.1	56.9	459.3	78.1	1.6
			5days	938.9	0.6	854.9	14.6	2.8

In Figure 3.2(a), two trends immediately appeared. First, there was a relatively large spread of cohesive energy, with values ranging from 400-1000 J/m^2. This large spread could indicate one of two things. First, cohesive energy as captured in this analysis was not precise enough to glean any useful information. However, an alternative explanation was that by only testing three samples, if one data point was an outlier, it would not be identifiable. While large factorial designs such as the one presented in this paper were interesting, they inherently reduce the number of replicates that are available in order to try and keep total number of tests under control. The second trend was that the slopes of the R-Curves, or the energy rate, appeared to be similar for all three replicates. This indicated that after the crack has formed and is propagating, the extension is relatively consistent.

In Figure 3.2(b), cohesive energy trends were matched expectations, with cohesive energy decreasing as the aging increased. As a material ages, it was expected that they cohesive nature of the material would deteriorate. However, the energy rates were not consistent, as the short term aging showed more brittle behavior versus no aging and the long term aging, it was expected that the energy rate would decrease as the aging time increased. However, Figure 3.2 contains only two sets of data. To fully explore the trends of the effects of mixture type, testing temperature, moisture condition, and aging on the crack initiation and propagation characterization, lines of equality were utilized and are shown in Figures 3.3-3.7.

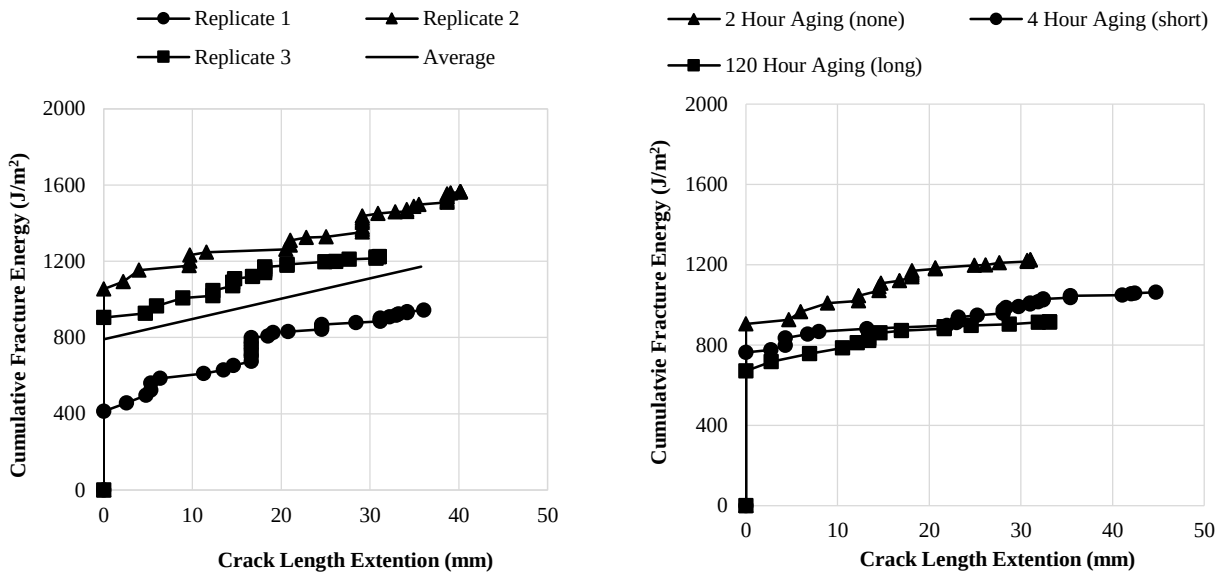

(a) (b)

Figure 3.2 Example R-Curves for HMA: (a) Three Replicates for HMA; (b) Three Levels of Aging for HMA Moisture Condition, -12°C

3.5.1 Effects of testing temperature

As seen in Figure 3.2 (a), the majority of data points fell above the line of equality, indicating that lower temperatures result in lower fracture energy for HMA and HR. This is reasonable as it was expected that lower temperatures create a more brittle (or elastic) material, decreasing the amount of energy that the HMA and HR mixtures absorb. The trend is not as clear, however, with the WR mixture, as the data points fell both above and below the line of equality.

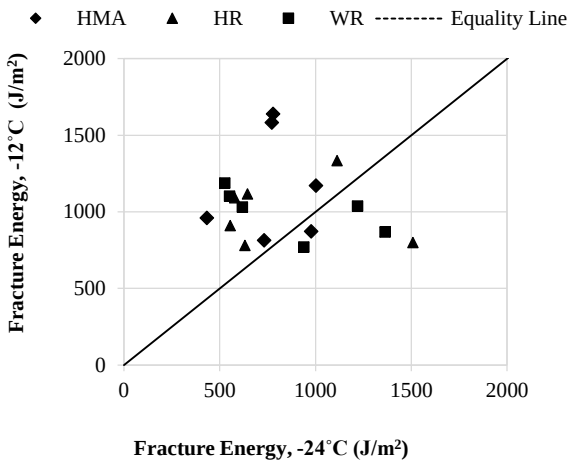

(a) Fracture energy

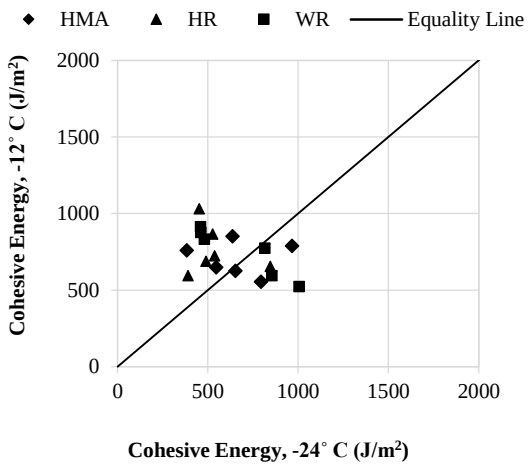

(b) Cohesive energy

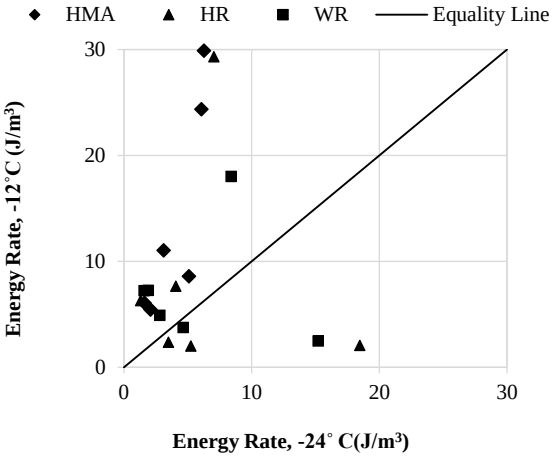

(c) Energy rate

Figure 3.3 Effects of Testing Temperature

As seen in Figure 3.2(b), the effects of testing temperature on cohesive energy were not clear, as the data did not show any clear trends around the line of equality. However, when Figure 3.2(a) and Figure 3.2(b) were compared, the data points for cohesive energy were more tightly clustered at the range of approximately 400 to 1000 J/m^2, despite the difference in temperature, whereas the fracture energy was spread over a larger range, approximately 600 to 1500 1000 J/m^2. This trend was also seen in Figures 3.3-3.5, which indicated that cohesive energy was less sensitive than fracture energy to testing temperature, moisture conditioning, and aging.

Therefore, there is a possibility that crack initiation may not be as effected by temperature, moisture conditioning, aging as crack propagation. However, this potential phenomenon should be explored in more detail in future work.

As seen in Figure 2(c), lower testing temperature leads to lower energy rate for all the HMA mixtures and most of the WR mixtures. This demonstrates that higher testing temperatures created more ductile cracking behavior, which aligns with previous fracture research findings (Braham et al., 2008). However, this trend was not as clear with HR, indicating that perhaps the addition of RAP to HMA influenced ductile versus brittle cracking behavior.

3.5.2 Effects of moisture conditioning

As can be seen in Figure 3.4, the effect of moisture condition on fracture energy was not consistent for HMA, HR, or WR mixtures. One potential reason might be that testing temperature, aging levels, and moisture conditioning interacted with each other, and moisture conditioning was not a strong enough factor to impact the fracture energy (Yang and Braham, 2015). The effect of moisture conditioning on cohesive energy was similar to fracture energy, there was no clear trend found.

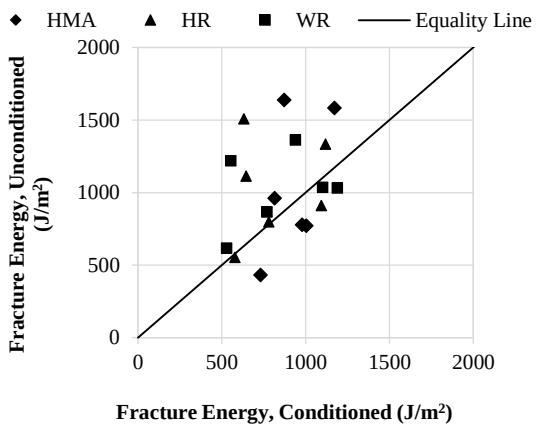

(a) Fracture energy

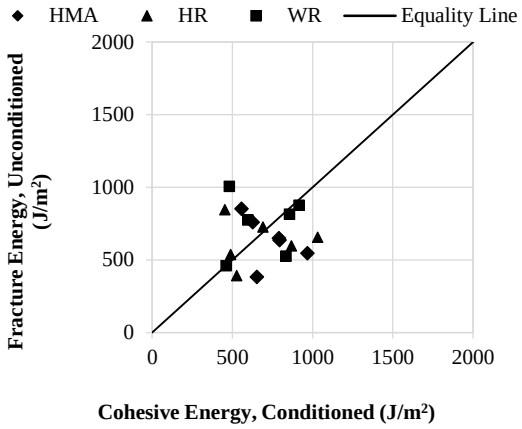

(b) Cohesive energy

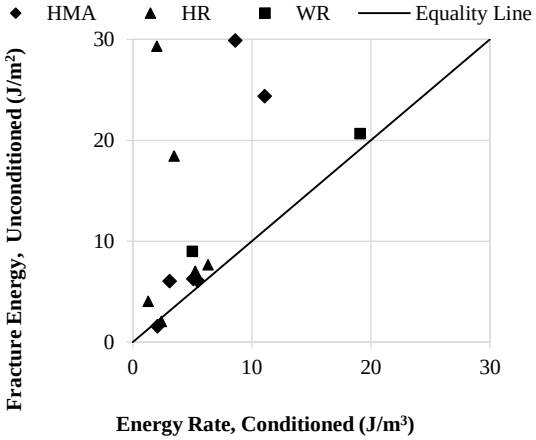

(c) Energy Rate

Figure 3.4 Effects of Moisture Conditioning

The effect of moisture condition on energy rate was clear; almost all the data points were above the line of equality, which means that after the crack initiation, it took less energy to grow a unit crack length for moisture conditioned specimens and the crack was more brittle in nature. For WR, the effect of moisture conditioning on energy rate was clear despite the different mixture type, aging, and test temperature.

3.5.3 Effects of short term aging

As illustrated in Figure 3.5, short term aging resulted in lower fracture energy for all three types of mixtures, but didn't necessarily lead to lower cohesive energy for all three mixtures. This again highlights that the energy required to initiate the crack, the cohesive energy, may not be as dependent on short term aging, while the energy required to propagate the crack is more dependent on short term aging. Finally, in general, short term aging resulted in lower energy, confirming previous fracture research that indicated aging increased the brittle behavior of asphalt concrete mixtures (Braham *et al.*, 2009).

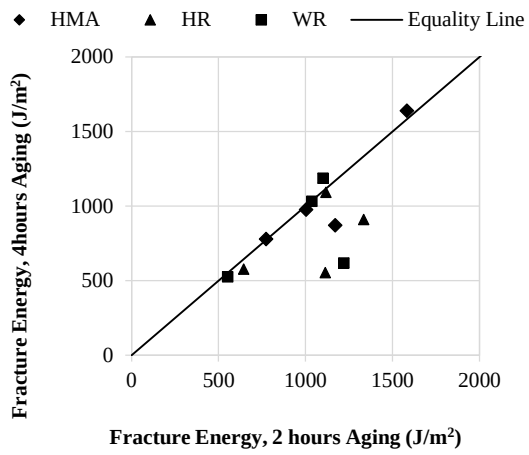

(a) Fracture energy

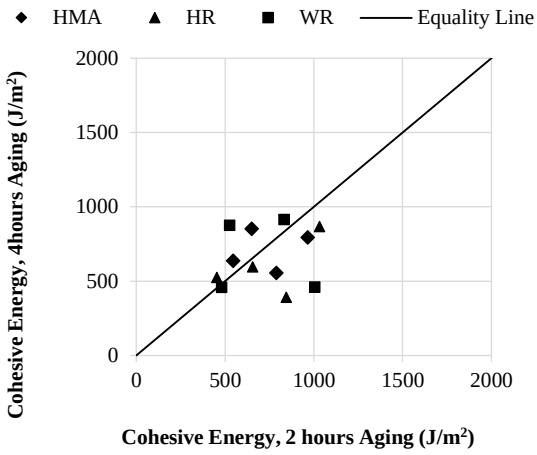

(b) Cohesive energy

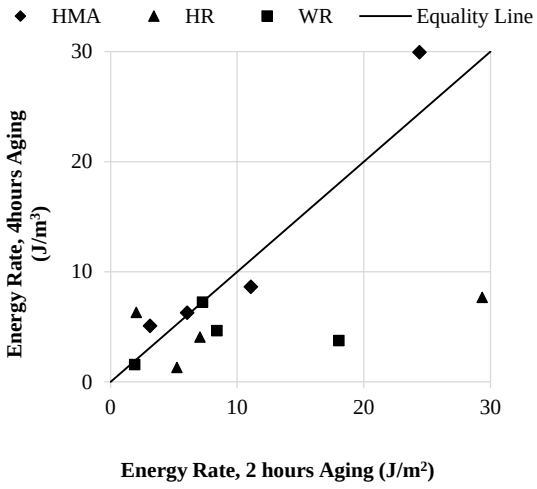

(c) Energy Rate

Figure 3.5 Effects of Short Term Aging

3.5.4 Effects of long term aging

As shown in Figure 3.6, long term aging led to lower fracture energy for HMA, which continued the aging trend found in the short term aging. However, this trend wasn't found for HR and WR, showing that perhaps the addition of RAP to mixtures affects the overall cracking characteristics of asphalt concrete. The effects of long term aging on cohesive energy fell on both sides of the line of equality, but most points fell below the line. As discussed above, however, the range of fracture energy was much tighter for cohesive energy versus the fracture energy, indicating that

long term aging may have less influence on the crack initiation versus the crack propagation. Finally, in general, long term aging lowered the energy rate. Specifically, all of the data points for HMA were below the line of equality, which demonstrated that the crack propagation consumed less energy when long term aged and the mixture was more brittle. In general, long term aging reduced the fracture energy, cohesive energy, and energy rate, which means that long term aging not only impacted the crack initiation, but also affected the crack propagation. It should be mentioned that both HR and WR used lab processed RAP. The RAP was processed by first freezing, then running through a lab-scale jaw crusher. Most RAP used in pavements goes through field scale crushing, so the use of lab-scale crushing may have introduced a significant factor that overshadowed the other factors. This was bolstered by the fact that the HMA mixtures usually showed a clearer trend.

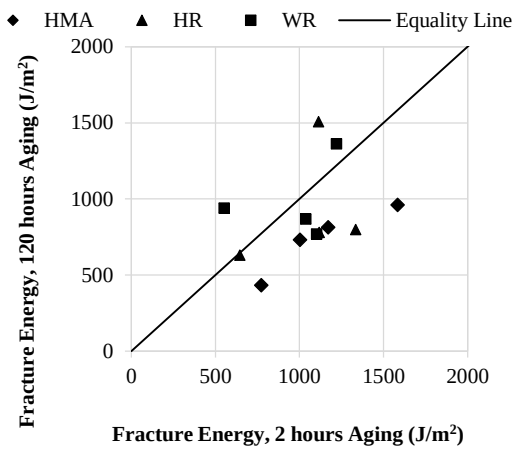

(a) Fracture energy

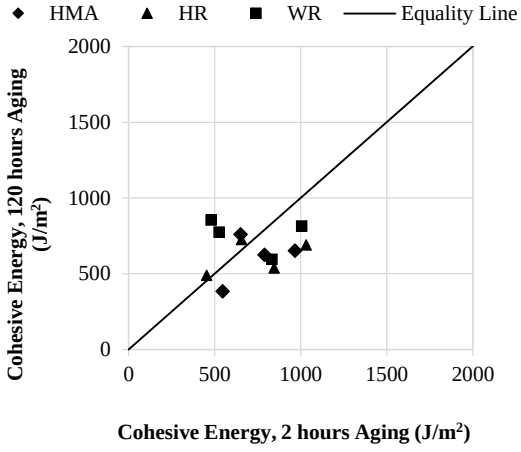

(b) Cohesive energy

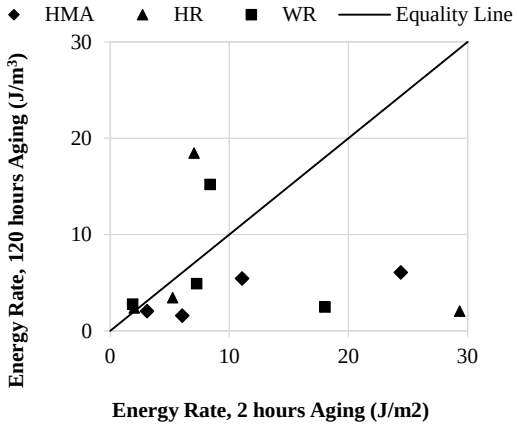

(c) Energy Rate

Figure 3.6 Effects of Long Term Aging

3.5.5 Statistical analysis

In order to test the hypothesis whether the mixture type, aging, condition and testing temperature was statistically significant with a 95% confidence on fracture energy, cohesive energy, and energy rate, an analysis of variance (ANOVA) were performed. The p-value results were shown in Table 3.3. It could be found that there are three p-values under 0.05. This indicates that three cases, effect of testing temperature on fracture energy, effect of testing temperature on energy rate, and effect of moisture condition on energy rate. This statistical analysis proved that

cohesive energy and energy rate are important complementary of fracture energy. For example, the moisture condition only impacted the energy rate, but it didn't impact the fracture energy and cohesive energy. None of the factors significantly impacted on cohesive energy, this results agreed that a narrow range of cohesive energy indicated cohesive energy is less sensitive to all factors. The full ANOVA tables are attached in Appendix B.

Table 3.3 P-value Summary of ANOVA for Fracture Energy, Cohesive Energy and Energy Rate

P-value	Fracture Energy	Cohesive Energy	Energy Rate
Mix Type	0.8763	0.6742	0.6150
Aging	0.2658	0.5369	0.2165
Moisture	0.0803	0.6220	0.0073
Temperature	0.0201	0.0711	0.0494

3.6 Summary and chapter conclusion

This preliminary R-Curve investigation of asphalt concrete constructed the R-Curve by using the SC(B) fracture test data to analyze the crack resistance of asphalt concrete. The initiation parameter cohesive energy, and the propagation parameter energy rate, were extracted from the R-Curves. It is found that cohesive energy was always in a narrower range (approximately 500-1000 J/m^2) compared to the fracture energy range (approximately 500-1700 J/m^2) over all combinations of aging and moisture conditions. The results of energy rate indicated that moisture and short term aging impact the crack propagation by reducing the resistance of crack growth. These results proved that R-Curves is a potentially useful tool to quantify the cracking resistance of asphalt concrete in both crack initiation and propagation. Three mixture included HMA, HMA with RAP and WMA with RAP were tested at two temperatures, -12°C, -24°C, three levels of aging (none aged, short term aged and long term aged), and two levels of moisture condition (none conditioned, and moisture conditioned). Fracture energy, cohesive energy and energy rate

were analyzed to evaluate the crack resistance of the three mixtures. The effects of aging and moisture condition on crack initiation and propagation were studied. In summary, the following conclusions can be made based on the test results analysis:

- Lower testing temperature leads to a lower energy rate for HMA and WR, this wasn't found in HR, which indicates that RAP may reduce the resistance to crack propagation but Warm mix could improve this propagation resistance when using RAP.
- Moisture condition does not impact the crack initiation but reduce the ability to resist crack propagation.
- Short term aging has the similar trend as moisture, it does not impact the ability to resist crack initiation but reduce the resistance to crack growth.
- The long term aging reduces the general fracture energy, cohesive energy and energy rate, in other words, it decreases the ability to resist cracking both in crack initiation and propagation.
- The R-Curve analyzed results and the statistical result proved that R-Curve is effective tool that can characterize the cracking behavior in asphalt concrete in both crack initiation and propagation.

This preliminary research of R-Curve proved that R-Curves rather than fracture energy gives more information of the quantification and characterization of the fracture resistance of asphalt concrete. R-Curves can potentially characterize the crack resistance in terms of crack imitation and propagation. However, the results of cohesive energy indicated it is not sensitive to temperature, aging, and moisture. The cohesive energy need to be further studied. The next chapter will discuss the further in depth research in R-Curve of asphalt concrete, a more effective

viable control need to be performed to differentiate the characterization of R-Curve, as the usage of RAP may result in high variation in test result which may hide the trend of the R-Curve. In addition, in this preliminary R-Curve study, it is realized in the image process that crack extension as one out of two components in R-Curve, need a further investigation. Due to the complexity of the crack pattern and the of the heterogeneous characterization of asphalt concrete, crack length as the normal crack quantification might not be adequate to fully characterize the crack growth. The crack extension will be defined more than a crack length in next chapter.

3.7 Reference

Anderson, Ted L., and T. L. Anderson. *Fracture Mechanics: Fundamentals and Applications*. CRC press, 2005.

Bertram, A., and J. F. Kalthoff. "Crack Propagation Toughness of Rock for the Range of Low to Very High Crack Speeds." Paper presented at the Advances in Fracture and Damage Mechanics, September 2, 2003 - September 4, 2003, Paderborn, Germany, 2003.

Brake, Nicholas Andres, and Karim Chatti. "Prediction of Transient and Steady-State Flexural Fatigue Crack Propagation in Concrete Using a Cyclic R-Curve." *Journal of Engineering Mechanics* 138, no. 4 (2012): 371-78.

Dave, Eshan V., Behzad Behnia, Sarfraz Ahmed, William G. Buttlar, and Henrique Reis. "Low Temperature Fracture Evaluation of Asphalt Mixtures Using Mechanical Testing and Acoustic Emissions Techniques." Paper presented at the Asphalt Paving Technology 2011, AAPT, March 27, 2011 - March 30, 2011, Tampa, FL, United states, 2011.

Du, J., M. D. Thouless, and A. F. Yee. "Development of a Process Zone in Rubber-Modified Epoxy Polymers." *International Journal of Fracture* 92, no. 3 (1999): 271-85.

Fett, T., D. Munz, R. D. Geraghty, and K. W. White. "Bridging Stress Determination by Evaluation of the R-Curve." *Journal of the European Ceramic Society* 20, no. 12 (2000): 2143-48.

Fett, T., D. "Influence of Specimen Geometry and Relative Crack Size on the R-Curve." *Engineering Fracture Mechanics* 66, no. 4 (2000): 375-86.

Fleck, N. A., M. P. F. Sutcliffe, S. Sivashanker, and X. J. Xin. "Compressive R-Curve of a Carbon Fibre-Epoxy Matrix Composite." *Composites Part B: Engineering* 27, no. 6 (1996): 531-41.

Ghafari, Sepehr, and Fereidoon Moghadas Nejad. "R-Curve Behavior and Crack Propagation Properties of Asphalt Concrete at Low Temperatures." *Journal of Civil Engineering and Management* 21, no. 5 (2015): 559-70.

Haynes, M. J., and R. P. Gangloff. "High Resolution R-Curve Characterization of the Fracture Toughness of Thin Sheet Aluminum Alloys." *Journal of Testing and Evaluation* 25, no. 1 (1997): 82-98.

Kim, Ji Sik, Young-Nam Kwon, and Kee-Sun Sohn. "Dynamic Visualization of Crack Tip Stress Field and Propagation Using the Mechano-Luminescence in Sral2o4:(Eu,Dy,Nd)." Paper presented at the 5th Pacific Rim International Conference on Advanced Materials and Processing, PRICM 2004, November 2, 2004 - November 5, 2004, Beijing, China, 2005.

Koh, Chulseung, and Reynaldo Roque. "Use of Nonuniform Stress-State Tests to Determine

Fracture Energy of Asphalt Mixtures Accurately." *Transportation Research Record*, no. 2181 (2010): 55-66.

Lach, R., S. Seidler, and W. Grellmann. "Resistance against the Intrinsic Rate of Fracture Mechanics Parameters for Polymeric Materials under Moderate Impact Loading." *Mechanics of Time-Dependent Materials* 9, no. 2-3 (2005): 103-19.

Li, X. J., and M. O. Marasteanu. "Using Semi Circular Bending Test to Evaluate Low Temperature Fracture Resistance for Asphalt Concrete." Paper presented at the Proceedings of the Society for Experimental Mechanics, Inc., 2010.

Li, Xue, and Mihai Marasteanu. "Evaluation of the Low Temperature Fracture Resistance of Asphalt Mixtures Using the Semi Circular Bend Test." Paper presented at the Asphalt Paving Technology 2004, March 8, 2004 - March 10, 2004, Baton Rouge, LA, United states, 2004.

Mobasher, Barzin, Michael S. Mamlouk, and How-Ming Lin. "Evaluation of Crack Propagation Properties of Asphalt Mixtures." *Journal of Transportation Engineering* 123, no. 5 (1997): 405-13.

Neshpor, G. S. "Some Special Features of the R-Curve and Its Use for Evaluating the Modulus of Rupture of Aluminum Alloys." *Industrial laboratory* 53, no. 5 (1987): 460-67.

Schmit, F., D. Bouvart, and D. Francois. "Ductile Fracture Characterization of Polycarbonate by the R-Curve Method." *International Journal of Fracture* 43, no. 2 (1990): 83-96.

Shah, M. B., J. L. Ferracane, and J. J. Kruzic. "R-Curve Behavior and Micromechanisms of Fracture in Resin Based Dental Restorative Composites." *Journal of the Mechanical Behavior of Biomedical Materials* 2, no. 5 (2009): 502-11.

Sundaresan, S., and B. Nageswara Rao. "Stress Intensity at the Initiation of Instability by R Curve." Paper presented at the 2014 International Mechanical Engineering Congress, IMEC 2014, June 13, 2014 - June 15, 2014, Tiruchirappalli, TN, India, 2014.

Suzuki, Kenji, Keisuke Tanaka, Yoshihisa Sakaida, and Hiroyuki Yamagishi. "R-Curve Behavior for Stable Crack Growth from Indentation Cracks in Alumina." *Zairyo/Journal of the Society of Materials Science, Japan* 44, no. 504 (1995): 1133-37.

Tanaka, K., and J. D. Harrison. "R Curve Approach to Cod and J for an Austenitic Steel." *International Journal of Pressure Vessels and Piping* 6, no. 3 (1978): 177-201.

Wagoner, Michael P., William G. Buttlar, Glaucio H. Paulino, and Philip Blankenship. "Investigation of the Fracture Resistance of Hot-Mix Asphalt Concrete Using a Disk-Shaped Compact Tension Test." 2005.

Wu, Ming, and Dale Wilson. "Residual Strength of Metal-Matrix Laminated Panels." Paper

presented at the Proceedings of the 1995 6th Symposium on Composites: Fatigue and Fracture, May 16, 1995 - May 18, 1995, Denver, CO, USA, 1997.

Chapter 4 R-Curve Research for Asphalt Concrete

4.1 Background

The preliminary R-Curve findings in Chapter 3 were collected from samples from a study focused on incorporated RAP and WMA technology into asphalt concrete. In chapter three, R-Curve for three types of asphalt concrete at different aging levels, moisture conditions, and temperature were constructed. Cohesive energy and energy rate were extracted to quantify the crack imitation and propagation. While this data provided a first glimpse to the potential benefits of utilizing R-Curves, it did not explore common variables in asphalt concrete design, common variables in testing conditions, and only used a single analysis technique. In this chapter, in order to evaluate this R-Curve method itself more comprehensively, there are three considerations to construct the experimental matrix. First, this expanded research of R-Curve intends to investigate the most fundamental variables in asphalt concrete: Nominal Maximum Aggregate Size (NMAS) and Performance Grade (PG) of asphalt cement. The theory of NMAS and PG has been established, it is clear that NMAS and PG grade is essential in the mix-design to control the cracking resistance performance. Second, as asphalt concrete is a viscoelastic material, the testing temperature and loading rate impact the crack behavior significantly. Viscous deformation always associates with the fracture process, it is important to know the energy dissipated in the system is used to create crack, or creep deformation. Third, R-Curve method highly depend on the crack extension analysis. However, crack pattern in a fracture test can be very complex. Conventionally, crack extension is defined as the growth of crack in length. Instead of a straight line, crack in asphalt concrete is usually random in shape, and it has branches and grows both in length and width. Thus, a simple definition of crack length extension may be too simplified to quantify the crack extension.

4.2 Chapter objective

This chapter investigates the next stage R-Curve research considering fundamental internal factors of NMAS and PG, external factors of testing temperature and loading rate. In addition, it expands the quantification of the crack extension during the crack growth in asphalt concrete.

4.3 Material and methods

In order to maximize the envelope of R-Curve in asphalt concrete, this chapter uses the experimental matrix shown in Table 4.1. The factors (including PG grade, Nominal Maximum Aggregate Size, testing temperature, and loading rate) and levels are chosen to expect significant difference in R-Curve behavior of asphalt concrete.

Table 4.1 Experimental Matrix for Chapter 4

Factors	**# of Levels**	**Level**
Performance Grade	2	PG 64-22, PG 76-22
NMAS	2	9.5mm, 25mm
Test Temperature	3	+24˚C, 0˚C, -24˚C
Loading Rate	2	0.03mm/min, 1.0mm/min

In a performance grade (PG), there are two numbers, for example, PG 76-22. These two number are converted from air temperature to pavement temperature in Celsius. The first one is from the maximum seven-day average pavement temperature of the year. Asphalt binder graded as PG76- should be able to perform well in this high temperature with a certain reliability. The second number is from the minimum pavement temperature in the year, asphalt binder graded as PG-22 is expected to perform without distress at this low temperature. In this study, the factor of PG grade has two levels, PG 76-22, and PG 64-22. These two are typical asphalt binders that are applied in Arkansas. Cracking is usually an issue at low temperature and these two asphalt

binders share the same lower limit in the PG. However, it is considered that the fracture behavior of these two binders in asphalt concrete can be very different too for the following reasons. First, the low temperature grading in a Superpave PG is graded by Bending Beam Rheometer (BBR). This BBR test uses a pure asphalt binder as the sample rather than a mixture, the binder performed in a different mechanism when mixed with aggregate. Second, PG 76-22 is usually styrene-butadiene-styrene (SBS) polymer modified asphalt binder whereas PG 64-22 is usually a neat binder without any modification. The purpose of the addition of polymer in the binder is the toughness increment at high temperature, while the polymer may also change the fracture behavior at low temperature without impacting on BBR results. Thus, this chapter is investigating the effects of these two type of binders on R-Curve of asphalt concrete.

NMAS 9.5mm is usually applied in surface course, whereas NMAS 25mm is usually placed in filed as the binder course in between surface course and base course. NMAS 9.5mm is a finer gradation than NMAS 25mm as illustrated in Figure 4.1. As known, the finer aggregate gradation has more surface area than the courser gradation, thus the binder content is usually higher in finer aggregate gradation to cover the surface area. In asphalt concrete, the binding between aggregate and asphalt binder is usually the weak point compare to the tensile strength of aggregate itself, so it is unlikely the crack occurs in a solid aggregate. It is usually observed crack growing in the asphalt binder filled voids of the asphalt concrete. Noticing that crack can be observed in an elongated or flat aggregate as well, but the content of elongated and flat aggregate is strictly controlled in a Superpave mix design. Besides, the gradation structures in the asphalt concrete can be very different due to the NMAS, which may result in significant fracture

toughness and fracture behavior. This chapter will look at the influence of the NMAS on the R-Curve behavior of the asphalt concrete.

Due to the viscoelasticity, time and temperature are vital in fracture behavior of asphalt concrete. This chapter use three testing temperature at: -24°C, 0°C and 24°C. The temperature of -24°C is chosen because of the lower limit of the PG grade for both binder is -22. -24°C is 2°C below the lower PG limit. This test temperature for fracture test was established by Braham *et al.* (2007) and was intended to within the range of glass transition temperature of the asphalt cement. 24°C is usually the ambient temperature, and significant amount of research was found to perform fracture test at ambient temperature. For example, Faruk *et al.* (2014) at Texas A&M Transportation Institute, found that the room temperature at 25 ºC, was the better suited for low binder content asphalt concrete in SC(B) test. Wu *et al.* (2005) at Louisiana Transportation Research Center perform the SC(B) test at 25°C, for the asphalt concrete contains the binder for PG 76-22 and PG70-22. However, it is considered that energy dissipated in the specimen during a fracture tests can be separated into three parts: fracture energy, recoverable strain energy, and creep strain energy. (Braham, 2008). This indicates that fracture is associated with the elastic deformation (recoverable) and viscous deformation (creep). Li and Marasteanu (2005) found that it took higher external work in a fracture test at higher testing temperature. This may indicate that the creep deformation is larger at higher testing temperature. In other words, the creep energy increases in the system as the increment of the testing temperature. This research cannot separate the three types of energy, but the three levels of testing temperature may promote a trend of the change of creep energy and elastic energy. Thus, -24°C, 0°C, and 24°C are chosen to expect to detect the trend. It is known that the effect of time and temperature can be converted by

the law of time-temperature superposition. Loading rate is the form of time in a fracture test, a faster loading rate at higher temperature may be equivalent to a slower loading rate at lower temperature. In this chapter, two loading rates are considered in the experimental matrix, 0.03mm/min, and 1.0mm/min, in the control of CMOD. Four replicates are performed for each factor at each level.

As the stiffness is an indicator to the viscoelastic behavior, dynamic modulus was tested for the material listed in the test matrix. In order to achieve the stiffness at SC(B) testing temperature of -24°C, it is decided to add a dynamic modulus testing temperature of -24°C instead of extrapolation values from the dynamic modulus master curve.

4.3.1 Mix design

A Superpave mix design was performed for the NMAS 9.5mm, and NMAS 25mm gradation, using PG 64-22 binder and targeting 4% air voids. The gradation of the NMAS 9.5mm and NMAS 25mm are illustrated in the Figure 4.1. In order to control the viable of binder content that could have added a confounding factor on the cracking behavior of asphalt concrete, this research uses the same binder contents for PG 76-22 binder and PG 64-22 binder. The binder contents in the mix design are listed in the Table 4.2. The compaction data is recorded during the compaction as illustrated in Figure 4.2, the percentage of theoretical maximum specific gravity (G_{mm}) is plotted versus gyration numbers. The testing sample compaction reduced the gyrations according to the compaction curve when compacting to achieve 7% air void to mimic the field air void immediately after the construction and as per standard practice. All the samples experienced two hours aging at the compaction temperature before the compaction.

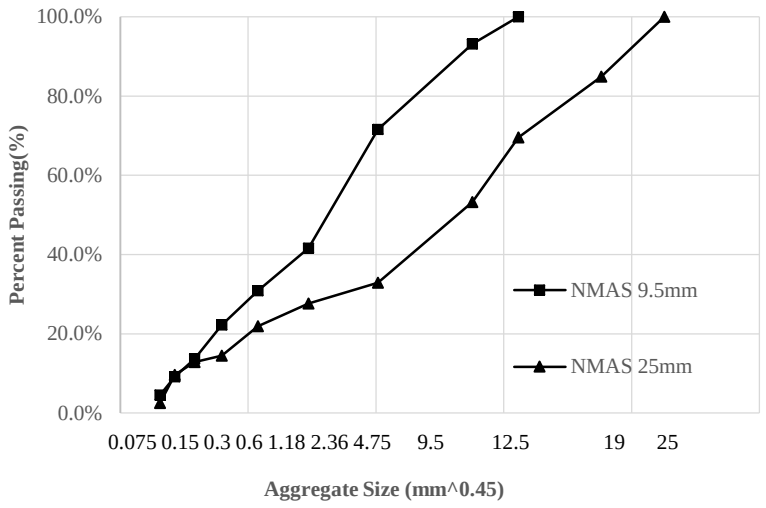

Figure 4.1 Gradation of Asphalt Mixture

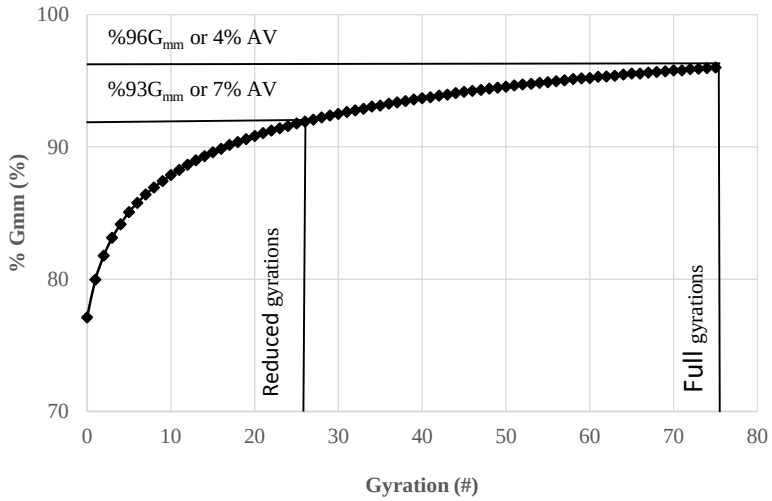

Figure 4.2 Compaction Curve

Table 4.2 Optimum Asphalt Binder Content

NMAS	Binder Content*
9.5mm	5.70%
25 mm	4.02%

(* binder content for both PG 64-22 and PG 76-22)

4.3.3 SC(B) test configuration

The SC(B) test configuration remains the same as in chapter two and three: SC(B) samples are tested on a MTS load frame with a 5kip load cell, a clip gauge is attached to the bottom center of the SC(B) to control the opening of the crack mouth. The same camera as preliminary research is setup to capture the images of one surface of the sample for crack growth analysis. The images captured are 18 megapixels, eight-bit monochrome grey scale, which means each pixel in the image has a grey value that ranges from 0 to 2^8. For the tests at loading rate of 1.00mm/min, the frame rate of 14 frame per second(fps) are applied, and a slower 0.2 fps is applied to the tests at loading rate 0.03mm/min due to the ram memory of the equipment. The illumination of the camera is improved by using two 60w, 60Hz LED bulbs, as shown in Figure 4.3. LED lights has cold light that would not radiate and heat up the SC(B) sample, which can help with the sample to remain at an even and constant temperature. A bulb level is used to ensure that the camera is level every after it is disturbed.

Figure 4.3 SC(B) Test Configuration, Before(left) and After(right) Test

4.3.2 Sample fabrication description

The geometry of the SC(B) sample also remained the same as in chapter two and three. Samples are cut from a 150mm gyratory compaction cylinder sample. The thickness of the sample is 25mm, and the notch is 1mm wide and 15mm deep at the bottom center of the sample. The only difference in sample fabrication as preliminary research is the orientation of the sample. In the preliminary research, samples are cut from three slices of the cylinder sample and then cut into halves, thus the six samples have three orientations from the cylinder height. As the air voids may vary in cylinder height, the SC(B) samples in preliminary research may have air void variation because of the orientation of the sample. As shown in Figure 4.4, the samples discussed in this chapter, are all cut from the middle height of the cylinder, so only one slice is cut from the cylinder and the slide is cut into two SC(B) samples.

Figure 4.4 SC(B) Sample Fabrication

4.3.4 Dynamic modulus of the material in test matrix

4.3.4.1 Test configuration and sample preparation

In this chapter, the dynamic modulus in indirect tensile (IDT) mode (Kim *et al.* 2004) is tested for the four type of HMA in the SC(B) experimental matrix: PG 76-22, NMAS 25mm; PG 76-22, NMAS 9.5mm; PG 64-22, NMAS 25mm; PG 64-22, NMAS 9.5mm. The IDT samples are tested under a MTS load frame with a 5kip load cell. Two pair of 38mm extensometers are attached in two surface sides of the IDT sample to measure the vertical and horizontal strain.

Five testing temperature are selected: -24°C, -10°C, 4°C, 21°C, 37°C and 54°C; -24°C is selected because of one of the SC(B) testing temperature is -24°C, and the other five temperatures are from the specification of uniaxial dynamic modulus, AASHTO T 342. Five frequencies are selected: 25Hz, 10 Hz, 5 Hz, 1 Hz, 0.5 Hz, and 0.1 Hz by following AAHTO T 342. The IDT samples are cut from the gyratory cylinder sample. The samples are targeting 40mm thickness slice orienting from the mid height of the cylinder sample. All the samples target 7% air void.

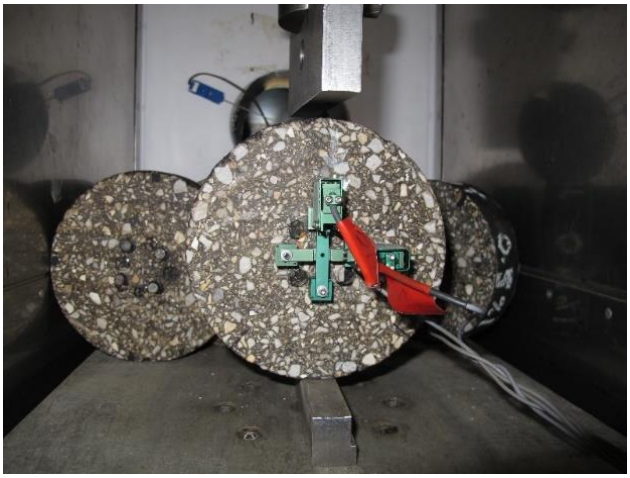

Figure 4.5 Dynamic Modulus in Indirect Tensile (IDT) Mode

4.3.4.2 Dynamic modulus master curve

At the testing temperature of 54°C, the strain level was not able to be controlled within the range of linear elastic, or 50-150 micron even with extreme low load. Thus, the data collected at 54°C are not applied to construct master curve. Besides, the data collected at 25Hz, and 10Hz are high in error, so those data are not applied to construct master curve as well. The master curves of dynamic modulus for the four mixtures are constructed by following AASHTO R62-13, using Equation 4.1.1 to Equation 4.1.4. An improved method that restricts initial coefficient of α, β, γ, a_1 and a_2 is applied to construct rational smoother master curves. (Yang *et al.*, 2015)

$$\log|E^*| = \delta + \frac{\alpha}{1+e^{\beta+\gamma\log(f_r)}} \qquad \textbf{Equation 4.1}$$

$$f_r = f \times a_T \qquad \textbf{Equation 4.2}$$

$$\boldsymbol{log a_T = a_1(T_R - T)^2 + a_2(T_R - T)} \qquad \textbf{Equation 4.3}$$

$$\boldsymbol{SSE = \sum_{i=1}^{N}(\log\left|\widehat{E}^*\right|_i - \log|E^*|_i)^2} \qquad \textbf{Equation 4.4}$$

Where;

$|E^*|_i$ = average measured dynamic modulus for each testing temperature and testing frequency combination, i, Mpa,

$\left|\hat{E}^*\right|_i$ = predicted dynamic modulus by Equation 4.1 for each testing temperature and testing frequency combination, i, Mpa,

N = total number of testing temperature and frequency combination,

SSE = square sum of error between measured and predicted dynamic modulus, and

$\alpha, \beta, \gamma, a_1, a_2$ = coefficient for best fitted curve in order to have lowest SSE.

The master curves for the four types of mixtures, NMAS9.5mm, PG 64-22; NMAS9.5mm, PG 76-22; NMAS25mm, PG 64-22; NMAS25mm, PG 76-22; are illustrated in Figure 4.6 a-d.

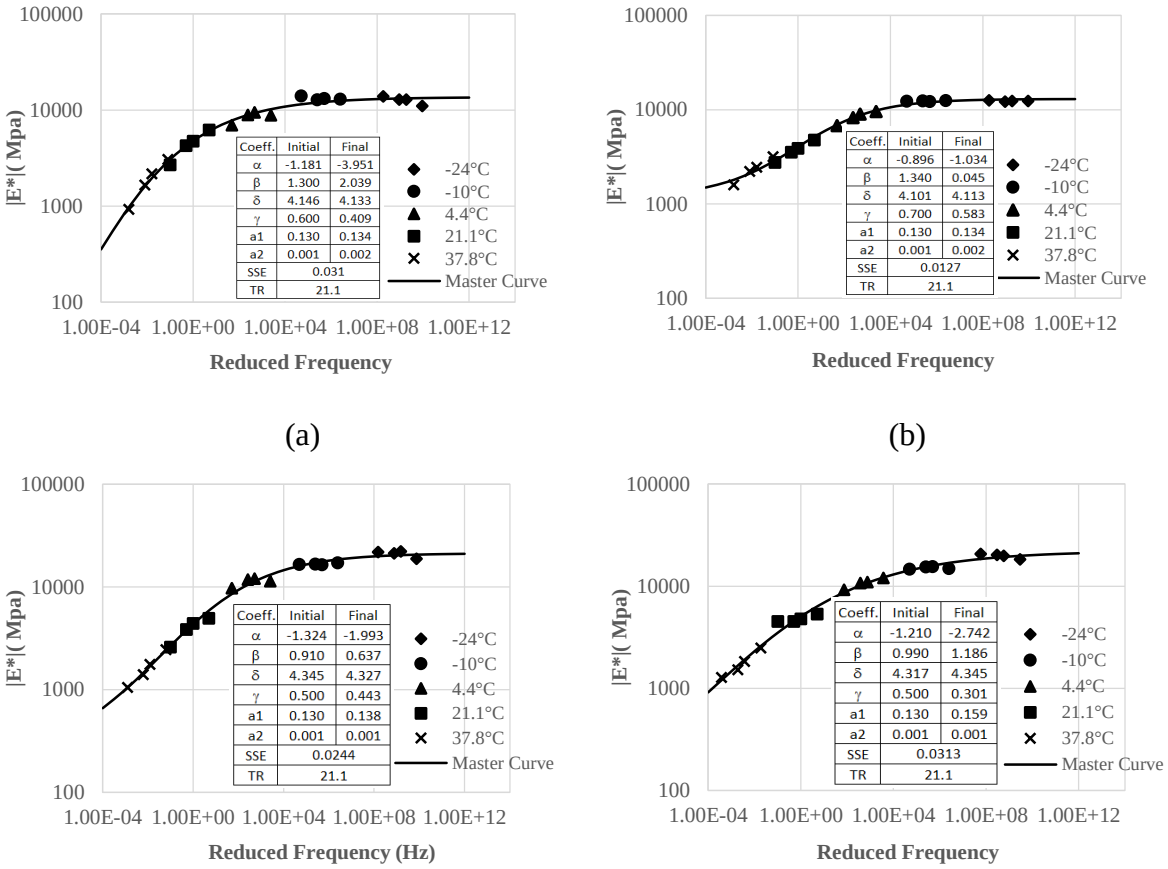

*SSE = sum of square error; TR = reference temperature in °C

Figure 4.6 Master Curves of Mixture with: (a) NMAS 9.5mm, PG 64-22; (b) NMAS 9.5mm, PG 76-22; (c) NMAS 25mm, PG 64-22; (d) NMAS 25mm, PG 76-22

In order to have a clear view that how the dynamic modulus varies among these four mixtures, these four master curves are plotted in Figure 4.7. As can be seen in the upper right corner of Figure 4.7, the modulus of the two mixtures with the NMAS25mm is higher than the other two mixtures with the NMAS9.5mm, while the difference in modulus between PG 76-22 and PG 64-22 are much smaller. In other words, at low temperature or high frequency, mixtures with NMAS25mm observed higher modulus than mixtures with NMAS9.5mm, while the binder PG 76-22 and PG 64-22 do not differentiate the modulus at low temperature. This trend is as expected because larger aggregate size is expected to lead to be tougher in modulus. And the

both binders are graded as -22 for the lower limit, which means they are expected to have the same performance at low temperature. In the lower left corner of Figure 4.7, it can be seen that the two mixtures with binder of PG 76-22 show higher modulus than the mixtures with binder of PG 64-22. In other words, mixtures with binder of PG 76-22 show higher modulus compare to mixtures with binder of PG 64-22. This trend is expected as well because polymer modification bump up two grades of the higher limit, and PG 76-22 is expected to be tougher at high temperature. Comparing the two mixtures with binder of PG 64-22 at higher temperature area, the mixture with NMAS25mm indicates higher modulus than NMAS 9.5mm, which is also as expected. However, comparing the two mixtures with binder of PG 76-22 at higher temperature area, the mixture with NMAS9.5mm indicates higher modulus. This is not expected because smaller aggregate size should result in lower modulus. But this unexceptional trend may indicate that at extreme high temperature, binder is more dominated in modulus compare to aggregate size.

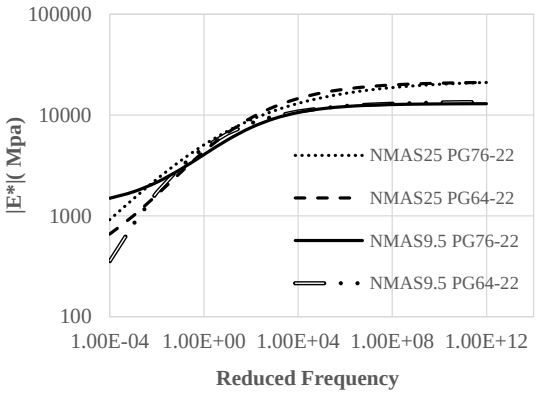

Figure 4.7 Master Curve Comparison

4.4 Tests results and discussion

To begin with, this chapter uses the same method that used in chapter three to construct R-Curves in the experimental matrix by plotting cumulative fracture energy versus crack length. Again, fracture energy, the crack initiation parameter cohesive energy, and crack propagation

parameter energy rate are extracted from the R-Curve to be analyzed. After that a new method to quantify the crack growth is developed to construct R-Curve, the energy rate data is analyzed again by using the new crack growth quantification. Finally, the creep damage in SC(B) test is discussed, and the dynamic modulus data is analyzed.

4.4.1 Fracture energy, cohesive energy and energy rate

SC(B) tests discussed in this chapter are performed at three testing temperatures: -24°C, 0°C, 24°C. However, it is found that, the tests performed at 24°C cannot be defined as fracture tests as crack cannot be detected in many of the tests while significant creep damage can be seen in the sample. This chapter will discuss the results of SC(B) tests at 24°C in section 4.4.3. This section only covers the results at the temperature of -24°C, and 0°C. These results are summarized in Table 4.3. Figure 4.8 illustrates a group of sample R-Curves for 25mm, PG 64-22 HMA at the loading rate of 0.03mm/min, with four replicates and the average R-Curve.

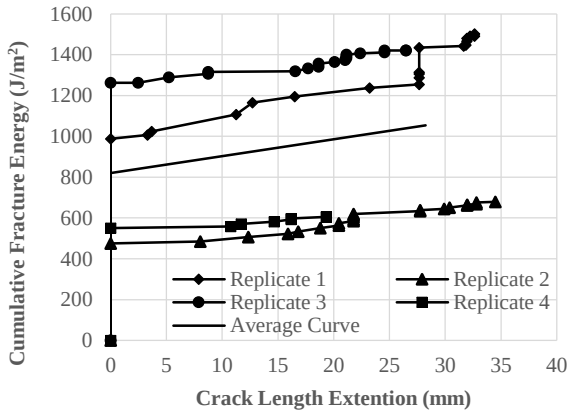

Figure 4.8 Sample R-Curves for 25mm, PG 64-22 HMA, at loading rate of 0.03mm/min

Table 4.3 Summary of Chapter 4's Test Results

Binder Grade	NMAS	Temp. °C	Loading Rate mm/min	F.E.* J/m^2	COV* of F.E. %	C.E.* J/m^2	COV of C. E. %	E. R.* J/m^3	COV of E. R. %
64-22	9.5	-24	0.03	357.5	11.6	342.8	11.8	0.4	98.3
			1.00	409.8	43.0	290.6	22.1	0.6	173.2
		0	0.03	981.2	12.8	630.3	19.1	9.9	42.9
			1.00	539.3	20.0	484.5	17.1	1.3	93.8
	25	-24	0.03	461.4	40.4	326.6	67.9	2.3	268.0
			1.00	393.0	27.0	393.0	27.0	0.0	N/A
		0	0.03	1053.9	44.9	820.9	45.7	7.7	72.5
			1.00	575.3	52.6	511.1	55.4	2.1	158.9
76-22	9.5	-24	0.03	352.0	13.4	338.3	13.3	0.4	58.0
			1.00	523.5	13.6	521.6	14.3	0.0	200.0
		0	0.03	806.8	26.1	658.4	26.8	26.8	7.5
			1.00	860.5	8.5	786.4	8.5	2.1	37.8
	25	-24	0.03	507.9	29.1	484.7	34.1	0.6	214.4
			1.00	256.6	20.0	256.6	20.0	0.0	N/A
		0	0.03	882.6	37.5	620.9	54.8	9.1	41.7
			1.00	1079.9	28.0	907.8	27.1	5.9	57.8

* F.E. = fracture energy
C.E. = cohesive energy
E. R. = energy rate
COV = coefficient of variance

Due to the heterogeneous characterization, the coefficient of variance (COV) for some of the results are very high, an analysis of variance (ANOVA) is performed to test the hypothesis whether the factors of binder grade, NMAS, temperature or loading rate is statistically significant on COV with a 95% confidence. As seen in Table 4.4, it is found that there are five p-values are under 0.05: factor of temperature on COV of energy rate; factor of NMAS on COV of fracture energy, COV of cohesive energy, and COV of energy rate; factor of loading rate on COV of energy rate. In other words, testing temperature be the reason to increase the heterogeneous on crack growth, however, it is not the reason to increase the heterogamous on fracture energy or cohesive energy. This is reasonable: asphalt concrete becomes more brittle and less viscous as

the temperature drops 0°C to -24°C, and crack at lower temperature imitates and grows in a much fast manner, which may increase uncertainty. Besides, the temperature change from -24°C to 0°C is not significant to cause the difference of variance for any form of energy (fracture energy and cohesive energy), which may indicate that the creep energy associated with cracking are not significantly different at these two temperatures. NMAS is a significant factor that cause a higher COV for fracture energy, cohesive energy, and energy rate. A larger NMAS has a different structure in gradation compare to a smaller NMAS. The angularity of larger aggregate leads to more contract area thus more aggregate interlock, this may increase the uncertainty of crack growth, and the work that is need to initiate a crack, or cohesive energy. The performance grade of binder is not significant at all to the COV of either fracture energy, cohesive energy or energy rate. Loading rate is only significant on the COV of energy rate. This is the same as the effect of temperature because of the viscous characterization: lower temperature can be equivalent to faster loading rate. A loading rate of 1.00mm/min can cause a significant different COV in energy rate compare to the loading rate of 0.03mm/min. The full ANOVA tables are seen in Appendix C.1-C.3.

Table 4.4 P-value Summary of ANOVA for COVs

p-value	COV of F.E.	COV of C.E.	COV of E.R.
Temperature	0.4696	0.3572	0.0004
NMAS	0.0115	0.0012	0.0089
Performance grade	0.1053	0.1702	0.0924
Loading rate	0.944	0.1008	0.0449

Also, ANOVA analysis is also performed to test the hypothesis whether these factors of binder grade, NMAS, temperature or loading rate is statistically significant on the crack initiation and propagation parameter: cohesive energy and energy rate. As seen in Table 4.5, there are three p-values are under 0.05: p-values from the factor of temperature on fracture energy, cohesive

energy, and energy rate. This results indicate that temperature significantly impact on fracture energy, cohesive energy, and energy rate. According to the ANOVA results, the other factors of NMAS, performance grade, and loading rate are not statistically significant. However, a further discussion of the results by using the technique of equality line figures is taken to expose the trend that is not statistically significant. The full ANOVA tables are seen in Appendix C.4-C.6.

Table 4.5 P-value Summary of ANOVA for Fracture Energy, Cohesive Energy and Energy Rate

p-value	**F. E.**	**C. E.**	**E. R.**
Temperature	0.0002	0.0005	0.0163
NMAS	0.5639	0.6032	0.5324
Performance grade	0.4517	0.1510	0.3566
Loading Rate	0.2560	0.8896	0.0584

4.4.1.1 Effect of performance grade of binder

According to the statistical analysis, the performance grade of binder is not significant to impact on the fracture energy, cohesive energy and energy rate. The equality line figures are plotted to check if there is any trend can be found. Take Figure 4.9(a) as an example, each point has an x-axis value of fracture energy for PG 64-22 binder, versus a y-value of fracture energy for PG 76-22 binder. All the other variables rather than binder type are fixed for each point. Thus, if the point falls below the equality line, the fracture energy of the PG 64-22 binder sample is higher; whereas if the point is above the equality line, the fracture energy of PG 76-22 binder sample is higher. In Figure 4.9(a), four points are above the equality line, three points are below while one point is close to the equality line. This result agrees with the ANOVA result, there is not a significant difference found between these two binders in fracture energy. Take a further look at the cohesive energy in Figure 4.9(b), there are less points fall below the equality line, which may indicate that the effect of the performance grade is stronger in impacting cohesive energy rather than fracture energy. The impaction of performance grade is not stronger in energy rate as seen in Figure 4.9(c). Noticed that these two type of binder are all graded to -22 for the lower limit in PG, and these SC(B) tests are all performed at low temperature of -24°C or 0°C. PG 76-22 and PG 64-22 are graded different at the high limit due to the polymer modification for the high temperature performance improvement such as rutting resistance, however, a slight effect of polymer modification on cohesive energy is detected. Five out of eight cases observed increase in cohesive energy. This is not statistically proved, but the sampling size in this research is relatively small, it is recommended to increase the statistical sample size in the future work. In summary, the polymer modification may have effect on cohesive energy despite the lower limit of the PG remains the same, but further research needs to be performed to verify.

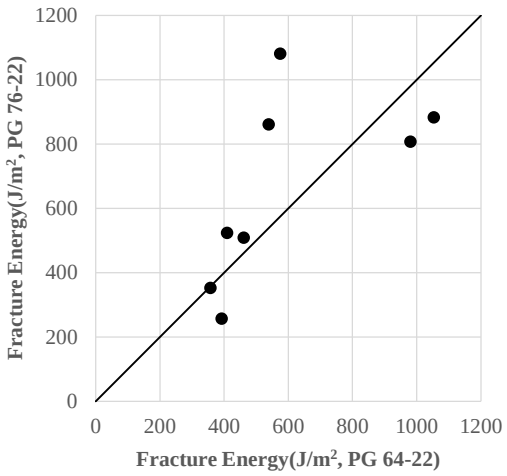

(a)

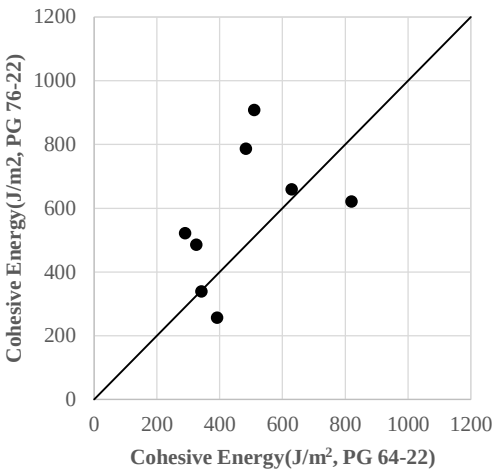

(b)

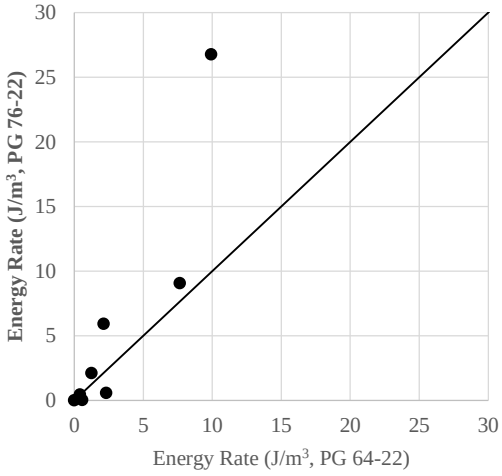

(c)

Figure 4.9 Effect of Performance Grade on Fracture Energy (a), Cohesive Energy (b), and Energy Rate (c)

4.4.1.2 Effect of NMAS

The equality line figures are applied to detect the effect of NMAS on fracture energy, cohesive energy and energy rate. As seen in Figure 4.10(a), six out of eight points are above the equality line, which means in most of the cases, bigger NMAS 25mm results in higher fracture energy than NMAS 9.5mm. This trend does not change much on cohesive energy, most of the five points out of eight are above the equality line while two points are close the line. Figure 4.10(c) shows the effect of NMAS on energy rate. In this figure, there is one point far away from all the other points. This point is the case of NMAS 9.5mm, PG 76-22, and loading rate 0.03mm/min. If taken this point out, for NMAS 9.5mm six out of eight points have the energy rate range from 0 to 2.1 J/m^3, and one point has the energy rate of $9.9J/m^3$, whereas there are five out of eight points have the energy rate range from 2.1 J/m^3 to 9.1 J/m^3. Although this is not proved by ANOVA, the equality line figure indicates that NMAS 25mm may lead to higher energy rate. In summary, NMAS 25mm indicates higher fracture energy, higher cohesive energy and higher energy rate in general. However, this conclusion needs to be verified with a larger amount of experiment.

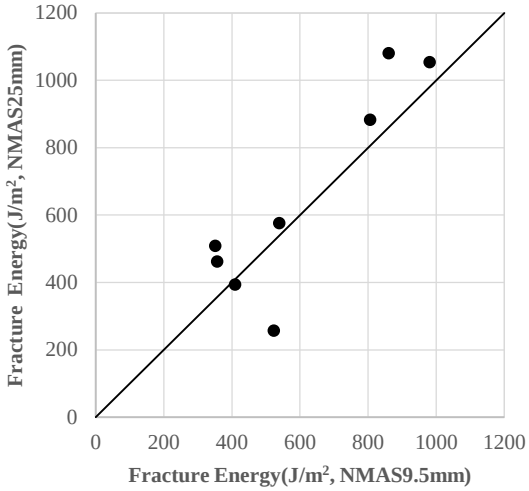

(a)

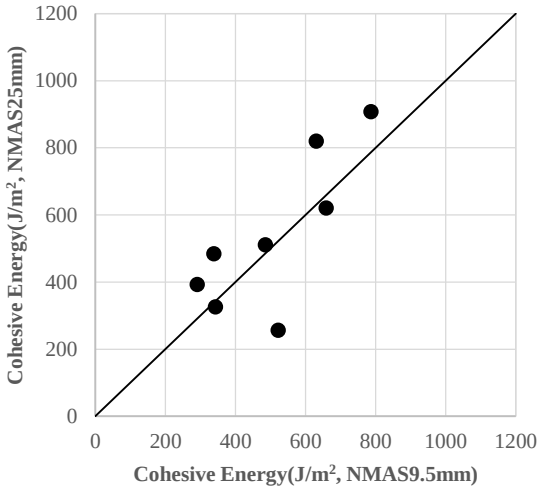

(b)

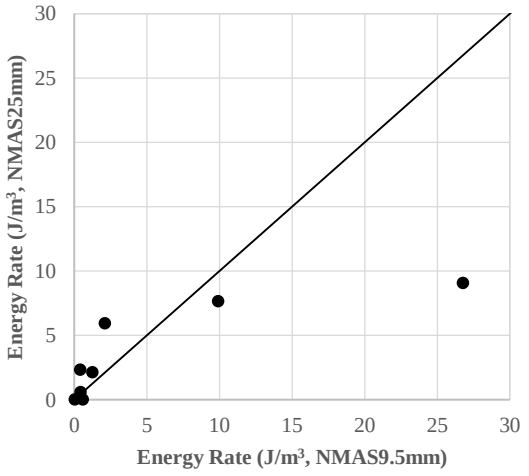

(c)

Figure 4.10 Effects of NMAS on Fracture Energy (a), Cohesive Energy (b), and Energy Rate (c)

4.4.1.2 Effect of testing temperature

The trend of effect of testing temperature is highly agreed with ANOVA: effect of testing temperature is significant on fracture energy, cohesive energy and energy rate. At the testing temperature of 0°C, fracture energy, cohesive energy and energy rate are always higher than they are at the testing temperature of -24°C. This can be a proof that at higher testing temperature, the total work may contain more creep dissipated energy. In this research, SC(B) tests are also performed at 24°C. In most of those cases, crack cannot even be detected, because the work applied on the sample may be totally used to create creep damage rather than crack. This will be discussed later but it is also a proof that as the testing temperature increase, there are more creep dissipated energy associated with the fracture.

In addition, as seen in Figure 4.11(c), most of the points are above the equality line and closer to the y-axis. Compared to Figure 4.11(a) and (b), in Figure 4.11 (c), the y-axis values at 0°C, is even more significantly higher than the x-axis value -24°C. This indicates that once the crack initiated, it consumes every small amount of energy to grow the crack, or the crack grows very fast after the initiation, most of the extern work applied on the sample dissipates into the cohesive energy. In other words, testing temperature has a larger impaction on crack propagation than crack initiation.

Still, these extractions (fracture energy, cohesive energy and energy rate) from R-Curve cannot separate the elastic portion, or recoverable strain energy, and viscous portion, or creep strain energy, from the fracture energy. But there is a trend of viscous portion increasing detected when testing temperature increases. Besides, this viscous portion increment may associate with crack

propagation more than crack initiation, because testing temperature has a larger impaction on crack propagation than crack initiation.

In summary, testing temperature significantly impacts on fracture energy, cohesive energy and energy rate. Higher testing temperature results in higher creep energy associated with fracture, and this higher creep energy associated with crack propagation more than crack initiation. Again, this finding needs to be verified with a large amount of experiment.

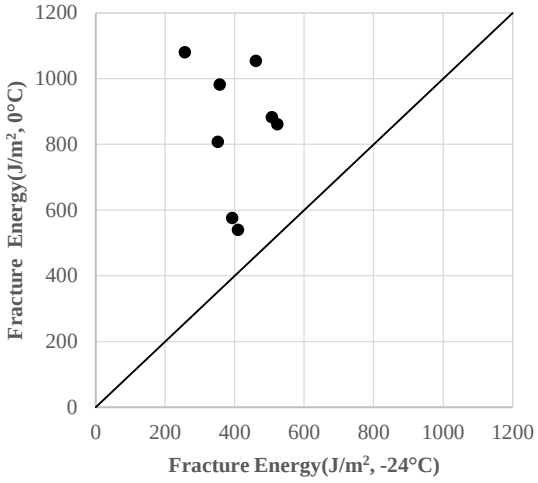

(a)

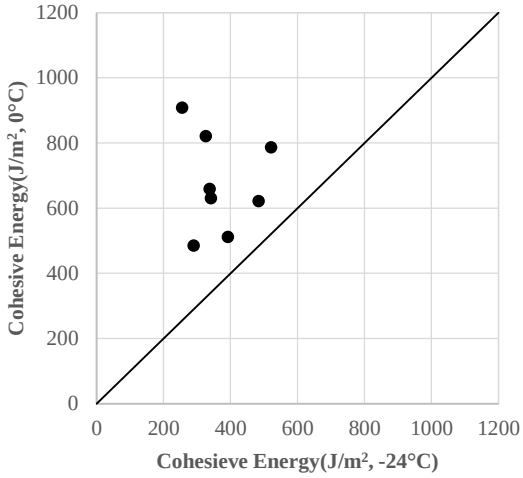

(b)

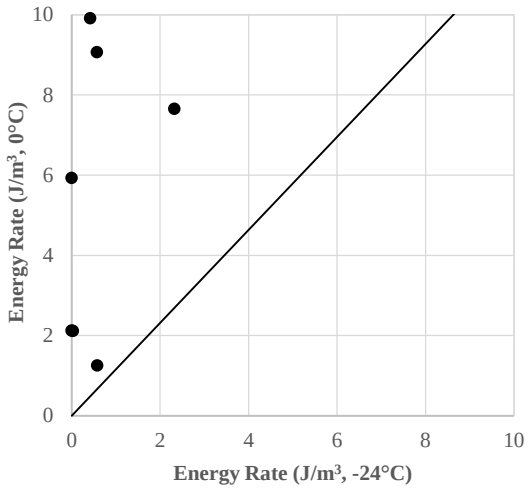

(c)

Figure 4.11 Effect of temperature on Fracture Energy (a), Cohesive Energy (b), and Energy Rate (c)

4.4.1.2 Effect of loading rate

The effect of loading rate may interact with the effect of testing temperature due to the viscoelastic behavior of asphalt concrete, or the equivalency between temperature and loading rate. As seen in Figure 4.12, the trend is not as clear as it is in Figure 4.11. In Figure 4.12 (a)-(b),

half of the points are above the equality line and half of the points are below the equality line. The effects of the loading rate on fracture energy and cohesive energy are hidden in equality line figures due to the interaction of temperature and loading rate. However, the trend of effect on energy rate is clear: Loading rate of 0.03mm/min results in higher energy rate. In other words, if the crack propagates slower, the crack growth consumes more external work. The same trend can be found in Figure 4.8(c): crack growth consumes more external work at higher testing temperature.

It is interesting to see that although the effects of fracture energy and cohesive energy can be hidden by equality line in Figure 4.12 (a)-(b), this effect of loading rate on energy rate is so strong and cannot be hidden because of the interaction. Due to the equivalency of temperature and loading rate at some extends, this is another prove that viscous portion energy associates with crack propagation more than crack initiation.

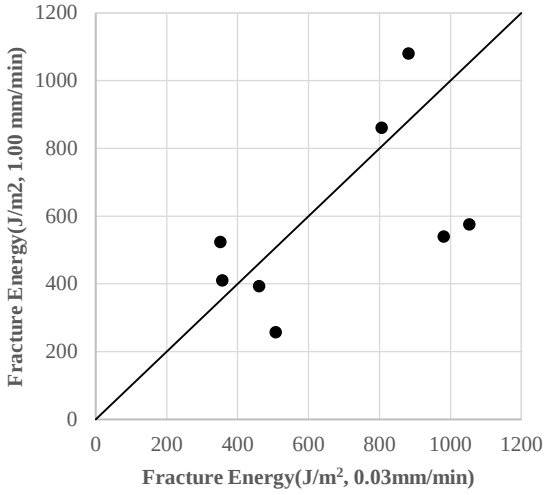

(a)

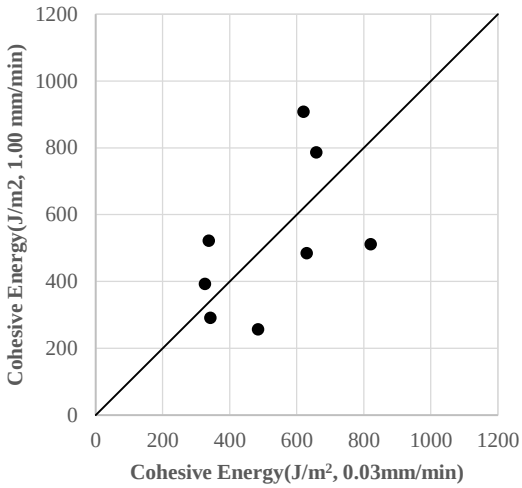

(b)

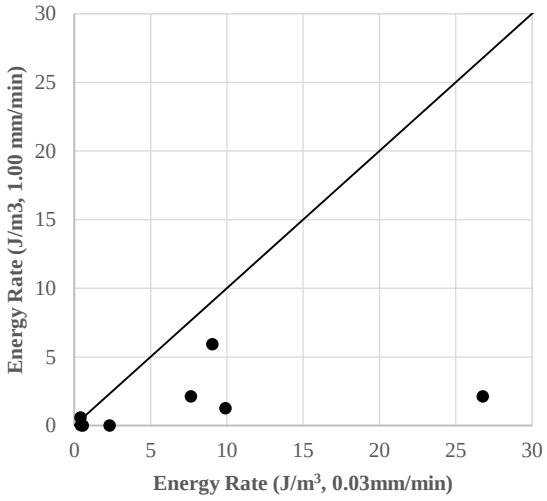

(c)

Figure 4.12 Effect of Loading Rate on Fracture Energy (a), Cohesive Energy (b), and Energy Rate (c)

4.4.2 Crack extension analysis

Before this point, all the crack extension discussed in this research is the extension in length. As discussed before, energy rate, which is highly related to crack extension, did not differentiate the effect of NMAS and binder type. This is not as expected. A potential reason might be the

measure of the crack extension. The crack growth in asphalt concrete or any other material can be complex. As illustrated in Figure 4.13, the crack grows from the beginning of arrow one to the end of arrow one, and then it stops growing from the end of arrow one but start to grow from the beginning of arrow two to the end of arrow two. After that, two cracks connect to each other at the location of arrow three. In this case, the length of crack is hard to be defined. In all this research, the crack is defined as the length from the crack tip to the notch tip. This may not be enough to fully quantify the crack extension because crack can open in width plus crack can have branches. As crack extension is one out of two components in the R-Curve, it is important to improve the definition of crack extension. Thanks to the image analysis, crack extension can also be defined as the crack area extension for two reasons: first, crack area can quantify the crack extension not only in length extend but also in width open; second, no matter how complex the crack pattern is, the definition of the crack area is much easier than crack length. The crack area is very practicable in image analysis. The following paragraph will discuss the development of quantification of crack area by image analysis. Notice that this is an attempt to explore appropriate crack extension, the result is preliminary.

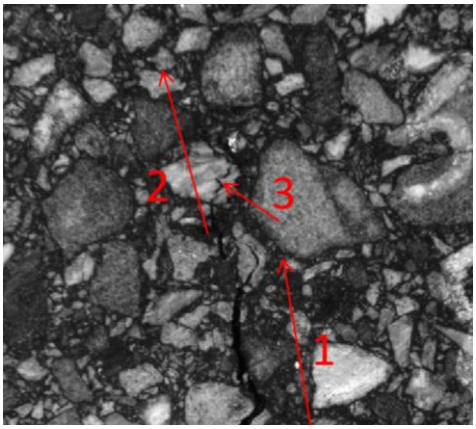

Figure 4.13 Crack Growth in Asphalt Concrete

The initial procedure to capture crack area extension in images includes three steps: first, as illustrated in Figure 4.14, establish an optimal static threshold value to isolate the crack in each image; second, count the number of pixels of isolated crack and compare with the reference image to capture the change; third, convert pixel into square millimeter.

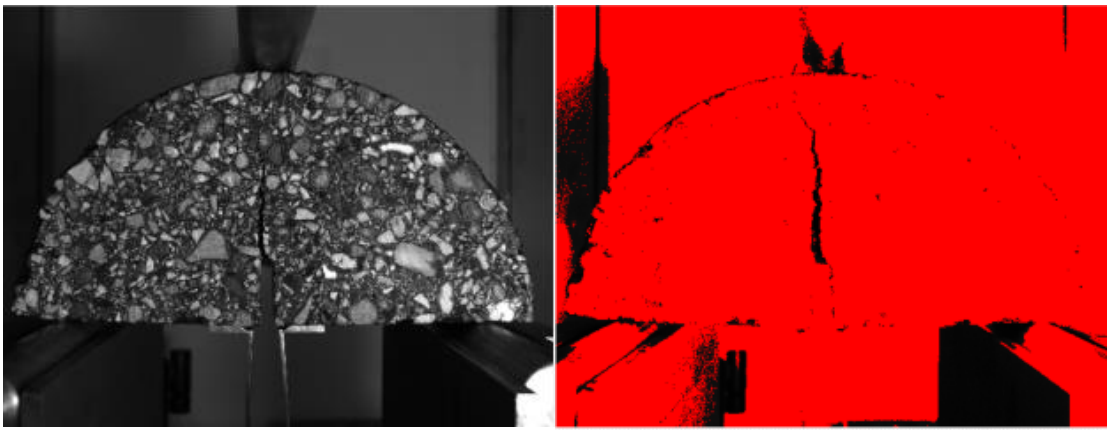

Figure 4.14 Isolation of Crack by Threshold Value

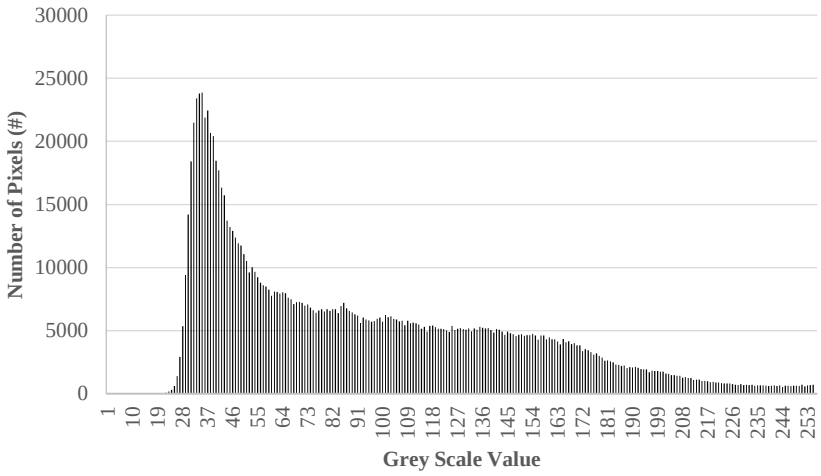

Figure 4.15 Example Histogram of One SC(B) Test Image

This method can capture the crack area extension when the crack is relatively large in size. However, when the crack is tiny at low testing temperature, there is difficulty to find out a static threshold value. Thus, another dynamic method is developed by using the histogram of the collected images. As shown in Figure 4.15 a histogram of an image counts the numbers of pixel

at each grey scale value. The camera used in this research is an eight-bit image depth, which means each pixel has 256 possible grey scale values. Thus, the x-axis in this histogram ranges from 0 to 256. This method follows five steps and calculated in Matlab®:

1. Calculate the histogram for each image in one SC(B) test;
2. Compare the histogram of each image with the reference image;
3. Find out the maximum change of the pixel numbers at one out of 256 grey scale values;
4. Use the maximum change of pixel numbers at one grey scale value as the crack area in current image;
5. Convert the pixel into square millimeter.

Figure 4.16 shows two examples of the crack area extension. The left figure captures the crack area extension by the images collected at a frame rate of 0.2fps, whereas the right figure is the crack area extension by the images collected at 10fps. The right figure has much lower noise compare to the left one. The cause of the higher noise in left figure can be the lower frame, and the frequency of the LED light. It can be seen that the noise in left figure occurs in a regular pace overtime. This method can be improved by using a continual illumination and faster frame rate. In addition, the image resolution in this research is 18 megapixels, and there is more than 100 pixels in $1mm^2$. This image resolution is sufficient to capture cracks in asphalt concrete, but improvement in grey scale depth may increase the accuracy of the analysis. However, the current captured crack area extension can still be valuable to construct R-Curves. The energy rate in the test matrix is updated by using the crack area extension as shown in Figure 4.17, the trend didn't change as the old figures that use crack length as extension.

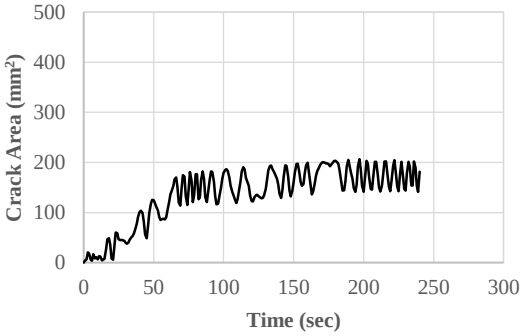

(a) 0.2fps

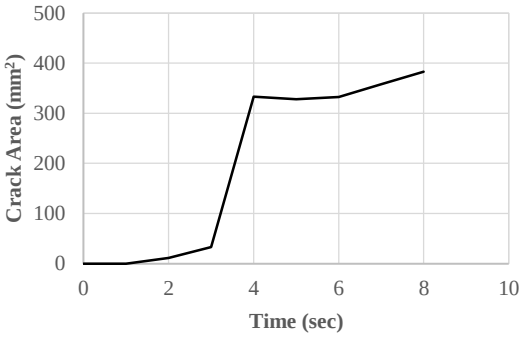

(b) 10fps

Figure 4.16 Example Crack Area Extension

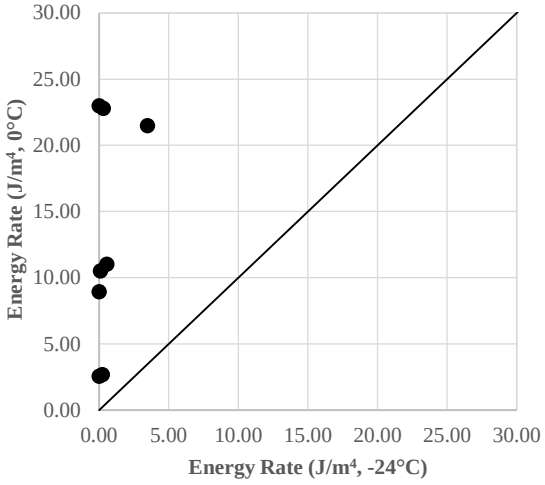

(a) Temperature

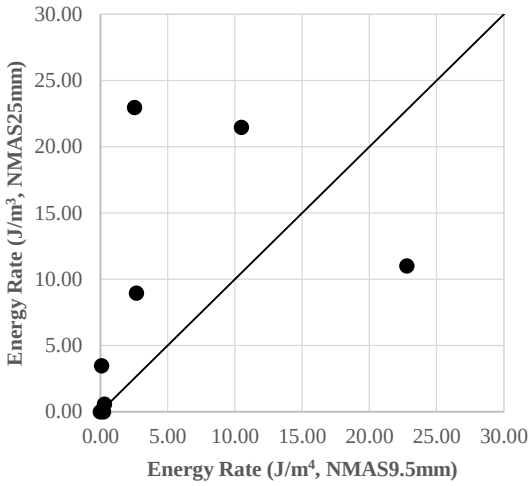

(b) NMAS

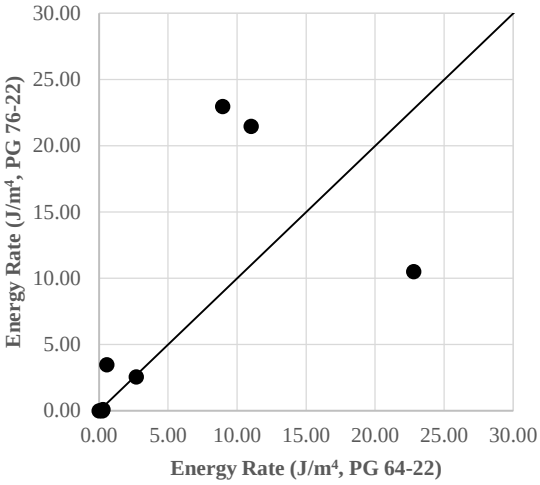

(c) Binder grade

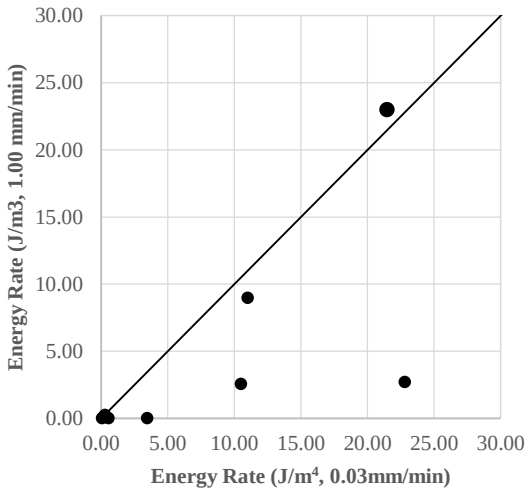

(d) Loading rate

Figure 4.17 Effect of Temperature, NMAS, binder Grade, and Loading Rate with Updated Energy Rate

4.4.3 Creep damage in fracture tests

At the testing temperature of 24°C, almost every SC(B) tests are not real fracture test because there is significant creep damage captured by the images. There are two types of creep damage observed in the SC(B) test at 24°C. First, the creep deformation forms in a rate that leads to crack mouth open in a faster rate than the set loading rate. In this situation, usually no crack can be

observed in the sample. This type of creep damage usually occurs at the loading rate of 0.03mm/min. The second type of creep damage is shown as in the Figure 4.18, the crack does not initiate form the notch tip, which means that the stress does not concentrate on the notch tip. The external work applied dominantly deforms the sample as permanent creep damage rather than create crack.

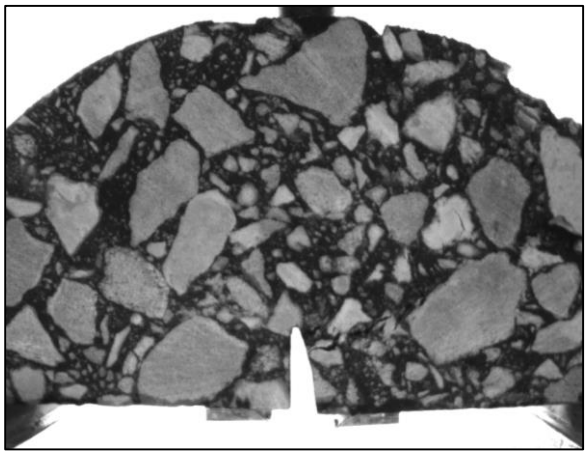

Figure 4.18 Creep Damage in SC(B) Test at 24°C, 1.00mm/min, NMAS 25mm, PG 76-22

4.5 Summary and chapter conclusion

In this chapter, the SC(B) tests are performed with the new designed experimental matrix to differentiate the crack characterization between materials. The factors of testing temperature, loading rate (0.3 mm/min and 1.0 mm/min), performance grade of binder (PG 64-22 and PG 76-22), and NMAS (9.5 mm and 25 mm) are considered in the experimental matrix. A clearer trend was found compare to chapter three. A new method of crack extension quantification using crack area is initially developed. The propagation parameter energy rate is updated by using the crack area extension. The following conclusions can be made based on the results analysis:

- Polymer modification may effect on crack initiation parameters of cohesive energy despite the lower limit of the PG remains the same;

- NMAS 25mm indicates higher fracture energy, higher cohesive energy and higher energy rate in general;
- The R-Curve results regarding binder type and NMAS does not completely agree with the dynamic modulus results, which reinforce that there are significant benefits to have both dynamic modulus and a form of cracking test to fully understand asphalt concrete;
- Testing temperature significantly impacts on fracture energy, cohesive energy and energy rate. Higher testing temperature results in higher creep energy associated with fracture, and this higher creep energy associated with crack propagation more than crack initiation.
- Loading rate of 0.03mm/min results in higher energy rate. Slow crack propagation consumes more external work;
- Crack area is an alternative of creak length to quantify the crack extension in R-Curve;
- Significant creep strain energy and creep damage increases as testing temperature increases. Fracture tests for R-Curve construction are suggested to be performed at low temperature rather than ambient temperature.

The above conclusions are made based on the results of ninety-six SC(B) tests, a further larger amount of tests are suggested to be performed to prove those conclusions. These conclusions suggest that R-Curve in asphalt concrete provided information of fracture behavior in terms of crack initiation and prorogation. The quantification of crack initiation and propagation can benefit the understanding the fracture mechanism in asphalt concrete.

4.6 Reference

Faruk, Abu N. M., Xiaodi Hu, Yuly Lopez, and Lubinda F. Walubita. "Using the Fracture Energy Index Concept to Characterize the Hma Cracking Resistance Potential under Monotonic Crack Testing." *International Journal of Pavement Research and Technology* 7, no. 1 (2014): 40-48.

Li, Xue, and Mihai O. Marasteanu. "Cohesive Modeling of Fracture in Asphalt Mixtures at Low Temperatures." *International Journal of Fracture* 136, no. 1-4 (2005): 285-308.

Wu, Zhong, Louay N. Mohammad, L. B. Wang, and Mary Ann Mull. "Fracture Resistance Characterization of Superpave Mixtures Using the Semi-Circular Bending Test." *Journal of ASTM International* 2, no. 3 (2005): 135-49.

Yang, Shu, and Braham, Andrew, Underwood, Shane., Hanz, Andrew., and Reinke, Gerald. "*Correlating Field Performance to Laboratory Dynamic Modulus from Indirect Tension and Torsion Bar"* Accepted by Journal of the Association of Asphalt Paving Technologists 2015

Chapter 5 Conclusions and Recommendations

5.1 Review of chapter objectives

Cracking, one of the most common types of distress in asphalt concrete, has been studied extensively both empirically and mechanistically. In recent years, fracture theory has emerged as one of the most promising paths to explore cracking behavior in the laboratory. However, most of the fracture theory research has focused on using a single number to quantify the fracture resistance of asphalt concrete--most frequently either the stress intensity factor, the fracture energy, or the J-Integral. An innovative method of quantifying the crack initiation and propagation was explored in the study, the method of Resistance Curve, or R-Curve. R-Curve is widely used in other materials, but was hardly found in asphalt concrete literature. This dissertation reviewed in depth the R-Curve application in many other materials to discover the benefits and challenges of utilizing R-Curve, methods of applying R-Curve, and analyzing R-Curve results. In order to fully explore the concept of R-Curve, first, the fracture energy of an asphalt concrete mixture modified with Recycled Asphalt Pavement (RAP) and Warm Mix Asphalt (WMA) additives was explored at multiple aging and moisture conditioning levels. This provided a base understanding of current fracture theory of a set of asphalt concrete mixtures and conditions. Second, R-Curve analysis techniques were applied to the same material, and preliminary findings concluded that R-Curve gave detailed information on crack initiation and propagation. Finally, a new test matrix exploring the effect of testing temperature, Nominal Maximum Aggregate Size (NMAS), binder grade, and loading rate was designed to explore the envelope of the R-Curve in asphalt concrete.

5.2 Conclusions

The first objective of this dissertation was to review the application of R-Curve in other materials. The general history of research in fracture of asphalt concrete was investigated. The research of fracture in asphalt concrete developed from empirical method to mechanical method in general. The history of fracture mechanics was also reviewed: linear elastic fracture mechanics, plastic-elastic fracture mechanics, and time-dependent fracture mechanics. In the application of fracture mechanics, the linear elastic theory was first applied in asphalt concrete, which simplified the material as a linear elastic material. Then, research of the nonlinear theory started to dominate the investigation of fracture in asphalt concrete, especially, the energy criterion: fracture energy was widely used as a quantitative of the fracture resistance of asphalt concrete. The R-Curve method looks at the fracture resistance in the view of energy criterion, which is widely applied in many materials but not asphalt concrete. Overall, the first object was met, and the need for research of R-Curve in asphalt concrete was established.

The second objective was the investigation of the current widely used fracture energy and viscoelastic analysis with dynamic modulus. This investigation was designed to evaluate the advantage and limitation of the application of fracture energy. In chapter two, the discussion of fracture energy is based on the SC(B) test on asphalt concrete. Fracture energy was used to quantify the fracture resistance performance. RAP usage, warm mix technology application, aging, and moisture were considered to address the concern in industry and academia. It was found that fracture energy as a single number can give direct simple information about fracture resistance; however, fracture energy may not be able to differentiate the fracture resistance of different materials. Also, as a single number, it cannot include the quantification of crack

initiation and propagation, which may be the reason this single number cannot differentiate the fracture resistance of different material. The experimental matrix considered the factors of RAP (0% and 25% RAP), aging (short term and long term aging per AASHTO R 30), and moisture (conditioned and unconditioned per AASHTO T 283), which could potentially change the mechanical behavior of the material, including fracture energy. In summary, the conclusions of the second objective were:

- Fracture energy was not able to always differentiate the cracking resistance performance of material among asphalt concrete without RAP, asphalt concrete with RAP, and warm mix asphalt with RAP.
- Moisture conditioned samples tended to have flatter dynamic modulus master curves, indicating that they become stiffer more quickly as temperature decreases versus unconditioned samples.
- After long term aging, all three asphalt concrete mixtures perform in a similar manner in dynamic modulus.
- The statistical analysis shows that WMA and RAP application results in a significantly different dynamic modulus at -10°C, but there is no significant difference at higher temperature. The effect of aging and moisture makes no significant difference to WMA and WR compared to HMA.
- Warm Mix Asphalt with RAP has similar compaction characteristics as Hot Mix Asphalt with RAP but at lower production and construction temperatures and 0.46% lower binder content. This lower asphalt binder content could lead to significant cost savings for the roadway owners without compromising performance.

The third objective was the construction and evaluation of R-Curves for the same material testing in the second objective. This objective was met as the R-Curve was successfully constructed for asphalt concrete in three mixture types, three aging levels, and two moisture condition levels. In addition to comparing the general shape of the R-Curve, parameters were developed by extracting information from the R-Curve including cohesive energy (theoretical crack initiation) and energy rate (theoretical crack propagation). R-Curve quantified the effect of aging and moisture on crack propagation as expected. Overall, the third objective was partially met by finding of cohesive energy and energy rate from the R-Curve. However, it was not clearly determined which factor affects the cohesive energy measurement. The same limitation as the second objective, the usage of RAP, aging and moisture may increase the variation and uncertainty, which may obscure the proper evaluation of the application of R-Curve of asphalt concrete. In summary, the conclusions of the third objective were:

- RAP can reduce the resistance to crack propagation of hot mix, while warm mix may improve the resistance when using RAP.
- Moisture conditioning does not impact the crack initiation but reduces the ability to resist crack propagation.
- Short term aging does not impact the ability to resist crack initiation but reduces the resistance to crack growth.
- The long term aging reduces the general fracture energy, cohesive energy and energy rate.
- The R-Curve analyzed results and the statistical result proved that R-Curve is an effective tool that can characterize the cracking behavior in asphalt concrete in both crack initiation and propagation.

The fourth objective was a further investigation of R-Curve in asphalt concrete. Due to the limitations caused by the existing externally imposed experimental matrix in the third objective, a new test matrix was designed to differentiate the material with the internal factors that dominate the material property: NMAS and binder type； and external factors that impact asphalt concrete behavior: temperature and loading rate. Overall, a clearer trend of R-Curve was found in this objective than in the third objective. The factors that have an impact on cohesive energy measurement were found to be testing temperature and NMAS. The dynamic modulus results does not completely agree with the R-Curve results, which indicates there are benefits to involve both dynamic modulus and R-Curve to fully understand asphalt concrete. In addition, these studies of R-Curve proved the existence of creep energy associated with the fracture, and that temperature is a significant factor that impacts the amount of creep damage associated with fracture. Because of the finding of creep damage, this objective was definitive that "cumulative fracture energy" as the fracture resistance may not be the most accurate quantification of cracking behavior, as the external work dissipated in the specimen included fracture energy, elastic strain energy, and creep strain energy. If the testing temperature is relatively high or the loading rate is relatively low, the creep portion can be extremely high which converts a "fracture test" into a "creep test". However, there is not an existing protocol to separate those three types of energy during lab testing. At this stage, using the external work as the fracture energy can still be considered valid, if the testing temperature is low. There is one limitation in the test matrix in the fourth objective: binder grade. Two binders used in the fourth objective have the same lower PG limit. Although it was found that polymer modification has an effect on the R-Curve, the effect of the lower limit in PG is important to investigate. Finally, in the fourth objective, a new

method that quantifies the crack extension in two dimensions is preliminarily developed during the image analysis. However, the noise in the image analysis is high and needs to be improved.

5.3 Recommendations

R-Curve has been investigated in asphalt concrete, and a large amount of materials have been evaluated by using R-Curve method. Due to the limitation that were found during the process of the research, there is still more research that needs to be performed. For the first objective, it is recommended that the literature continue tracking the R-Curve method development in other materials stays up to date, as the application of fracture mechanics is more developed in materials such as metal, polymer, and composite.

The second objective of this research is the investigation of the current widely applied fracture energy in asphalt concrete. There is plenty of research on fracture energy comprehensively; however, there is an issue on the separation of recoverable strain energy and creep strain energy from the fracture energy. If the fracture energy can be isolated in measurement from the total external work in fracture testing, a more appropriate evaluation of the general fracture resistance can be performed.

The third and fourth objectives of this research are the construction and application of R-Curve in asphalt concrete. There are four recommendations on further research of R-Curve in asphalt concrete. First, it is recommended that a wider range of PG be investigated, so that the effect of PG on R-Curve can be understood. Second, it is recommended the recoverable strain energy and creep strain energy measurement be separated from the fracture energy. Alternatively, a proper

testing temperature of the fracture test needs to be selected to ensure that the fracture energy is dominated in the total energy dissipation. Third, in this research, only one test configuration was performed in R-Curve research. Forth, it is noticed that most R-Curves at low temperature may be unstable cracking, and future work shall study the correlation between test temperature, loading rate and instability of crack growth. It is known that R-Curve is geometry dependent, other testing configurations included SE(B), DC(T) and also the geometry size effect need to be studied. In this research all the SC(B) sample are fixed in geometry with sample width of 25mm, the dependence of sample width on R-Curve should be investigated to address the stress status in field. Fourth, image analysis for the crack extension is recommended for further study: improvement of grey scale depth rather than the resolution of the camera sensor is recommended.

Reference

Ahmed, Sarfraz, Eshan V. Dave, Behzad Behnia, William G. Buttlar, and Marvin Exline. "Fracture Characterization of Gap-Graded Asphalt Mixtures and Thin Bonded Wearing Courses." *International Journal of Pavement Research and Technology* 3, no. 3 (2010): 128-34.

Ameli, A., M. Papini, J. A. Schroeder, and J. K. Spelt. "Fracture R-Curve Characterization of Toughened Epoxy Adhesives." *Engineering Fracture Mechanics* 77, no. 3 (2010): 521-34.

Anderson, Richard M., and Linda M. Braun. "Technique for the R-Curve Determination of Y-Tzp Using Indentation-Produced Flaws." *Journal of the American Ceramic Society* 73, no. 10 (1990): 3059-62.

Anderson, Ted L., and T. L. Anderson. *Fracture Mechanics: Fundamentals and Applications*. CRC press, 2005.

Bajaj, Devendra, and Dwayne D. Arola. "On the R-Curve Behavior of Human Tooth Enamel." *Biomaterials* 30, no. 23-24 (2009): 4037-46.

Bertram, A., and J. F. Kalthoff. "Crack Propagation Toughness of Rock for the Range of Low to Very High Crack Speeds." Paper presented at the Advances in Fracture and Damage Mechanics, September 2, 2003 - September 4, 2003, Paderborn, Germany, 2003.

Bhasin, Amit, and Dallas N. Little. "Application of Microcalorimeter to Characterize Adhesion between Asphalt Binders and Aggregates." *Journal of Materials in Civil Engineering* 21, no. 6 (2009): 235-43.

Birgisson, B., A. Montepara, E. Romeo, R. Roncella, G. Tebaldi, and R. Roque. "The Use of Digital Image Correlation for Accurate Determination of Fracture Energy Density in Hot Mix Asphalt (Hma)." Paper presented at the 6th RILEM International Conference on Cracking in Pavements, June 16, 2008 - June 18, 2008, Chicago, IL, United states, 2008.

Birgisson, Bjorn, Antonio Montepara, John Napier, Elena Romeo, Riccardo Roncella, and Gabriele Tebaldi. "Micromechanical Analyses for Measurement and Prediction of Hot-Mix Asphalt Fracture Energy." Paper presented at the Bituminous Paving Mixtures, 2006.

Birgisson, Bjorn, Antonio Montepara, Elena Romeo, Reynaldo Roque, Riccardo Roncella, and Gabriele Tebaldi. "Determination of Fundamental Tensile Failure Limits of Mixtures." Paper presented at the Asphalt Paving Technology 2007 AAPT, March 11, 2007 - March 14, 2007, San Antonio, TX, United states, 2007.

Birgisson, Bjorn, Reynaldo Roque, and Gale C. Page. "Performance-Based Fracture Criterion for Evaluation of Moisture Susceptibility in Hot-Mix Asphalt." 2004.

Braham, Andrew F., William G. Buttlar, Timothy R. Clyne, Mihai O. Marasteanu, and Mugurel I. Turos. "The Effect of Long-Term Laboratory Aging on Asphalt Concrete Fracture Energy." Paper presented at the Asphalt Paving Technology 2009, AAPT, March 15, 2009 - March 18, 2009, Minneapolis, MN, United states, 2009.

Braham, Andrew F., William G. Buttlar, and Mihai O. Marasteanu. "Effect of Binder Type, Aggregate, and Mixture Composition on Fracture Energy of Hot-Mix Asphalt in Cold Climates." *Transportation Research Record*, no. 2001 (2007): 102-09.

Braham, Andrew Franz. *Fracture Characteristics of Asphalt Concrete in Mode I, Mode Ii, and Mixed-Mode*. ProQuest, 2008.

Braham, Andrew, and Caleb Mudford. "Development of Fracture Resistance Curves for Asphalt Concrete." *Journal of Materials in Civil Engineering* 25, no. 11 (2013): 1631-37.

Brake, Nicholas Andres, and Karim Chatti. "Prediction of Transient and Steady-State Flexural Fatigue Crack Propagation in Concrete Using a Cyclic R-Curve." *Journal of Engineering Mechanics* 138, no. 4 (2012): 371-78.

Cesar, Paulo Francisco, Vinicius Rosa, Marcelo Mendes Pinto, Humberto Naoyuki Yoshimura, and Luoyu Roy Xu. "Effect of Ion Exchange on R-Curve Behavior of a Dental Porcelain." *Journal of Materials Science* 46, no. 1 (2011): 117-22.

Chan, Kwai S., and Daniel P. Nicolella. "Micromechanical Modeling of R-Curve Behaviors in Human Cortical Bone." *Journal of the Mechanical Behavior of Biomedical Materials* 16, no. 1 (2012): 136-52.

Chen, Xiang, Randy K. Nanstad, and Mikhail A. Sokolov. "J-R Curve Determination for Disk-

Shaped Compact Specimens Based on the Normalization Method and the Direct Current Potential Drop Technique." Paper presented at the 6th International Symposium on Small Specimen Test Techniques, January 29, 2014 - January 31, 2014, Houston, TX, United states, 2015.

Cheng, DingXin, Dallas N. Little, Robert L. Lytton, and James C. Holste. "Surface Energy Measurement of Asphalt and Its Application to Predicting Fatigue and Healing in Asphalt Mixtures." 2002.

Dave, Eshan V., Behzad Behnia, Sarfraz Ahmed, William G. Buttlar, and Henrique Reis. "Low Temperature Fracture Evaluation of Asphalt Mixtures Using Mechanical Testing and Acoustic Emissions Techniques." Paper presented at the Asphalt Paving Technology 2011, AAPT, March 27, 2011 - March 30, 2011, Tampa, FL, United states, 2011.

Dave, Eshan V., and William G. Buttlar. "Thermal Reflective Cracking of Asphalt Concrete Overlays." *International Journal of Pavement Engineering* 11, no. 6 (2010): 477-88.

de Castro, P. M. S. T. "R-Curve Behaviour of a Structural Steel." *Engineering Fracture Mechanics* 19, no. 2 (1984): 341-57.

Dongre, Rai, M. G. Sharma, and D. A. Anderson. "Development of Fracture Criterion for Asphalt Mixes at Low Temperatures." *Transportation Research Record*, no. 1228 (1989): 94-105.

Du, J., M. D. Thouless, and A. F. Yee. "Development of a Process Zone in Rubber-Modified Epoxy Polymers." *International Journal of Fracture* 92, no. 3 (1999): 271-85.

Elseifi, Mostafa A., Louay N. Mohammad, Hao Ying, and Samuel Cooper Iii. "Modeling and Evaluation of the Cracking Resistance of Asphalt Mixtures Using the Semi-Circular Bending Test at Intermediate Temperatures." Paper presented at the Asphalt Paving Technology 2012, AAPT, April 1, 2012 - April 4, 2012, Austin, TX, United states, 2012.

Faruk, Abu N. M., Xiaodi Hu, Yuly Lopez, and Lubinda F. Walubita. "Using the Fracture Energy Index Concept to Characterize the Hma Cracking Resistance Potential under Monotonic Crack Testing." *International Journal of Pavement Research and Technology* 7, no. 1 (2014): 40-48.

Fett, T., D. Munz, R. D. Geraghty, and K. W. White. "Bridging Stress Determination by Evaluation of the R-Curve." *Journal of the European Ceramic Society* 20, no. 12 (2000): 2143-48.

Fett, T., D. Munz, R. D. Geraghty, and K. W. White. "Influence of Specimen Geometry and Relative Crack Size on the R-Curve." *Engineering Fracture Mechanics* 66, no. 4 (2000): 375-86.

Fischer, David S., and Christopher A. Schuh. "Effect of a Rising R-Curve on the Sliding Wear of Silicon-Disilicide in Situ Composites." *Journal of the American Ceramic Society* 95, no. 4 (2012): 1406-13.

Fleck, N. A., M. P. F. Sutcliffe, S. Sivashanker, and X. J. Xin. "Compressive R-Curve of a Carbon Fibre-Epoxy Matrix Composite." *Composites Part B: Engineering* 27, no. 6 (1996): 531-41.

Ghafari, Sepehr, and Fereidoon Moghadas Nejad. "R-Curve Behavior and Crack Propagation Properties of Asphalt Concrete at Low Temperatures." *Journal of Civil Engineering and Management* 21, no. 5 (2015): 559-70.

Gopalakrishnan, Karthik, and John J. Mecholsky. "Mixed-Mode Fracture in an R-Curve Material." *Engineering Fracture Mechanics* 79 (2012): 380-88.

Griffith, Alan A. "The Phenomena of Rupture and Flow in Solids." *Philosophical transactions of the royal society of london. Series A, containing papers of a mathematical or physical character* 221 (1921): 163-98.

Gutkin, R., M. L. Laffan, S. T. Pinho, P. Robinson, and P. T. Curtis. "Modelling the R-Curve Effect and Its Specimen-Dependence." *International Journal of Solids and Structures* 48, no. 11-12 (2011): 1767-77.

Haynes, M. J., and R. P. Gangloff. "High Resolution R-Curve Characterization of the Fracture Toughness of Thin Sheet Aluminum Alloys." *Journal of Testing and Evaluation* 25, no. 1 (1997): 82-98.

Howson, Jonathan, Eyad Masad, Dallas Little, and Emad Kassem. "Relationship between Bond Energy and Total Work of Fracture for Asphalt Binder-Aggregate Systems." Paper

presented at the Asphalt Paving Technology 2012, AAPT, April 1, 2012 - April 4, 2012, Austin, TX, United states, 2012.

Irwin, G. R., and J. A. Kies. "Critical Energy Rate Analysis of Fracture Strength." *Welding Journal* 33, no. 4 (1954): 193-8.

Jeon, Changwoo, Choongnyun Paul Kim, Hyoung Seop Kim, and Sunghak Lee. "Interpretation of Fracture Toughness and R-Curve Behavior by Direct Observation of Microfracture Process in Ti-Based Dendrite-Containing Amorphous Alloys." *Metallurgical and Materials Transactions A: Physical Metallurgy and Materials Science* 46, no. 4 (2015): 1588-96.

Kavanagh, Leonnie N. "A 9-Year Evaluation of Field Cracking and Rutting Performance of Sps-9 Superpave Experiment." 2004.

Kim, Jaeseung, Reynaldo Roque, and Bjorn Birgisson. "Integration of Thermal Fracture in the Hma Fracture Model." Paper presented at the 2008 Annual Meeting of the Association of Asphalt Paving Technologists, AAPT, April 25, 2008 - April 30, 2008, Philadelphia, PA, United states, 2008.

Kim, Ji Sik, Young-Nam Kwon, and Kee-Sun Sohn. "Dynamic Visualization of Crack Tip Stress Field and Propagation Using the Mechano-Luminescence in Sral2o4:(Eu,Dy,Nd)." Paper presented at the 5th Pacific Rim International Conference on Advanced Materials and Processing, PRICM 2004, November 2, 2004 - November 5, 2004, Beijing, China, 2005.

Kim, Kwang W., and M. El Hussein. "Variation of Fracture Toughness of Asphalt Concrete under Low Temperatures." *Construction and Building Materials* 11, no. 7-8 (1997): 403-11.

Kim, Minkyum, Louay Mohammad, and Mostafa Elseifi. "Characterization of Fracture Properties of Asphalt Mixtures as Measured by Semicircular Bend Test and Indirect Tension Test." *Transportation Research Record*, no. 2296 (2012): 115-24.

Koh, Chulseung, and Reynaldo Roque. "Use of Nonuniform Stress-State Tests to Determine Fracture Energy of Asphalt Mixtures Accurately." *Transportation Research Record*, no. 2181 (2010): 55-66.

Kuai, Haidong, Hyun Jong Lee, Goangseup Zi, and Sungho Mun. "Application of Generalized J-Integral to Crack Propagation Modeling of Asphalt Concrete under Repeated Loading." *Transportation Research Record*, no. 2127 (2009): 72-81.

Lach, R., S. Seidler, and W. Grellmann. "Resistance against the Intrinsic Rate of Fracture Mechanics Parameters for Polymeric Materials under Moderate Impact Loading." *Mechanics of Time-Dependent Materials* 9, no. 2-3 (2005): 103-19.

Li, X. J., and M. O. Marasteanu. "Using Semi Circular Bending Test to Evaluate Low Temperature Fracture Resistance for Asphalt Concrete." Paper presented at the Proceedings of the Society for Experimental Mechanics, Inc., 2010.

Li, Xue, and Mihai Marasteanu. "Evaluation of the Low Temperature Fracture Resistance of Asphalt Mixtures Using the Semi Circular Bend Test." Paper presented at the Asphalt Paving Technology 2004, March 8, 2004 - March 10, 2004, Baton Rouge, LA, United states, 2004.

Li, Xue, and Mihai O. Marasteanu. "Cohesive Modeling of Fracture in Asphalt Mixtures at Low Temperatures." *International Journal of Fracture* 136, no. 1-4 (2005): 285-308.

Lin, Jia, Yu Huang, and Houan Zhang. "Damage Resistance, R-Curve Behavior and Toughening Mechanisms of Zrb2-Based Composites with Sic Whiskers and Zro2 Fibers." *Ceramics International* 41, no. 2 (2015): 2690-98.

Luo, Xue. "Characterization of Fatigue Cracking and Healing of Asphalt Mixtures." ProQuest LLC, 2012.

Luo, Xue, Rong Luo, and Robert L. Lytton. "Energy-Based Crack Initiation Criterion for Viscoelastoplastic Materials with Distributed Cracks." *Journal of Engineering Mechanics* 141, no. 2 (2015).

Majidzadeh, K., E. M. Kauffmann, and D. V. Ramsamooj. "Application of Fracture Mechanics in the Analysis of Pavement Fatigue." 1971 1970.

Marasteanu, Mihai, William Buttlar, Hussain Bahia, Christopher Williams, Ki Hoon Moon, Eyoab Zegey Teshale, Augusto Cannone Falchetto, *et al.* "Investigation of Low Temperature Cracking in Asphalt Pavements National Pooled Fund Study–Phase Ii."

(2012).

McCabe, D. E. "Fracture Toughness Evaluation by R-Curve Methods." 1973.

Miller, J. S., and W. Y. Bellinger. "Distress Identification Manual for the Long-Term Pavement Performance (Ltpp) Project." FHWA-RD-03, 2003.

Moavenzadeh, Fred. "Asphalt Fracture." 1967.

Mobasher, Barzin, Michael S. Mamlouk, and How-Ming Lin. "Evaluation of Crack Propagation Properties of Asphalt Mixtures." *Journal of Transportation Engineering* 123, no. 5 (1997): 405-13.

Neshpor, G. S. "Some Special Features of the R-Curve and Its Use for Evaluating the Modulus of Rupture of Aluminum Alloys." *Industrial laboratory* 53, no. 5 (1987): 460-67.

Novak, Stephen R. "Resistance to Plane-Stress Fracture (R-Curve Behavior) of A572 Structural Steel." In *Mechanics of Crack Growth*: ASTM International, 1976.

Ouchterlony, Finn. "Simple R-Curve Approach to Fracture Toughness Testing of Rock Core Specimens." Paper presented at the Proceedings 23rd Symposium on Rock Mechanics, Berkeley, Calif, USA, 1982.

Paris, P., and F. Erdogan. "Critical Analysis of Crack Propagation Laws." *American Society of Mechanical Engineers -- Transactions -- Journal of Basic Engineering* 85, no. 4 (1963): 528-34.

Ramsamooj, D. V. "Prediction of Fatigue Life of Asphalt Concrete Beams from Fracture Tests." *Journal of Testing & Evaluation* 19, no. 3 (1991): 231-39.

Reynolds, Anthony P. "Comparison of R-Curve Methodologies for Ranking the Toughness of Aluminum Alloys." *Journal of Testing and Evaluation* 24, no. 6 (1996): 406-10.

Ruth, Byron E., Reynaldo Roque, Bensa Nukunya, Richard Davis, Mihai Marasteanu, William Vavrik, Frank Fee, *et al.* "Aggregate Gradation Characterization Factors and Their Relationships to Fracture Energy and Failure Strain of Asphalt Mixtures." Paper

presented at the Asphalt Paving Technology 2002, March 18, 2002 - March 20, 2002, Colorado Springs, CO, United states, 2002.

Sahu, M. K., J. Chattopadhyay, and B. K. Dutta. "Transferability of Specimen J-R Curve to Straight Pipe with Circumferential Surface Flaw." *Fatigue and Fracture of Engineering Materials and Structures* 35, no. 5 (2012): 476-87.

Saxena, Ashok. *Nonlinear Fracture Mechanics for Engineers*. CRC press, 1998.

Schmit, F., D. Bouvart, and D. Francois. "Ductile Fracture Characterization of Polycarbonate by the R-Curve Method." *International Journal of Fracture* 43, no. 2 (1990): 83-96.

Shah, M. B., J. L. Ferracane, and J. J. Kruzic. "R-Curve Behavior and Micromechanisms of Fracture in Resin Based Dental Restorative Composites." *Journal of the Mechanical Behavior of Biomedical Materials* 2, no. 5 (2009): 502-11.

Siverns, M. J., and A. T. Price. "Crack Propagation under Creep Conditions in a Quenched 2 One Quarter Chromium 1 Molybdenum Steel." *International Journal of Fracture* 9, no. 2 (1973): 199-207.

Sundaresan, S., and B. Nageswara Rao. "Stress Intensity at the Initiation of Instability by R Curve." Paper presented at the 2014 International Mechanical Engineering Congress, IMEC 2014, June 13, 2014 - June 15, 2014, Tiruchirappalli, TN, India, 2014.

Suzuki, Kenji, Keisuke Tanaka, Yoshihisa Sakaida, and Hiroyuki Yamagishi. "R-Curve Behavior for Stable Crack Growth from Indentation Cracks in Alumina." *Zairyo/Journal of the Society of Materials Science, Japan* 44, no. 504 (1995): 1133-37.

Tanaka, K., and J. D. Harrison. "R Curve Approach to Cod and J for an Austenitic Steel." *International Journal of Pressure Vessels and Piping* 6, no. 3 (1978): 177-201.

Wagoner, Michael P., and William G. Buttlar. "Influence of Specimen Size on Fracture Energy of Asphalt Concrete." Paper presented at the Asphalt Paving Technology 2007 AAPT, March 11, 2007 - March 14, 2007, San Antonio, TX, United states, 2007.

Wagoner, Michael P., William G. Buttlar, and Glaucio H. Paulino. "Development of a Single-Edge Notched Beam Test for Asphalt Concrete Mixtures." *Journal of Testing and Evaluation* 33, no. 6 (2005): 452-60.

Wagoner, Michael P., William G. Buttlar, Glaucio H. Paulino, and Philip Blankenship. "Investigation of the Fracture Resistance of Hot-Mix Asphalt Concrete Using a Disk-Shaped Compact Tension Test." 2005.

Wagoner, Michael P., William G. Buttlar, Glaucio H. Paulino, Philip Blankenship, Reynaldo Roque, Wu Rongzong, Adriaan De Bondt, *et al.* "Laboratory Testing Suite for Characterization of Asphalt Concrete Mixtures Obtained from Field Cores." Paper presented at the Association of Asphalt Paving Technologists -Proceedings of the Technical Sessions 2006 Annual Meeting, March 27, 2006 - March 29, 2006, Savannah, GA, United states, 2006.

Walubita, Lubinda F., Geoffrey S. Simate, Edward Ofori-Abebresse, Amy Epps Martin, Robert L. Lytton, and Luis E. Sanabria. "Mathematical Formulation of Hma Crack Initiation and Crack Propagation Models Based on Continuum Fracture-Mechanics and Work-Potential Theory." *International Journal of Fatigue* 40 (2012): 112-19.

Wu, Ming, and Dale Wilson. "Residual Strength of Metal-Matrix Laminated Panels." Paper presented at the Proceedings of the 1995 6th Symposium on Composites: Fatigue and Fracture, May 16, 1995 - May 18, 1995, Denver, CO, USA, 1997.

Wu, Zhong, Louay N. Mohammad, L. B. Wang, and Mary Ann Mull. "Fracture Resistance Characterization of Superpave Mixtures Using the Semi-Circular Bending Test." *Journal of ASTM International* 2, no. 3 (2005): 135-49.

Xi, Yunping, and Zdenek P. Bazant. "Analysis of Crack Propagation in Concrete Structures by Markov Chain Model and R-Curve Method." Paper presented at the Proceedings of the 1996 7th Specialty Conference on Probabilistic Mechanics and Structural Reliability, August 7, 1996 - August 9, 1996, Worcester, MA, USA, 1996.

Yang, Kwanho, C. James Hwang, and John A. Rice. "New Testing Method for Ceramic R-Curve Determination at Elevated Temperatures." Paper presented at the Proceedings of the 1994 International Mechanical Engineering Congress and Exposition, November 6, 1994 - November 11, 1994, Chicago, IL, USA, 1994.

Yang, Shu, and Andrew Braham. R-curves characterisation analysis for asphalt concrete. *International Journal of Pavement Engineering*:1-10, 2016.

Yang, Shu, Andrew Braham, Lianfang Wang, and Qingkai Wang. Influence of aging and moisture on laboratory performance of asphalt concrete. *Construction and Building*

Materials 115:527-535, 2016.

Zhou, Peng, Ping Hu, Xinghong Zhang, Wenbo Han, and Youhua Fan. "R-Curve Behavior of Laminated Zrbinf2/Inf-Sic Ceramic with Strong Interfaces." *International Journal of Refractory Metals and Hard Materials* 52 (2015): 12-16.

Appendix A Tables from Chapter 2

Table A.1 Analysis of Variance of |E*| at -10ºC, 25Hz

Source	Sum Sq.	d.f.	Mean Sq.	F	p-value
Mix	9.82E+07	2	4.91E+07	12.31	0.020
Age	5.23E+06	2	2.62E+06	0.66	0.567
Condition	3.35E+07	1	3.35E+07	8.41	0.044
Mix*Age	4.46E+07	4	1.11E+07	2.79	0.172
Mix*Condition	2.22E+06	2	1.11E+06	0.28	0.770
Age*Condition	2.19E+07	2	1.10E+07	2.75	0.177
Error	1.60E+07	4	3.99E+06		
Total	2.22E+08	17			

Table A.2 Analysis of Variance of |E*| at -10ºC, 10Hz

Source	Sum Sq.	d.f.	Mean Sq.	F	p-value
Mix	1.48E+08	2	7.38E+07	10.82	0.024
Age	1.65E+07	2	8.24E+06	1.21	0.389
Condition	2.41E+07	1	2.41E+07	3.53	0.134
Mix*Age	5.33E+07	4	1.33E+07	1.95	0.266
Mix*Condition	2.85E+06	2	1.43E+06	0.21	0.820
Age*Condition	5.00E+07	2	2.50E+07	3.66	0.125
Error	2.73E+07	4	6.82E+06		
Total	3.22E+08	17			

Table A.3 Analysis of Variance of |E*| at -10ºC, 5Hz

Source	Sum Sq.	d.f.	Mean Sq.	F	p-value
Mix	1.25E+08	2	6.26E+07	11.54	0.022
Age	1.41E+07	2	7.03E+06	1.3	0.368
Condition	2.54E+07	1	2.54E+07	4.68	0.097
Mix*Age	4.15E+07	4	1.04E+07	1.91	0.273
Mix*Condition	2.39E+06	2	1.20E+06	0.22	0.811
Age*Condition	4.42E+07	2	2.21E+07	4.07	0.108
Error	2.17E+07	4	5.42E+06		
Total	2.74E+08	17			

Table A.4 Analysis of Variance of |E*| at -10ºC, 1Hz

Source	Sum Sq.	d.f.	Mean Sq.	F	p-value
Mix	1.33E+08	2	66320941	16.87	0.011
Age	1.52E+07	2	7620042.1	1.94	0.258
Condition	1.98E+07	1	19824006	5.04	0.088
Mix*Age	4.01E+07	4	10016568	2.55	0.194
Mix*Condition	1.23E+06	2	614392.1	0.16	0.860
Age*Condition	4.15E+07	2	20730327	5.27	0.076
Error	1.57E+07	4	3930663.2		
Total	2.66E+08	17			

Table A.5 Analysis of Variance of |E*| at -10ºC, 0.5Hz

Source	Sum Sq.	d.f.	Mean Sq.	F	p-value
Mix	1.66E+08	2	8.30E+07	24.1	0.006
Age	9.88E+06	2	4.94E+06	1.43	0.339
Condition	3.48E+07	1	3.48E+07	10.09	0.034
Mix*Age	5.48E+07	4	1.37E+07	3.98	0.105
Mix*Condition	8.79E+06	2	4.40E+06	1.28	0.373
Age*Condition	2.64E+07	2	1.32E+07	3.84	0.117
Error	1.38E+07	4	3.44E+06		
Total	3.14E+08	17			

Table A.6 Analysis of Variance of |E*| at -10ºC, 0.1Hz

Source	Sum Sq.	d.f.	Mean Sq.	F	p-value
Mix	1.29E+08	2	6.47E+07	22.43	0.007
Age	1.43E+07	2	7.16E+06	2.48	0.199
Condition	2.01E+07	1	2.01E+07	6.97	0.058
Mix*Age	4.01E+07	4	1.00E+07	3.48	0.127
Mix*Condition	4.55E+06	2	2.27E+06	0.79	0.515
Age*Condition	2.57E+07	2	1.29E+07	4.46	0.096
Error	1.15E+07	4	2.88E+06		
Total	2.46E+08	17			

Table A.7 Analysis of Variance of |E*| at 4ºC, 25Hz

Source	Sum Sq.	d.f.	Mean Sq.	F	p-value
Mix	3.67E+07	2	1.84E+07	3.04	0.158
Age	1.67E+07	2	8.35E+06	1.38	0.350
Condition	3.56E+06	1	3.56E+06	0.59	0.486
Mix*Age	1.91E+07	4	4.77E+06	0.79	0.589
Mix*Condition	1.90E+07	2	9.52E+06	1.57	0.313
Age*Condition	1.85E+07	2	9.26E+06	1.53	0.321
Error	2.42E+07	4	6.05E+06		
Total	1.38E+08	17			

Table A.8 Analysis of Variance of |E*| at 4ºC, 10Hz

Source	Sum Sq.	d.f.	Mean Sq.	F	p-value
Mix	4.58E+07	2	2.29E+07	2.59	0.190
Age	2.00E+07	2	1.00E+07	1.13	0.408
Condition	1.49E+06	1	1.49E+06	0.17	0.702
Mix*Age	2.13E+07	4	5.34E+06	0.6	0.682
Mix*Condition	2.61E+07	2	1.31E+07	1.48	0.331
Age*Condition	3.16E+07	2	1.58E+07	1.79	0.279
Error	3.54E+07	4	8.85E+06		
Total	1.82E+08	17			

Table A.9 Analysis of Variance of |E*| at 4ºC, 5Hz

Source	Sum Sq.	d.f.	Mean Sq.	F	p-value
Mix	4.68E+07	2	2.34E+07	2.97	0.162
Age	2.22E+07	2	1.11E+07	1.41	0.345
Condition	1.24E+06	1	1.24E+06	0.16	0.712
Mix*Age	2.09E+07	4	5.22E+06	0.66	0.651
Mix*Condition	2.48E+07	2	1.24E+07	1.57	0.313
Age*Condition	2.48E+07	2	1.24E+07	1.57	0.314
Error	3.16E+07	4	7.89E+06		
Total	1.72E+08	17			

Table A.10 Analysis of Variance of |E*| at 4ºC, 1Hz

Source	Sum Sq.	d.f.	Mean Sq.	F	p-value
Mix	41073978.1	2	20536989	3.11	0.153
Age	18456483.4	2	9228241.7	1.4	0.346
Condition	199080.5	1	199080.5	0.03	0.871
Mix*Age	10443633.2	4	2610908.3	0.4	0.804
Mix*Condition	16956471	2	8478235.5	1.29	0.371
Age*Condition	22723226.3	2	11361613	1.72	0.289
Error	26377069.7	4	6594267.4		
Total	136229942	17			

Table A.11 Analysis of Variance of |E*| at 4ºC, 0.5Hz

Source	Sum Sq.	d.f.	Mean Sq.	F	p-value
Mix	30918233.4	2	15459117	3.43	0.136
Age	21947944.8	2	10973972	2.43	0.204
Condition	739328	1	739328	0.16	0.706
Mix*Age	12394244.9	4	3098561.2	0.69	0.637
Mix*Condition	17423497	2	8711748.5	1.93	0.259
Age*Condition	15245227	2	7622613.5	1.69	0.294
Error	18035260	4	4508815		
Total	116703735	17			

Table A.12 Analysis of Variance of |E*| at 4ºC, 0.1Hz

Source	Sum Sq.	d.f.	Mean Sq.	F	p-value
Mix	19602026.3	2	9801013.2	3.67	0.124
Age	17997072.3	2	8998536.2	3.37	0.139
Condition	420138.9	1	420138.9	0.16	0.712
Mix*Age	7775411.3	4	1943852.8	0.73	0.617
Mix*Condition	10936168.1	2	5468084.1	2.05	0.244
Age*Condition	8540008.1	2	4270004.1	1.6	0.309
Error	10682438.9	4	2670609.7		
Total	75953264	17			

Table A.13 Analysis of Variance of |E*| at 21ºC, 25Hz

Source	Sum Sq.	d.f.	Mean Sq.	F	p-value
Mix	54042432.1	2	27021216	5.77	0.066
Age	2840547.4	2	1420273.7	0.3	0.754
Condition	18477120.5	1	18477121	3.95	0.118
Mix*Age	11263798.9	4	2815949.7	0.6	0.683
Mix*Condition	13781590.3	2	6890795.2	1.47	0.332
Age*Condition	594901	2	297450.5	0.06	0.939
Error	18725294.7	4	4681323.7		
Total	119725685	17			

Table A.14 Analysis of Variance of |E*| at 21ºC, 10Hz

Source	Sum Sq.	d.f.	Mean Sq.	F	p-value
Mix	12789387.4	2	6394693.7	1.55	0.317
Age	16672787.4	2	8336393.7	2.03	0.247
Condition	4512.5	1	4512.5	0	0.975
Mix*Age	6287086.22	4	1571771.6	0.38	0.813
Mix*Condition	4157162.33	2	2078581.2	0.51	0.637
Age*Condition	9916092.33	2	4958046.2	1.21	0.389
Error	16455209.3	4	4113802.3		
Total	66282237.6	17			

Table A.15 Analysis of Variance of |E*| at 21ºC, 5Hz

Source	Sum Sq.	d.f.	Mean Sq.	F	p-value
Mix	8637214.3	2	4318607.2	1.28	0.372
Age	14491790.3	2	7245895.2	2.15	0.232
Condition	22684.5	1	22684.5	0.01	0.939
Mix*Age	6121653.3	4	1530413.3	0.45	0.769
Mix*Condition	4013832.3	2	2006916.2	0.6	0.594
Age*Condition	8082736.3	2	4041368.2	1.2	0.391
Error	13487099.3	4	3371774.8		
Total	54857010.5	17			

Table A.16 Analysis of Variance of |E*| at 21ºC, 1Hz

Source	Sum Sq.	d.f.	Mean Sq.	F	p-value
Mix	3288389.8	2	1644194.9	0.92	0.469
Age	8752022.1	2	4376011.1	2.45	0.202
Condition	69564.5	1	69564.5	0.04	0.853
Mix*Age	4345345.9	4	1086336.5	0.61	0.679
Mix*Condition	2803745.3	2	1401872.7	0.79	0.515
Age*Condition	4534308.3	2	2267154.2	1.27	0.374
Error	7133570.3	4	1783392.6		
Total	30926946.3	17			

Table A.17 Analysis of Variance of |E*| at 21ºC, 0.5Hz

Source	Sum Sq.	d.f.	Mean Sq.	F	p-value
Mix	3288389.8	2	1644194.9	0.92	0.469
Age	8752022.1	2	4376011.1	2.45	0.202
Condition	69564.5	1	69564.5	0.04	0.853
Mix*Age	4345345.9	4	1086336.5	0.61	0.679
Mix*Condition	2803745.3	2	1401872.7	0.79	0.515
Age*Condition	4534308.3	2	2267154.2	1.27	0.374
Error	7133570.3	4	1783392.6		
Total	30926946.3	17			

Table A.18 Analysis of Variance of |E*| at 21ºC, 0.1Hz

Source	Sum Sq.	d.f.	Mean Sq.	F	p-value
Mix	520620.4	2	260310.2	0.62	0.582
Age	3340344.4	2	1670172.2	3.99	0.111
Condition	74755.6	1	74755.6	0.18	0.694
Mix*Age	1978874.2	4	494718.6	1.18	0.437
Mix*Condition	535987.1	2	267993.6	0.64	0.574
Age*Condition	780508.4	2	390254.2	0.93	0.465
Error	1672672.9	4	418168.2		
Total	8903763.1	17			

Table A.19 Analysis of Variance of |E*| at 37ºC, 25Hz

Source	Sum Sq.	d.f.	Mean Sq.	F	p-value
Mix	1194016.8	2	597008.4	1.31	0.366
Age	2045773.4	2	1022886.7	2.24	0.223
Condition	2327043.6	1	2327043.6	5.09	0.087
Mix*Age	1195813.2	4	298953.3	0.65	0.654
Mix*Condition	714525.4	2	357262.7	0.78	0.517
Age*Condition	1724915.4	2	862457.7	1.89	0.265
Error	1827294.6	4	456823.6		
Total	11029382.4	17			

Table A.20 Analysis of Variance of |E*| at 37ºC, 10Hz

Source	Sum Sq.	d.f.	Mean Sq.	F	p-value
Mix	394970.1	2	197485.1	0.46	0.663
Age	1456174.8	2	728087.4	1.68	0.295
Condition	1868244.5	1	1868244.5	4.32	0.106
Mix*Age	1480594.2	4	370148.6	0.86	0.559
Mix*Condition	695224.3	2	347612.2	0.8	0.509
Age*Condition	1164866.3	2	582433.2	1.35	0.357
Error	1731651.3	4	432912.8		
Total	8791725.6	17			

Table A.21 Analysis of Variance of |E*| at 37ºC, 5Hz

Source	Sum Sq.	d.f.	Mean Sq.	F	p-value
Mix	601573	2	300786.5	1.06	0.428
Age	1213246.3	2	606623.2	2.13	0.234
Condition	753582.7	1	753582.7	2.65	0.179
Mix*Age	752604.7	4	188151.2	0.66	0.650
Mix*Condition	372160.8	2	186080.4	0.65	0.568
Age*Condition	1054963.4	2	527481.7	1.86	0.269
Error	1136873.6	4	284218.4		
Total	5885004.5	17			

Table A.22 Analysis of Variance of |E*| at 37ºC, 1Hz

Source	Sum Sq.	d.f.	Mean Sq.	F	p-value
Mix	217546.3	2	108773.2	1.2	0.392
Age	450916.3	2	225458.2	2.48	0.199
Condition	163973.6	1	163973.6	1.8	0.251
Mix*Age	243232.3	4	60808.1	0.67	0.647
Mix*Condition	130393.4	2	65196.7	0.72	0.542
Age*Condition	304780.8	2	152390.4	1.68	0.296
Error	363809.2	4	90952.3		
Total	1874652	17			

Table A.23 Analysis of Variance of |E*| at 37ºC, 0.5Hz

Source	Sum Sq.	d.f.	Mean Sq.	F	p-value
Mix	142828.4	2	71414.2	1.2	0.390
Age	272163.1	2	136081.6	2.29	0.217
Condition	98272.2	1	98272.2	1.66	0.267
Mix*Age	155338.2	4	38834.6	0.65	0.654
Mix*Condition	92727.1	2	46363.6	0.78	0.517
Age*Condition	189749.8	2	94874.9	1.6	0.309
Error	237224.9	4	59306.2		
Total	1188303.8	17			

Table A.24 Analysis of Variance of |E*| at 37ºC, 0.1Hz

Source	Sum Sq.	d.f.	Mean Sq.	F	p-value
Mix	49321	2	24660.5	1.32	0.362
Age	100681	2	50340.5	2.7	0.181
Condition	19404.5	1	19404.5	1.04	0.365
Mix*Age	47785	4	11946.2	0.64	0.661
Mix*Condition	25981	2	12990.5	0.7	0.550
Age*Condition	57490.3	2	28745.2	1.54	0.318
Error	74451.7	4	18612.9		
Total	375114.5	17			

Table A.25 Analysis of Variance of |E*| at 54ºC, 25Hz

Source	Sum Sq.	d.f.	Mean Sq.	F	p-value
Mix	300538.8	2	150269.4	4.04	0.110
Age	207704.8	2	103852.4	2.8	0.174
Condition	38456.9	1	38456.9	1.04	0.367
Mix*Age	273212.9	4	68303.2	1.84	0.285
Mix*Condition	43734.8	2	21867.4	0.59	0.597
Age*Condition	96220.1	2	48110.1	1.3	0.368
Error	148602.2	4	37150.6		
Total	1108470.4	17			

Table A.26 Analysis of Variance of |E*| at 54ºC, 10Hz

Source	Sum Sq.	d.f.	Mean Sq.	F	p-value
Mix	182460.1	2	91230.1	2.5	0.197
Age	164680.4	2	82340.2	2.26	0.221
Condition	11858	1	11858	0.33	0.599
Mix*Age	183359.6	4	45839.9	1.26	0.415
Mix*Condition	65816.3	2	32908.2	0.9	0.475
Age*Condition	67692	2	33846	0.93	0.466
Error	145780.7	4	36445.2		
Total	821647.1	17			

Table A.27 Analysis of Variance of |E*| at 54ºC, 5Hz

Source	Sum Sq.	d.f.	Mean Sq.	F	p-value
Mix	106064.1	2	53032.1	2.25	0.221
Age	93890.8	2	46945.4	1.99	0.251
Condition	3901.4	1	3901.4	0.17	0.705
Mix*Age	111761.2	4	27940.3	1.19	0.436
Mix*Condition	46296.8	2	23148.4	0.98	0.450
Age*Condition	41204.1	2	20602.1	0.87	0.484
Error	94199.2	4	23549.8		
Total	497317.6	17			

Table A.28 Analysis of Variance of |E*| at 54ºC, 1Hz

Source	Sum Sq.	d.f.	Mean Sq.	F	p-value
Mix	34520.1	2	17260.1	2.03	0.247
Age	35971.4	2	17985.7	2.11	0.237
Condition	227.6	1	227.6	0.03	0.878
Mix*Age	36509.2	4	9127.3	1.07	0.474
Mix*Condition	20584.8	2	10292.4	1.21	0.389
Age*Condition	18407.4	2	9203.7	1.08	0.422
Error	34085.2	4	8521.3		
Total	180305.8	17			

Table A.29 Analysis of Variance of |E*| at 54ºC, 0.5Hz

Source	Sum Sq.	d.f.	Mean Sq.	F	p-value
Mix	32157	2	16078.5	2.22	0.225
Age	27571	2	13785.5	1.9	0.263
Condition	2913.4	1	2913.4	0.4	0.561
Mix*Age	29876	4	7469	1.03	0.489
Mix*Condition	11802.8	2	5901.4	0.81	0.506
Age*Condition	12726.8	2	6363.4	0.88	0.483
Error	29035.6	4	7258.9		
Total	146082.5	17			

Table A.30 Analysis of Variance of |E*| at 54ºC, 0.1Hz

Source	Sum Sq.	d.f.	Mean Sq.	F	p-value
Mix	11113	2	5556.5	1.5	0.327
Age	11077.3	2	5538.67	1.49	0.328
Condition	2312	1	2312	0.62	0.474
Mix*Age	13072.7	4	3268.17	0.88	0.548
Mix*Condition	8386.3	2	4193.17	1.13	0.409
Age*Condition	7777.3	2	3888.67	1.05	0.431
Error	14865.3	4	3716.33		
Total	68604	17			

Appendix B Tables from Chapter 3

Table B.1 Analysis of Variance of Fracture Energy

Source	Sum Sq.	d.f.	Mean Sq.	F	p-value
Mix Type	20704.6	2	10352.3	0.13	0.8763
Aging	216469.1	2	108234.6	1.39	0.2658
Moisture	256171.0	1	256171	3.28	0.0803
Temperature	471923.2	1	471923.2	6.05	0.0201
Error	2262278.8	29	78009.6		
Total	3227546.7	35			

Table B.2 Analysis of Variance of Cohesive Energy

Source	Sum Sq.	d.f.	Mean Sq.	F	p
Mix Type	25969.7	2	12984.8	0.4	0.6742
Aging	41295.8	2	20647.9	0.64	0.5369
Moisture	8070.0	1	8070	0.25	0.622
Temperature	114018.8	1	114018.8	3.51	0.0711
Error	942260.1	29	32491.7		
Total	1131614.4	35			

Table B.3 Analysis of Variance of Energy Rate

Source	Sum Sq.	d.f.	Mean Sq.	F	p
Mix Type	42.5	2	21.272	0.49	0.615
Aging	138.9	2	69.443	1.61	0.2165
Moisture	358.7	1	358.724	8.34	0.0073
Temperature	181.1	1	181.082	4.21	0.0494
Error	1247.9	29	43.031		
Total	1969.1	35			

Appendix C Tables from Chapter 4

Table C.1 Analysis of Variance of Fracture Energy COV

Source	Sum Sq.	d.f.	Mean Sq.	F	p
Temperature	65.21	1	65.21	0.56	0.4696
NMAS	1064.39	1	1064.39	9.16	0.0115
PG	361.95	1	361.95	3.11	0.1053
Loading rate	0.6	1	0.6	0.01	0.944
Error	1278.46	11	116.22		
Total	2770.6	15			

Table C.2 Analysis of Variance of Cohesive Energy COV

Source	Sum Sq.	d.f.	Mean Sq.	F	p
Temperature	121	1	121	0.92	0.3572
NMAS	2475.06	1	2475.06	18.89	0.0012
PG	282.24	1	282.24	2.15	0.1702
Loading rate	420.25	1	420.25	3.21	0.1008
Error	1441.44	11	131.04		
Total	4740	15			

Table C.3 Analysis of Variance of Energy Rate COV

Source	Sum Sq.	d.f.	Mean Sq.	F	p
Temperature	51000	1	51000	30.01	0.0004
NMAS	18773.1	1	18773.1	11.05	0.0089
PG	6023.7	1	6023.7	3.55	0.0924
Loading rate	9208.5	1	9208.5	5.42	0.0449
Error	15292.5	11	1699.2		
Total	82453.1	15			

Table C.4 Analysis of Variance of Fracture Energy

Source	Sum Sq.	d.f.	Mean Sq.	F	p
Temperature	773432.3	1	773432.3	30.33	0.0002
NMAS	9025	1	9025	0.35	0.5639
PG	15525.2	1	15525.2	0.61	0.4517
Loading rate	36614.8	1	36614.8	1.44	0.256
Error	280466.6	11	25497		
Total	1115064	15			

Table C.5 Analysis of Variance of Cohesive Energy

Source	Sum Sq.	d.f.	Mean Sq.	F	p
Temperature	380103.1	1	380103.1	24.13	0.0005
NMAS	4512.5	1	4512.5	0.29	0.6032
PG	37529.4	1	37529.4	2.38	0.151
Loading rate	317.7	1	317.7	0.02	0.8896
Error	173291.1	11	15753.7		
Total	595753.7	15			

Table C.6 Analysis of Variance of Energy Rate

Source	Sum Sq.	d.f.	Mean Sq.	F	p
Temperature	229.523	1	229.523	8.01	0.0163
NMAS	11.902	1	11.902	0.42	0.5324
PG	26.522	1	26.522	0.93	0.3566
Loading rate	127.69	1	127.69	4.46	0.0584
Error	315.073	11	28.643		
Total	710.71	15			